NASA Technical Memorandum 89144

Langley Aerospace Test Highlights 1986

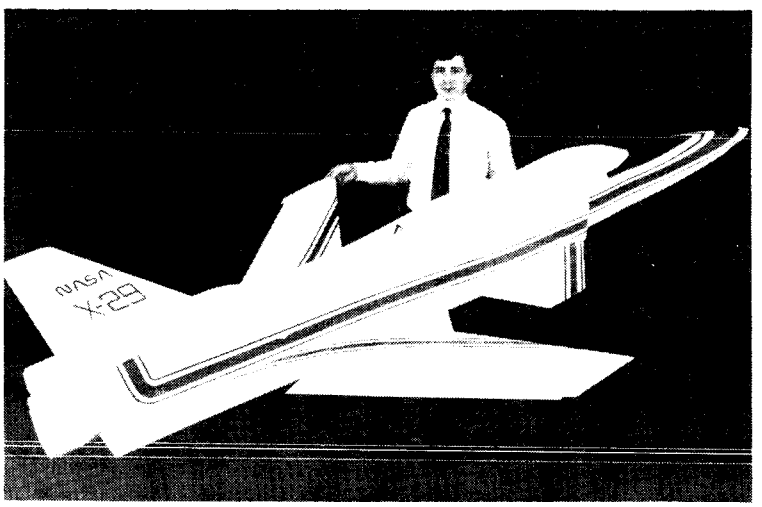

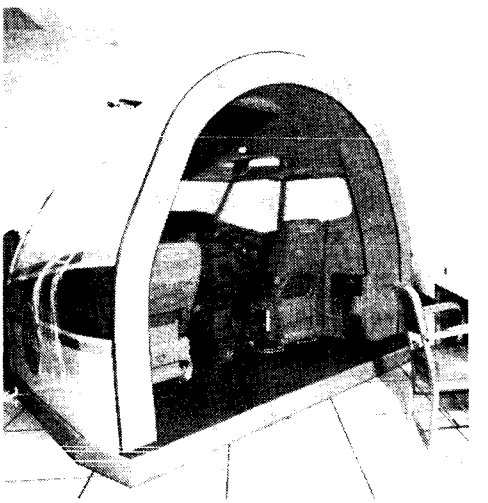

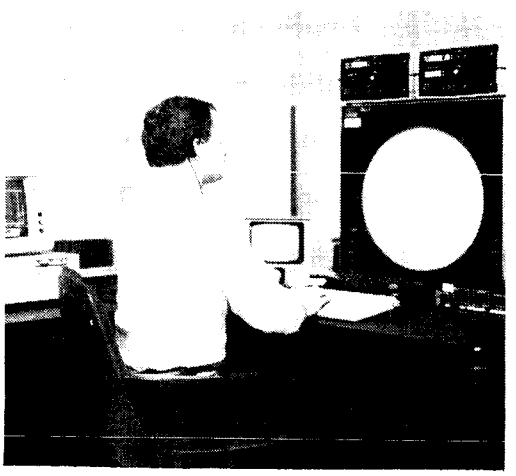

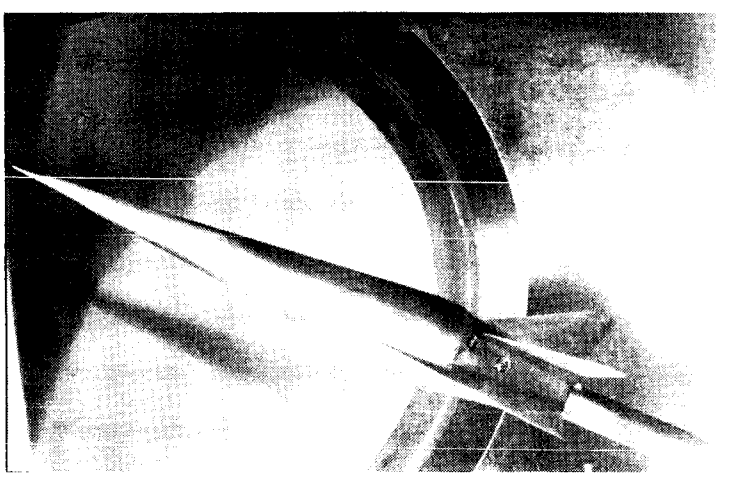

NASA
National Aeronautics and
Space Administration

NASA Technical Memorandum 89144

Langley Aerospace Test Highlights 1986

National Aeronautics and
Space Administration

Langley Research Center
Hampton, Virginia 23665-5225

Foreword

The role of the Langley Research Center is to perform basic and applied research necessary for the advancement of aeronautics and space flight, to generate new and advanced concepts for the accomplishment of related national goals, and to provide research advice, technological support, and assistance to other NASA installations, other government agencies, and industry. This report highlights some of the significant tests that were performed during calendar year 1986 in Langley Research Center test facilities, a number of which are unique in the world. The report illustrates both the broad range of the research and technology activities at the Langley Research Center and the contributions of this work toward maintaining United States leadership in aeronautics and space research. Other highlights of Langley research and technology for 1986 are described in *Research and Technology 1986 Annual Report of the Langley Research Center*. Further information about both reports is available from the Office of the Chief Scientist, Mail Stop 103, Langley Research Center, Hampton, Virginia 23665 (804-865-3316).

Richard H. Petersen
Director

Availability Information

For additional information on any highlight, contact the individual identified with the highlight. This individual is generally either a member or a leader of the research group. Commercial telephone users may dial the listed extension preceded by (804) 865. Telephone users with access to the Federal Telecommunications System (FTS) may dial the extension preceded by 928.

Contents

30- by 60-Foot Tunnel

The Langley 30- by 60-Foot Tunnel is a continuous-flow open-throat double-return tunnel powered by two 4000-horsepower electric motors, each driving a four-blade 35.5-ft-diameter fan. The tunnel test section is 30 ft high and 60 ft wide and is capable of speeds up to 100 mph. The tunnel was first put into operation in 1931 and has been used continuously since then to study the low-speed aerodynamics of commercial and military aircraft. The large open-throat test section lends itself readily to tests of large-scale models and to unique test methods with small-scale models.

Large-scale and full-scale aircraft tests are conducted with the strut mounting system. This test method can handle airplanes up to the size of present-day light twin-engine airplanes. Such tests provide static aerodynamic performance and stability and control data, including the measurement of power effects, wing pressure distributions, and flow visualization.

Small-scale models can be tested to determine both static and dynamic aerodynamics. For all captive tests, the models are sting mounted with internal strain-gauge balances. The captive test methods include conventional static tests for performance and stability and control, forced-oscillation tests for aerodynamic damping, and rotary tests for spin aerodynamics. Dynamically scaled subscale models, properly instrumented, are also freely flown in the large test section with a simple tether to study their dynamic stability characteristics at low speed and at high angles of attack. A small computer is used in this free-flight test technique to represent the important characteristics of the airplane flight control system. The Langley 12-Foot Low-Speed Tunnel, which is used extensively for static tests prior to entry in the 30- by 60-Foot Tunnel, is an atmospheric wind tunnel with a 12-ft octagonal cross section for model testing. The tunnel serves as a diagnostic facility for exploratory research primarily in the area of high-angle-of-attack stability and control studies of various airplane and spacecraft configurations. Preliminary tests are conducted in the 12-Foot Low-Speed Tunnel on simple models prior to testing higher speed facilities on more sophisticated models, to obtain more efficient test planning and effective use of occupancy time in higher speed facilities.

Ground Effect on STOVL Fighter Configuration in Hover

Tests were made in the 30- by 60-Foot Tunnel using the tunnel compressed air supply and an experimental boom assembly to obtain information on the influence of ground proximity on the powered lift of an 0.15-scale model of the General Dynamics E-7 supersonic STOVL (short takeoff and vertical landing) fighter configuration in the hover mode. The E-7 configuration has an ejector system located forward of the center of gravity in the wing root section of a large clipped delta wing and a vectorable core nozzle located aft of the center of gravity to provide the lift and balance required for STOVL capability. During hovering flight, altitude control of the aircraft is provided by small reaction jet thrusters located in the nose, wing, and tail sections. These control jets were unpowered for this investigation.

Measurements made at different heights of the diffuser exit plane above the ground are presented

relative to a reference condition arbitrarily chosen to correspond to the full-scale vehicle at a height of 20 ft. Data for the wing ejector and core flow operation simultaneously indicate that a loss in lift occurred as the vehicle approached the ground. The summed results of individual test data showed a larger lift loss than was measured. The difference between the curves is believed to be due to the presence of a jet fountain that exists between the ejectors and core nozzle and alleviates some of the lift loss due to ground effect.

(Donald R. Riley, 2184)

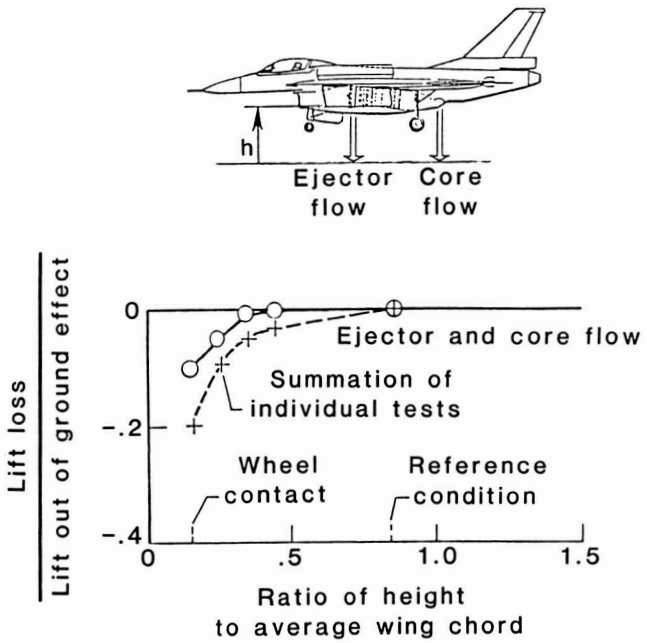

Ground effect tests of E-7 powered lift model in hover.

Effect of Forebody Geometry on High Angle-of-Attack Stability

A research program is under way to provide a systematic low-speed wind tunnel data base on the effects of forebody geometry on aircraft static and dynamic stability at high angles of attack. As part of this program, a series of wind tunnel tests of a generic, variable-geometry fighter model have been conducted in the 12-Foot Low-Speed Tunnel. Conventional force and moment tests were conducted to determine static stability characteristics, and single degree-of-freedom free-to-roll tests were conducted to study the wing rock susceptibility. Flow visualization data were obtained to aid in the analysis of the complex flow phenomena involved.

Test results have shown large effects of forebody cross-sectional shape on static and dynamic stability. The forebody shape affected static directional stability by the formation of vortices which produced stabilizing or destabilizing forces on the forebody of the model. Lateral stability was affected by coupling of the forebody and wing flow fields. This coupling and associated flow lag effects were seen to induce wing rock for several of the test configurations.

Forebody/wing proximity was found to directly affect the coupling of the two flow fields and as a result influenced both static and dynamic stability at high angles of attack. The combination of forebody geometry and proximity factors produced static lateral/directional stability characteristics that range from highly stable to highly unstable and configurations that were well damped in roll to those that exhibited very large-amplitude wing rock. A general trend was observed whereby configurations that had the highest levels of static lateral stability also tended to exhibit the largest amplitude wing rock, whereas configurations that were statically unstable were very resistant to wing rock.

(Jay M. Brandon, 2184)

L-83-11,376

Generic flexible geometry fighter model.

Low-Turbulence Pressure Tunnel

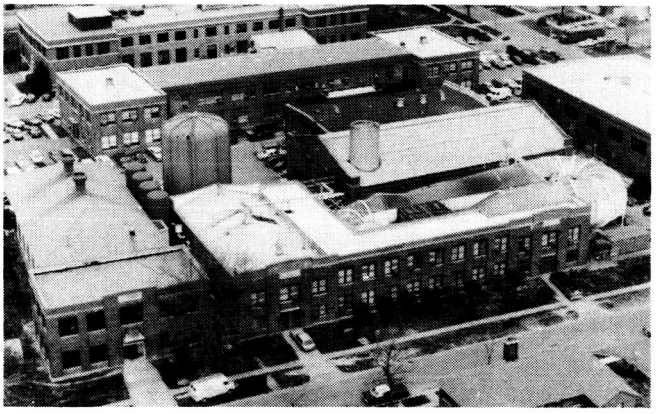

The Langley Low-Turbulence Pressure Tunnel (LTPT) is a single-return closed-circuit tunnel that can be operated at pressures from near vacuum to 10 atm. The test section is rectangular in shape (3 ft wide and 7.5 ft in height and length), and the contraction ratio is 17.6:1. The LTPT is capable of testing at Mach numbers from 0.05 to 0.50 and unit Reynolds numbers from 0.1×10^6 to 15×10^6 per foot. The tunnel has provisions for removal of the sidewall boundary layer by means of a closed-loop suction system mounted inside the pressure chamber. This system utilizes slotted vertical sidewalls just ahead of the model test section, and the removed air is reinjected through an annular slot downstream of the test section. A flow control system allows the flow and pressure requirements to be varied as dictated by tunnel operation. This system can be used to provide boundary-layer control (BLC) for low-drag airfoil research.

A BLC system for high-lift airfoil testing is also available. This system utilizes compressed dry air and involves tangential blowing from slots located on the sidewall mounting endplates. Flowmeters can be used to monitor the amount of air blown into the tunnel. An automatically controlled vent valve is utilized to remove the air injected into the tunnel by this system. A high-lift model support and force balance system is provided to handle both single-element and multiple-element airfoils.

The measured turbulence level of the LTPT is very low due to the large contraction ratio and the many fine-mesh antiturbulence screens. The excellent flow quality of this facility makes it particularly suitable for testing low-drag airfoils. Recent flow quality measurements in the LTPT indicate that the velocity fluctuations in the test section range from 0.025 percent at Mach 0.05 to 0.30 percent at Mach 0.20 at the highest unit Reynolds number.

The drive system is a 2000-horsepower direct-current motor with power supplied from a motor-generator set. The tunnel stagnation temperature is controlled by a heat exchanger, which provides both heating and cooling via steam injectors and modulated valves that control the flow volume of water through a set of coils.

Low Reynolds Number Airfoil Research

Recent interest in incompressible low Reynolds number aerodynamics has increased in regard to both military and civilian applications. Chord Reynolds numbers below 500,000 are usually identified as being in this classification. Applications are varied and include remotely piloted vehicles at high altitudes, sail planes, ultralight human-powered vehicles, wind turbines, and propellers.

Although the design and evaluation techniques for airfoil sections at chord Reynolds numbers above 500,000 are well developed, serious problems related to boundary-layer separation and transition have been encountered at Reynolds numbers below 500,000. Presently available design and analysis methods generally do not adequately model the flow phenomena because of the effects of large laminar separation bubbles. Experimental results obtained on the Eppler 387 airfoil at low Reynolds numbers in several wind tunnels have shown large differences in airfoil performance. This is not surprising

because of the sensitivity of the airfoil boundary layer to free-stream disturbances and model contour accuracy. Also, the model pressures and forces are very small and difficult to measure.

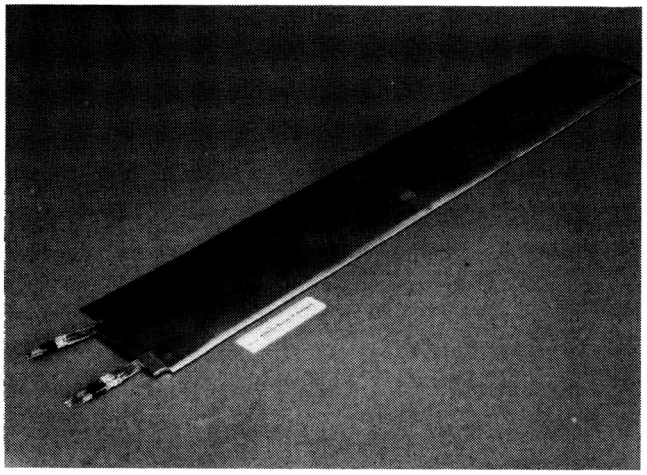

L-86-1165

Eppler 387 airfoil model tested in LTPT.

Tests have been conducted in the LTPT on a pressure model of the Eppler 387 airfoil (shown in the first figure) to develop test techniques for low Reynolds number aerodynamics. The LTPT was selected because of its excellent flow quality and precision pressure instrumentation.

Typical pressure data are shown in the second figure for the Eppler 387 airfoil at a Reynolds number R of 100,000, Mach number M of 0.03, and angle of attack α of 0°. Large differences between experimental and theoretical results are indicated on the upper surface of the airfoil due to the presence of a long laminar separation bubble. Separation and reattachment locations were determined from oil-flow studies.

(Robert J. McGhee, 4516)

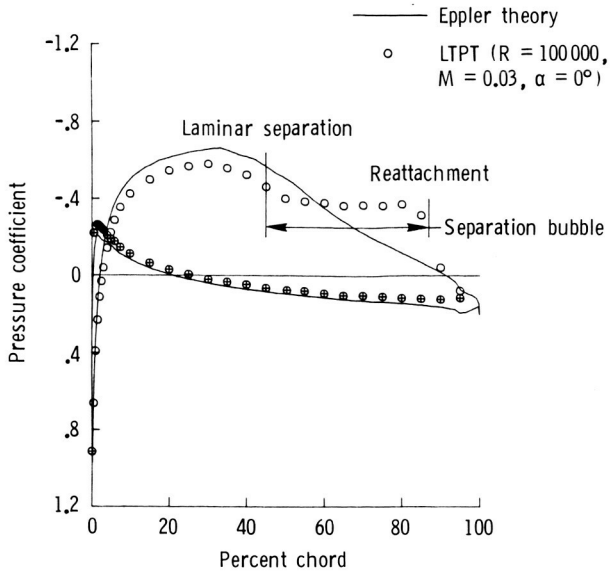

Experimental and theoretical pressure data for Eppler 387 airfoil.

High Reynolds Number Investigation of Cylinders With Perforations and Protrusions

The effects of perforations and protrusions on a circular cylinder have been studied on a new off-shore oil structure design through a cooperative test program with Bethlehem Steel Corporation. The study of flow fields on or about circular cylinders has been the focus of attention throughout aerodynamic history because the cylinder is one of the most commonly occurring shapes in engineering structures.

Because off-shore structures often approach exposed heights of 600 ft, aerodynamic loading is critical to the stability of these structures. This high Reynolds number application of the circular cylinder is unique because although the Reynolds number must approach 6×10^6, the Mach number must remain below 0.15. To avoid large and costly models, the LTPT was determined to be the only possible facility for this test. In addition to the steady loading characteristics, it is also important to determine the unsteady effects that vary dramatically at high Reynolds numbers.

Although considerable data are available on smooth circular cylinders at subcritical Reynolds numbers, a sparsity of data exists at high Reynolds numbers or with cylinders having spanwise perforations and protrusions. This study examines seven cylinder configurations, including a baseline smooth cylinder, at Reynolds numbers ranging from 5×10^5 to 6×10^6. (This range is generally considered the transcritical and supercritical regime for a smooth circular cylinder.) An objective of this study was to determine the general behavior of these seven configurations. The study included examining drag coefficients, Reynolds number effects, Strouhal numbers, wake symmetry, and three-dimensional effects.

Typical results indicate that drag coefficients for cylinders with protrusions and perforations approached four times those of the baseline configuration. The unsteady loading characteristics were on the order of 20 percent of the mean loads. Bethlehem Steel Corporation plans to integrate these data into the new off-shore oil structure design.

(P. Calvin Stainback, 4516)

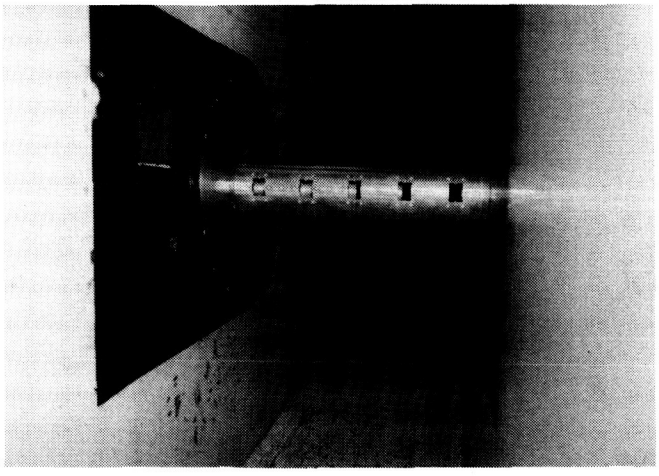

L-86-3318

Circular cylinder model in LTPT.

20-Foot Vertical Spin Tunnel

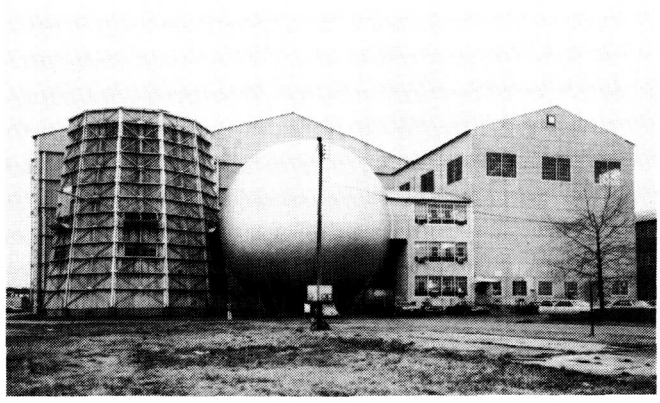

The Langley 20-Foot Vertical Spin Tunnel is the only operational spin tunnel in the United States and one of only two in the free world. The tunnel, which is used to investigate spin characteristics of dynamically scaled aircraft models, is a vertical tunnel with a closed-circuit annular return passage. The vertical test section has 12 sides and is 20 ft wide and 25 ft high. The test medium is air. Tunnel speed can be varied from 0 to 90 ft/sec with accelerations to 15 ft/sec^2. This facility is powered by a 1300-horsepower main drive.

Spin recovery characteristics are studied by remote actuation of the aerodynamic controls of models to predetermined positions. Force and moment testing is performed with a gooseneck rotary-arm model support, which permits angles of attack from 0° to ±90° and sideslip angles from 0° to ±20°. Motion picture and video records are used to record the spinning and recovery characteristics in the spin tunnel tests. Force and moment data from the rotary balance tests are recorded in coefficient form and stored on magnetic tapes.

Pressure Measurement Tests on Tail of Spinning Model

Past research has shown that the location of the horizontal tail with respect to the vertical tail can cause dramatic changes in the spin and recovery characteristics of airplanes. Data were not available for use in analysis of the horizontal tail interference effects on the vertical tail during a spin until rotary balance tests were recently conducted to measure the pressure distribution over the empennage and aft fuselage of an Australian trainer model at steady-spin conditions.

It was previously thought that part of the vertical tail above the horizontal tail provided some damping to the spin (antispin). Results from the pressure tests indicate however that the horizontal tail causes an interference effect on the vertical tail that, in turn, produces a propelling moment in a spin. The rotary balance pressure measurement technique has demonstrated for the first time the complex flow interaction relationship between the vertical and horizontal tails for an airplane undergoing spin motions. This technique is a valuable research tool for analyzing spin

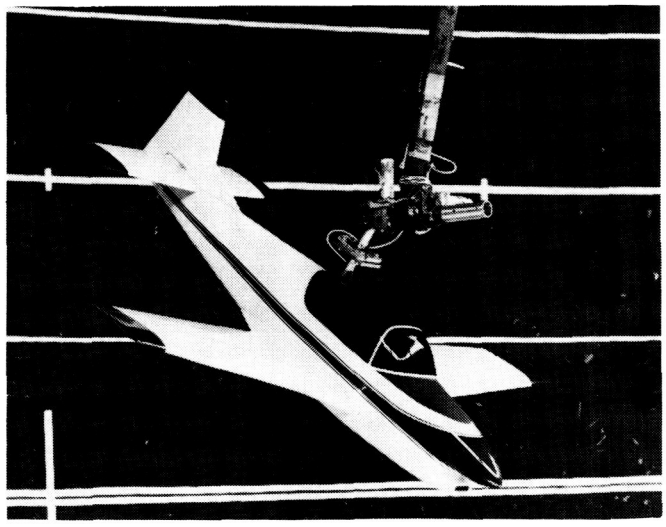

L-83-4,450

Australian trainer model mounted on rotary-balance rig in 20-Foot Vertical Spin Tunnel.

aerodynamics and for determining the influences of airplane components, such as wing, fuselage, and tails, on spin characteristics. Such information gives the designer increased confidence for providing desired spin and recovery characteristics on new aircraft early in the development process.
(James S. Bowman, Jr., 2244)

7- by 10-Foot High-Speed Tunnel

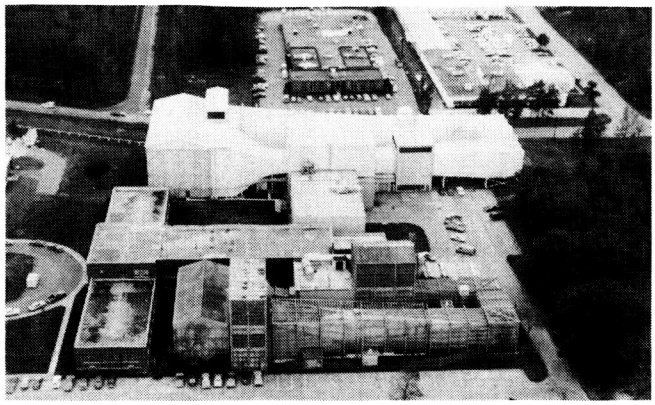

The Langley 7- by 10-Foot High-Speed Tunnel is a closed-circuit single-return continuous-flow atmospheric tunnel with a test section 6.6 ft high, 9.6 ft wide, and 10 ft long. The tunnel is fan driven and is powered by a 14,000-horsepower electric motor. It operates over a Mach number range from 0.2 to 0.9 to produce a maximum Reynolds number of 4×10^6 per foot. In addition to static testing of complete and semispan models, the facility is equipped for both steady-state roll and oscillatory stability testing.

The facility has an important role in a wide range of basic and applied aerodynamics research, including advanced vortex lift concepts, fuel-conservative aircraft design technology, highly maneuverable aircraft concepts, and the development of improved aerodynamic theories such as the difficult separated-flow and jet interaction effects needed for computer-aided design and analysis.

The 7- by 10-Foot High-Speed Tunnel is currently having new fan blades installed and has not been operational the past year. Work is scheduled to be completed in 1988.

14- by 22-Foot Subsonic Tunnel

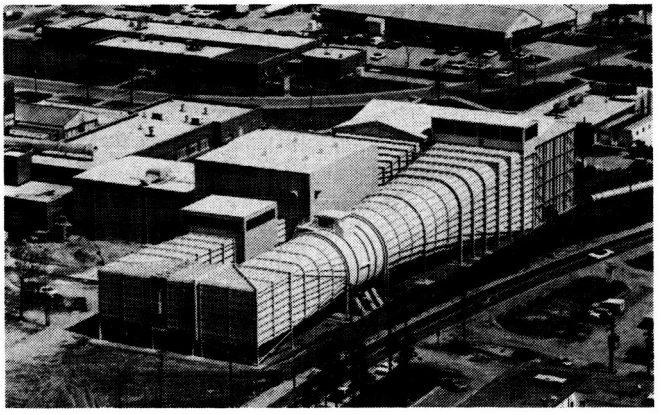

The Langley 14- by 22-Foot Subsonic Tunnel (formerly the 4- by 7-Meter Tunnel) is used for low-speed testing of powered and unpowered models of various fixed- and rotary-wing civil and military aircraft. The tunnel is powered by an 8000-horsepower electrical drive system, which can provide precise tunnel speed control from 0 to 318 ft/s with the Reynolds number per foot ranging from 0 to 2.1×10^6. The test section is 14.5 ft high, 21.8 ft wide, and approximately 50 ft long. The tunnel can be operated as a closed tunnel with slotted walls or as one or more open configurations when the side walls and ceiling are removed to allow extra testing capability, such as flow visualization and acoustic tests. The tunnel is equipped with a two-component laser velocimeter system. Furthermore, boundary-layer suction on the floor at the entrance to the test section and a moving-belt ground board for operation at test section flow velocities up to 111 ft/s can be installed for ground effect tests.

Modifications for improved aerodynamic and acoustic testing.

Langley has recently completed significant modifications to the 14- by 22-Foot Subsonic Tunnel to improve and expand its aerodynamic and acoustic test capability. One of the more significant aerodynamic improvements was achieved through the use of flow deflectors installed downstream of the first corner of the tunnel circuit to improve the performance of the tunnel fan. The deflectors resulted in a more uniform velocity distribution into the tunnel drive system and eliminated regions of large-scale flow separation in the return leg of the tunnel circuit.

A new turbulence reduction system consisting of a grid, a honeycomb, and four fine-mesh screens dramatically reduced the level of longitudinal turbulence intensity in the tunnel test section. This system provided a reduction in turbulence of 50 percent or more for the closed test section configuration. Periodic flow pulsations that occurred at several speeds in the unmodified configuration of the open test section were eliminated by installation of a new flow collector.

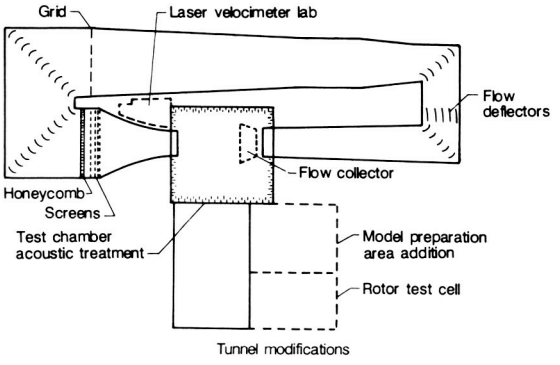

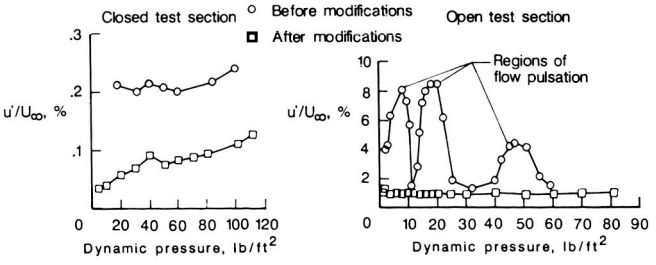

Effect of flow improvement modifications on longitudinal turbulence intensity (u'/U_∞).

Acoustic reverberations in the open test section were reduced through the use of sound-absorbing panels on the test chamber walls. A major operational improvement was achieved through the construction of a specially designed laser velocimeter laboratory for setup and maintenance of the two-component laser velocimetry system. Finally, an addition to the model preparation area which includes a support system and rotor test cell provides the capability to assemble and test rotor models in hovering conditions prior to actual entry into the tunnel.

(Zachary T. Applin, 4872)

Thrust Reverser Investigation on Jet Transport Model in Ground Effect

A wind tunnel investigation has been conducted in the 14- by 22-Foot Subsonic Tunnel to determine the sensitivity of thrust reverser performance to variations in inlet-to-exit mass flow ratio and to obtain a better understanding of the reversed engine flow field through velocity measurements and flow visualization.

A modern jet transport model was used in the tests, and three thrust-reverser designs representing cascade, target, and four-door configurations were studied. A high-pressure air system was used to simulate the engine exhaust flow and to power an ejector for engine inlet flow. The engine simulators were mounted on a separate support system alongside the airplane model. Separate controls were used for inlet and exhaust flows so that mass-flow ratios could be varied. Force and moment data were obtained on the aircraft model, along with ground-board pressure data. Flow visualization was performed by using smoke in the wind tunnel free stream, water spray in the reversed engine flow, and a sheet of laser light for illumination.

The ratio of inlet-to-exit mass flow was varied over a wide range of forward speeds, and in all cases the effects of mass-flow ratio on configuration aerodynamics were minor. This result is significant because it shows that effective thrust reverser research can be conducted on simplified models without the additional expense and complexity of providing for both inlet and exhaust flow simulation. With respect to the effects of forward speed, the cascade configuration was least sensitive to changes in free-stream velocity, while the four-door configuration was the most sensitive. All reverser plumes propagated farther upstream on a fixed ground plane than on a moving-belt ground plane as was expected. Overall aerodynamic characteristics of the airplane with reversers operating were highly configuration dependent and different for each reverser arrangement.

(Gregory M. Gatlin and P. Frank Quinto, 3611)

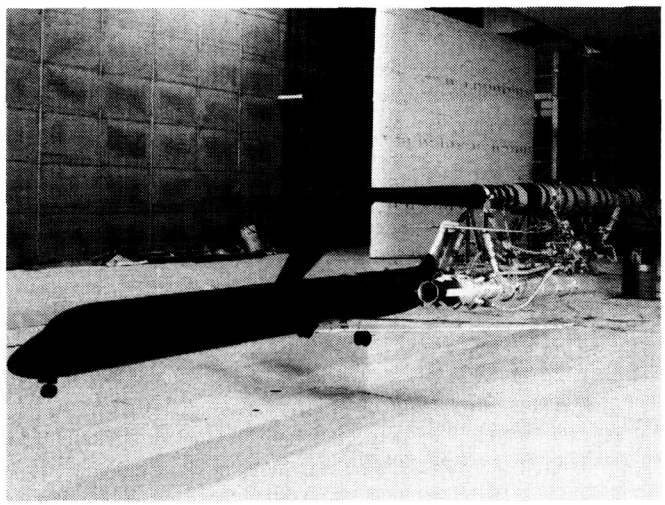

L-86-5370

Thrust reverser test apparatus.

Turboprop Installation Effects

Tests were conducted in the 14- by 22-Foot Subsonic Tunnel to study the basic aerodynamic and stability and control characteristics of a twin turboprop aircraft model with pusher propellers mounted on the aft fuselage. The wind tunnel model used in the test was representative of a 1/4-scale model of a typical twin-engine general-aviation aircraft with a T-tail. The model was tested through an angle-of-attack range from $-8°$ to $36°$ and an angle-of-sideslip range from $-20°$ to $20°$ with the propellers off, the propellers operating

at maximum power, and one propeller at maximum power and the other propeller feathered to simulate one engine out.

The model had aerodynamic characteristics that were generally as expected, except in terms of poststall behavior. The investigation revealed that an unrecoverable stall was more likely to occur if the propellers were not operating and that this likelihood was increased when the aircraft was configured with deflected landing flaps. Further tests are scheduled to evaluate model modifications in order to correct the stall problem, and diagnostic experiments are planned to study the mechanism responsible for the observed characteristics.
(Dana J. Dunham, 3611)

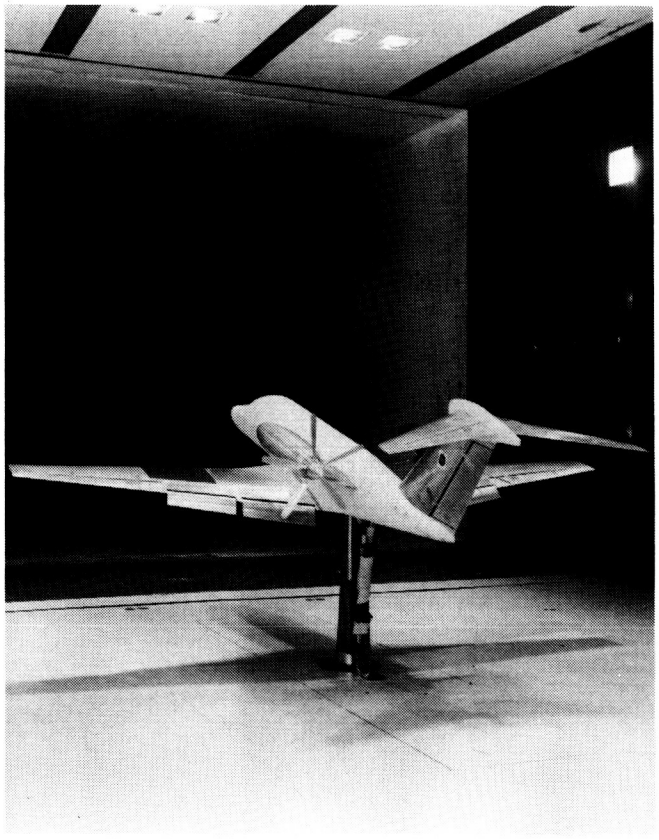

L-86-4913

Turboprop model installed for testing.

Sheared Wing-Tip Drag Reduction Research

Classical linear-wing theory based on planar-wing wakes shows that maximum lifting efficiency can be realized with an elliptical-wing planform. For the last decade, design of vertical winglets to reduce induced drag was based on classical linear theory. Recent applications of modern nonlinear aerodynamic theory in which the wing wake is allowed to deflect and roll up have shown that planar, sheared wing tips can provide lower induced drag penalty than classical elliptical planforms. A sheared wing tip is characterized by sweepback of its leading and trailing edge.

An advanced, low-drag, high aspect-ratio subsonic wing with several sheared wing-tip configurations was recently tested in the 14- by 22-Foot Subsonic Tunnel (as shown in the figure). Sheared tips with leading-edge sweep angles of 45° to 60° were tested and showed very good agreement with numerical predictions. A 10-percent reduction in induced drag was found for the 60° wing-tip sweep angle at cruise condition.

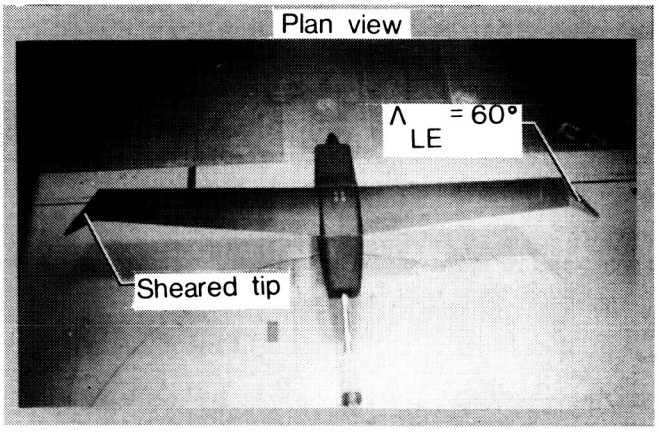

60° *sheared wing-tip configuration.*

At high angles of attack, a stable leading-edge vortex generated by the sheared wing tips may provide significant vortex lift. Vortex lift on these tips could increase stall/spin departure resistance and reduce buffet at approach conditions. Approach buffet is a problem that has made the application of winglets to transport wings difficult.

Further wind tunnel and flight tests, using aircraft from the Flight Research Facility, are planned to investigate both cruise and high angle-of-attack performance of sheared tips at low and high subsonic speeds.
(Bruce J. Holmes, 3274)

RECOUP Plume Simulation Test

Wind tunnel plume simulation tests of the Resource Recovery Facility (RECOUP) were conducted in the 14- by 22-Foot Subsonic Tunnel. The purposes of the tests were to verify analytically predicted plume downwash from the two existing 90-ft exhaust stacks and to test higher stacks for plume downwash. A 1/200-scale model (10-ft diameter), which consisted of stack, trees, and structures within a 1000-ft radius of the stack, was constructed. Testing simulated an atmospheric wind speed of 9 mph and stack exhaust velocity of 50 ft/s. A heated copper block, with small passageways, vaporized liquid propylene glycol, passed the vapor through the exhaust stack, and simulated smoke. A helium-nitrogen gas mixture acted as the carrier gas and, when heated by the block, simulated the positive buoyancy of the RECOUP exhaust. The model was mounted on a turntable and tested over 360° at 45° increments to determine wind direction effects. Stack heights of 90, 200, 250, and 300 ft were simulated.

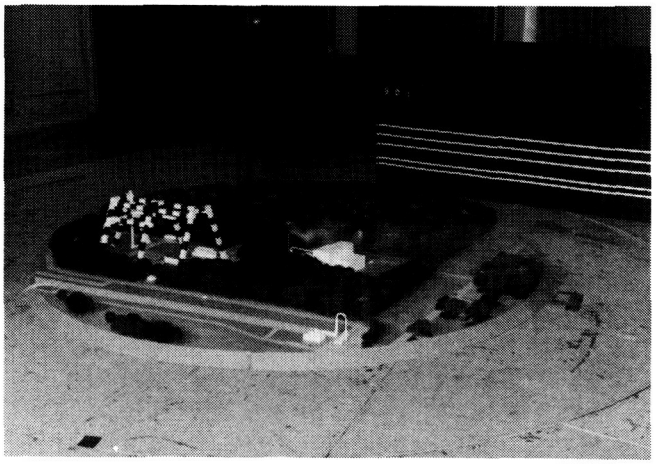

L-86-3191

1/200-scale model of RECOUP in 14- by 22-Foot Subsonic Tunnel.

The results of the tests showed significant aerodynamic building downwash with the 90-ft stack. No building downwash was observed with the higher stacks. Tests that simulated the 200- and 250-ft stacks showed plume spreading when the 240-ft-high Impact Dynamics Research Facility was upwind of the RECOUP facility. These tests and extensive plume spreading analyses were the bases for recommending a 250-ft-high exhaust stack at the RECOUP facility.
(William S. Lassiter, 4508)

8-Foot Transonic Pressure Tunnel

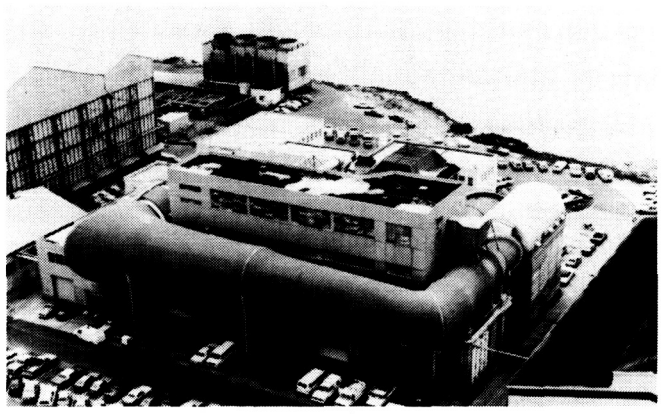

The Langley 8-Foot Transonic Pressure Tunnel (TPT) is a closed-circuit single-return variable-density continuous-flow wind tunnel. The test section walls are slotted (5 percent porosity) at the top and bottom, with solid sidewalls fitted with windows for schlieren flow visualization. In 1982, the facility was modified for flow quality improvements and reconfigured for low drag testing of a large-chord swept laminar-flow control airfoil at transonic speeds. A honeycomb and screens were permanently installed in the settling chamber to suppress the turbulence level in the test section. A contoured liner was installed on all four walls of the test section to simulate interference-free flow about an infinite yawed wing. This contoured liner produces a contraction ratio of 25:1 and covers existing floor and ceiling slots. An adjustable sonic throat is also located at the end of the test section to block upstream propagation of diffuser noise.

The combination of honeycomb, screens, and choke provides a very low disturbance level in the test region at transonic speeds. Except for the honeycomb and screens, the changes are reversible. In the current configuration, the stagnation pressure can be varied from about 0.25 to 1.25 atm up to a Mach number of less than 0.85 with the transonic slots closed by the liner. The stagnation temperature is controlled by water-cooled fins upstream of the settling chamber. Tunnel air can be dried by a dryer that uses silica gel desiccant to prevent fogging due to expansion in the high-speed nozzle.

Basic Aerodynamic Research Facility modification

The great strides that have been made in the area of computational fluid dynamics (CFD) are often limited only by the lack of understanding in the physics of flow mechanics. To gain a greater understanding of such physics, particularly at transonic speeds, it is necessary for experimental researchers to develop advanced facilities and measuring techniques. These flow diagnostic techniques include three-dimensional laser velocimetry (LV), hot-wire anemometry, and multidimensional pressure probes. Many of these techniques are still in the development stage or are very complex, and results are difficult to interpret.

Experiments have been designed which are intended to bring these flow diagnostic technologies "off the workbench" and apply them in a production mode to transonic flow fields. As a first step, the Basic Aerodynamic Research Facility, which is part of the 8-Foot TPT complex, was modified with a new 18-in. × 18-in. × 55-in. LV test section. This small wind tunnel is ideal for direct comparisons of different transonic flow diagnostic techniques. The sidewalls incorporated in the test section enable the researcher to economically configure the wind tunnel for either two- or three-dimensional models. The tunnel will also act as a test bed for pilot studies to be performed in larger wind tunnels such as the 8-Foot TPT.

Rebuilding the test section to accommodate the windows for the three-dimensional LV system required a new corner slot design. This design was implemented and the test section was calibrated over a Mach number range of 0.1 to 1.30. Preliminary fluctuating pressure measures indicated that the turbulence levels were approximately 0.08 percent at a Mach number of 0.8.

P. Calvin Stainback, 4516)

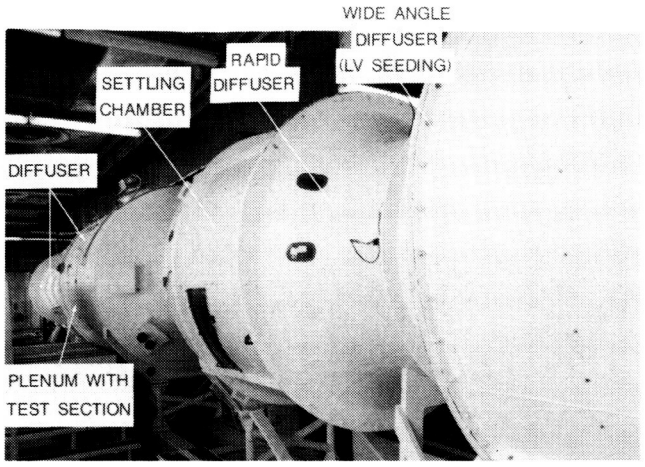

Basic Aerodynamic Research Facility exterior view, looking downstream.

Laminar-Flow Control Tests

An experiment has been designed to investigate the physical phenomena associated with laminar flow and low-profile drag on advanced swept supercritical airfoils. These tests allow the evaluation and documentation of the combination of suction control laminarization and supercritical airfoil technology at conditions typical of high-performance transports.

Performance testing with the laminar-flow control (LFC) experiment, installed in the 8-Foot TPT, has been ongoing since September 1982. Two suction concepts will be evaluated in separate wind tunnel tests for their ability to maintain laminar flow over the same airfoil geometry. One concept involves removal of the slow moving air near the surface through discretely spaced fine slots along the airfoil span. The other concept accomplishes this by suction through porous spanwise strips.

Results on the swept airfoil with discrete slots indicate that full-chord suction laminarization can be achieved with very low drag up to high speeds and high Reynolds numbers. Suction laminarization over an extensive supercritical zone was also obtained for high chord Reynolds numbers before transition moved forward. Overall slotted surface results demonstrated that LFC and supercritical airfoil technologies are compatible with low drag, depending on the extent of the suction laminarization zone applied.

The second wing of the same aerodynamic contour, but with a porous rather than slotted skin on the upper surface, has been tested. A comparison of initial results over the same Reynolds number range with those for the slotted wing indicates that considerably less laminar flow was obtained. Two possible causes for this difference are the surface skin waviness, inherent in the porous surface design, and insufficient suction. The suction surface metering system has been modified, and additional suction pumps have been installed. The wing is being reinstalled for further tests.

(Cuyler W. Brooks, 2631)

Transonic Dynamics Tunnel

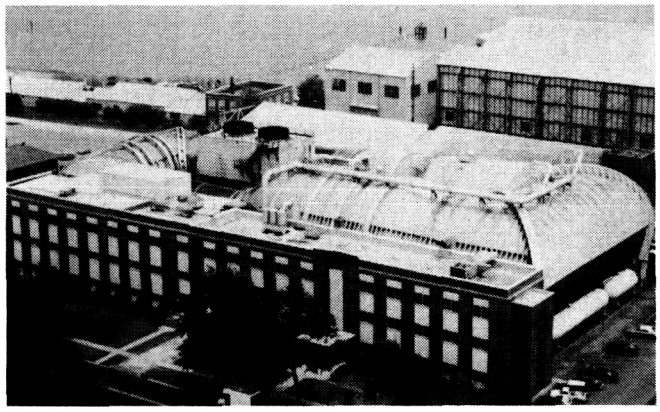

Conversion of the original Langley 19-Foot Pressure Tunnel into the Transonic Dynamics Tunnel (TDT) was begun in the late 1950's to satisfy the need for a large transonic wind tunnel dedicated specifically to work on the dynamics and aeroelastic problems associated with the development of high-speed aircraft. Since the facility became operational in 1960, it has been used almost exclusively to clear new designs for safety from flutter and buffet, to evaluate solutions to aeroelastic problems, and to research aeroelastic phenomena at transonic speeds.

The tunnel is a slotted-throat single-return closed-circuit wind tunnel with a 16-ft^2 test section. The stagnation pressure can be varied from slightly above atmospheric to near vacuum, and the Mach number can be varied from 0 to 1.2. Both test section Mach number and density are continuously controllable. The facility can use either air or Freon 12 as the test medium. Freon is usually used because it has several advantages over air as a test medium for dynamically scaled aeroelastic model testing. The tunnel has a Freon reclamation system so that the gas can be purified and reused.

The facility is equipped with many features uniquely suited to dynamic and aeroelasticity testing. These include a computerized data acquisition system especially designed to rapidly process large quantities of dynamic data, a means of rapidly reducing test section Mach number and dynamic pressure to protect models from damage when aeroelastic instabilities occur, a system of oscillating vanes to generate sinusoidal variations in tunnel flow angle for use in gust response studies, and special mount systems which enable simulation of airplane free-flight dynamic motions.

During much of 1985, the tunnel complex was modified to provide 50-percent higher test dynamic pressures in the transonic speed range. The test medium density capability was increased by 50 percent in that speed range, which allows models to be built 50 percent heavier and still meet the mass density scaling ratios required for proper modeling of full-size aircraft. For strength considerations, this becomes very significant as full-size aircraft become more structurally efficient. To provide this increased density capability, the existing fan motor was rewound to increase the power rating from 20,000 to 30,000 hp. Additional tunnel cooling capacity was provided to accommodate the increased tunnel power limit. Other major modifications included changes to the electrical power distribution system and installation of a new speed control system.

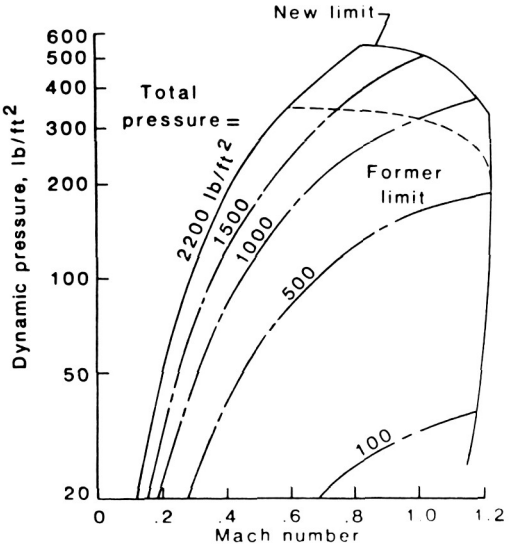

Former and present operational boundaries of TDT.

Adaptive Flutter Suppression System

A 1/4-scale, cable-mounted F-16 aeroelastic model equipped with an Adaptive Flutter Suppression System (AFSS) was tested in the TDT in a joint USAF/NASA/General Dynamics test. The model is shown in the figure along with a sketch that illustrates the AFSS operation. Accelerometers were used to measure wing motion. The AFSS digital computer was located in the control room. Computer-generated signals were sent to the flaperons to provide a continuous low-amplitude random excitation to the model. The resultant wing motion was measured, and a mathematical representation of the model was determined by using an analysis implemented on the digital computer. Using this derived mathematical model, a control law was then developed to suppress flutter.

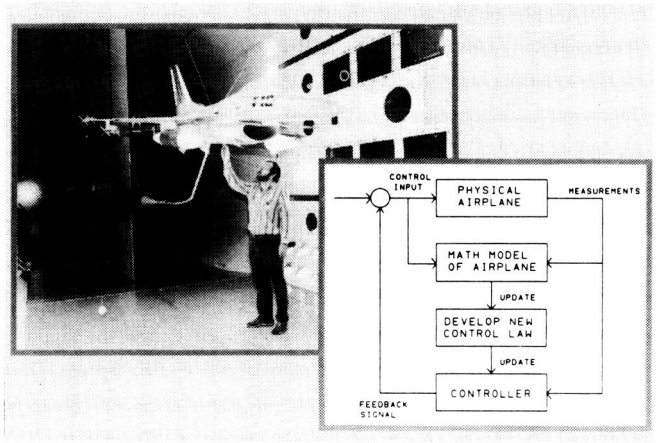

L-86-8600

Adaptive flutter suppression evaluation in TDT tests.

Flutter data were obtained with the AFSS both on and off for three flutter-critical store configurations. System-on testing began below the flutter boundary and proceeded above the system-off flutter boundary. The adaptive control law would update approximately four times per minute. Although this update rate is too slow for practical airplane applications, it was adequate for the purposes of this study. Mach number and dynamic pressure were increased until maximum test conditions were achieved or until a control law was developed which could not suppress flutter (at which time control was switched automatically to a previously tested nonadaptive control law that acted as a "flutter stopper"). The maximum demonstrated improvement in flutter dynamic pressure was approximately 22 percent.

(F. W. Cazier, Jr., and Moses G. Farmer, 2661)

Advanced Technology Wing Model

Utilizing wing flexibility to provide control power is a technological concept that would be a useful capability for an advanced high-performance fighter vehicle. This concept would use multiple active control surfaces to provide variation in the wing shape for roll and maneuver load control. The objective of the present advanced technology wing tests was to obtain a data base of measured static aerodynamic forces and moments due to multiple control surface deflections. A 1/6-scale, full-span configuration, designed and built by Rockwell International Corporation, was tested in the TDT as part of a cooperative program with the Air Force Wright-Aeronautical Laboratories. This model was mounted to a tunnel sting arrangement that allowed the complete model freedom to roll about an axis near the sting centerline. Model loads were measured using a six-component balance. A hydraulic brake located on the sting at the rear of the model was used to prevent roll motion throughout most of these early tests. In the figure, the complete model system is shown mounted in the wind tunnel. The wings of the model were aeroelastically tailored to obtain the desired wing structural stiffness properties. The model had eight large control surfaces, two each on the leading and trailing edges of both wing panels.

Data for calculating roll control effectiveness of each control surface were obtained by moving the surfaces through their allowable deflection ranges at various tunnel conditions. The roll moment versus dynamic pressure (shown in the figure) demonstrates the roll power effectiveness for several of the control surfaces tested. In addition, model loads and actuator frequency response data for various combinations of control surface deflections and model angle of attack were measured for several tunnel conditions. These data were obtained with the

model hydraulic roll brake on to prevent roll motion. The model was also flutter cleared throughout the test operating envelope. At the conclusion of these tests, the model hydraulic roll brake was released, and the model roll capability was thoroughly checked out with the use of these data. Control laws will be developed by NASA and Rockwell International Corporation and implemented on digital computers. Experimental evaluation of these roll control concepts will be made in a second TDT entry, which is scheduled for calendar year 1987.

(Maynard C. Sandford and Stanley R. Cole, 2661)

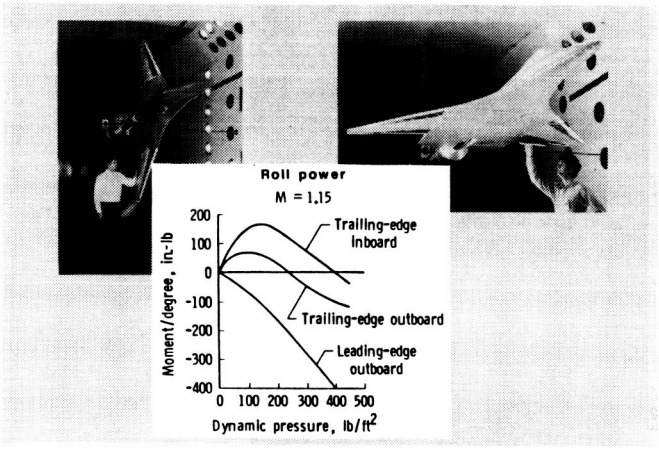

Active flexible wing model tested in TDT.

Active Control of DAST ARW-2 Wing Semispan

In 1983 tests were made in the TDT with the DAST (drones for aerodynamic and structural testing) ARW-2 (aeroelastic research wing number 2) right semispan cantilevered to the tunnel wall. During flutter clearance testing large-amplitude lowly damped motion occurred in the transonic region and led, by extrapolation of a measure of the damping estimates, to the prediction of an instability near a Mach number of 0.90 for a range of dynamic pressures.

A second series of tests of the right semispan were conducted in the TDT in January 1986. One of the objectives of these tests was to use an active control law to add damping in the critical mode and thereby suppress the apparent instability. Constrained optimization techniques were employed to design a control law that uses compensated acceleration feedback to drive an outboard trailing-edge control surface. The model of the plant used in the control law design was based solely upon a limited amount of forced response data available from the previous and second series of tests.

Results from these second tests have shown that, although the damping in the critical mode becomes quite small and reaches a minimum near Mach 0.92, there is no instability with the control law off. As shown in the figure, the control law added significant damping in the critical mode for all test conditions through a Mach number of 0.90. The control law also added significant damping at a Mach number of 0.92 for the lower dynamic pressure test condition ($Q = 151$ lb/ft^2) but not for the higher dynamic pressure test condition ($Q = 323$ lb/ft^2). Two conditions contributed to the loss of effectiveness at a Mach number of 0.92 at the higher dynamic pressure test condition. The first condition was that the flow over the wing became separated and turbulent in the region of the control surface as Mach number increased; the second condition was that the control law was scheduled to increase the frequency at which damping was added as a function of both dynamic pressure and Mach number. Although the frequency of the wing oscillation initially increased with Mach number and dynamic pressure, it later

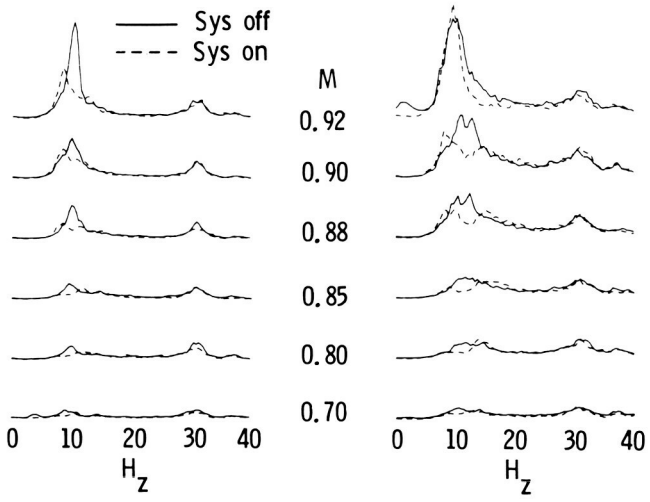

ARW-2 accelerometer peak hold responses.

decreased to approximately 10 Hz at $M = 0.92$ and $Q = 323$ lb/ft^2, which was considerably below the 12.28-Hz frequency of peak effort for the control law at this test condition.

(William M. Adams, Jr., 3744)

Unanticipated Flutter Characteristics of New Composite A-6 Wing

A 1/4-size dynamically scaled aeroelastic model of the A-6 Intruder airplane was tested in the TDT to determine the flutter characteristics of the wing with and without external stores. The store configurations to be studied were selected from those expected to be most commonly used and to have the most impact on flutter. The semispan model mounted in the wind tunnel is shown in the figure. The aerodynamic effects of the fuselage on the wing were accounted for by using a rigid fuselage fairing. The model wing was attached to the wall through a specially designed fixture that simulated the wing-fuselage attachment flexibility.

A total of eight configurations were tested at transonic Mach numbers. The tests of the clean wing, both with and without pylons, showed that the flutter characteristics of the basic wing were satisfactory. The flutter boundary was well outside the airplane planned operating envelope. The flutter characteristics of some of the key external store configurations were not satisfactory and were quite different from what had been predicted by analysis prior to the test. Some illustrative flutter results are shown in the figure for a configuration with a 300-gal fuel tank mounted on each of the two inboard pylons. Also included is the calculated flutter boundary. Aerodynamic forces on the tanks were not included in this analysis because they were thought to have a second-order effect. The experimental data show an almost constant dynamic pressure flutter boundary, whereas the analytical data show a typical transonic "bucket-like" boundary. To aid in further understanding these experimental results, flutter tests were conducted with the large fuel tanks replaced by "pencil" stores that were thin streamlined bodies having the same inertial properties as the fuel tanks. As shown in the figure, these data have a Mach number effect as predicted analytically. These results indicate that store unsteady aerodynamics play an important role in the flutter mechanism for the new A-6 wing design.

(Stanley R. Cole and Jose A. Rivera, 2661)

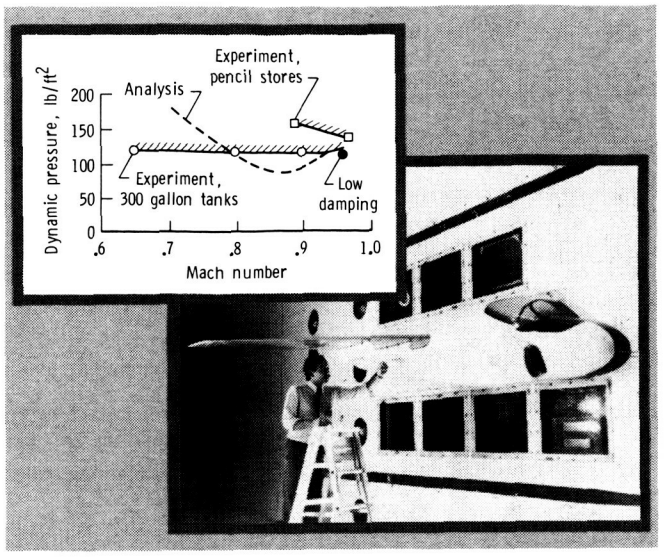

L-86-3108

Uncanted flutter characteristics of new composite A-6 wing identified in TDT tests.

16-Foot Transonic Tunnel

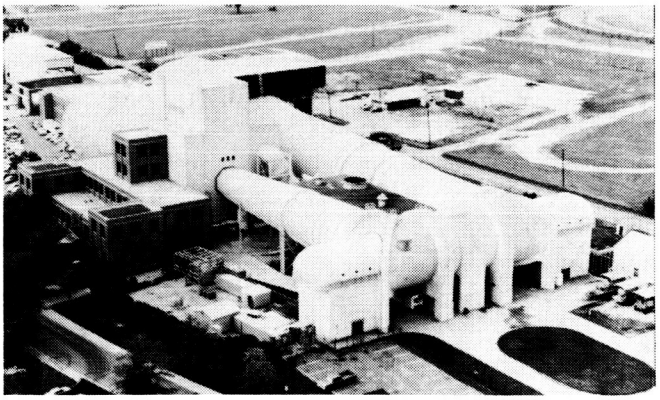

The Langley 16-Foot Transonic Tunnel is a closed-circuit single-return continuous-flow atmospheric tunnel. Speeds up to Mach 1.05 are obtained with the tunnel main-drive fans, and speeds from Mach 1.05 up to Mach 1.30 are obtained with a combination of main-drive and test section plenum suction. The slotted octagonal test section measures 15.5 ft across the flats. The tunnel is equipped with an air exchanger with adjustable intake and exit vanes to provide some temperature control. This facility has a main drive 60,000 horsepower, and a 36,000-horsepower compressor provides test section plenum suction.

This tunnel is used for force, moment, pressure, flow visualization, and propulsion-airframe integration studies. Model mounting consists of sting, sting-strut, and fixed-strut arrangements. Propulsion simulation studies are made with dry, cold, high-pressure air.

Thrust Vectoring Control From Canted Nozzles

Significant advantages in air combat are gained by the ability of the aircraft to maneuver at angles of attack greater than those of current fighter aircraft. The angle-of-attack envelope of current fighters, however, is limited by a combination of degraded stability characteristics and inadequate control effectiveness. One promising means of providing large control moments that are not dependent on angle of attack and dynamic pressures, as are aerodynamic controls, is vectoring the engine exhaust. One concept that can provide control moments in both the pitch and yaw planes is canting the nozzles. With the nozzles canted, pitching moment is obtained by symmetric nozzle pitch vectoring whereas yawing moment is produced from asymmetric pitch vectoring. To explore the potential of this concept, tests were recently conducted on a twin-engine general research model with two-dimensional (2-D) convergent-divergent (C-D) nozzles at Mach numbers from 0.20 to 1.20, angles of attack up to 27°, and nozzle pressure ratios up to 7.0. Nozzle cant angle and pitch vector angle were also varied.

The results of this investigation indicate that significant levels of combined pitch and yaw control moments were generated with the canted nozzles. The increment in control moment that resulted from pitch or yaw vectoring remained essentially

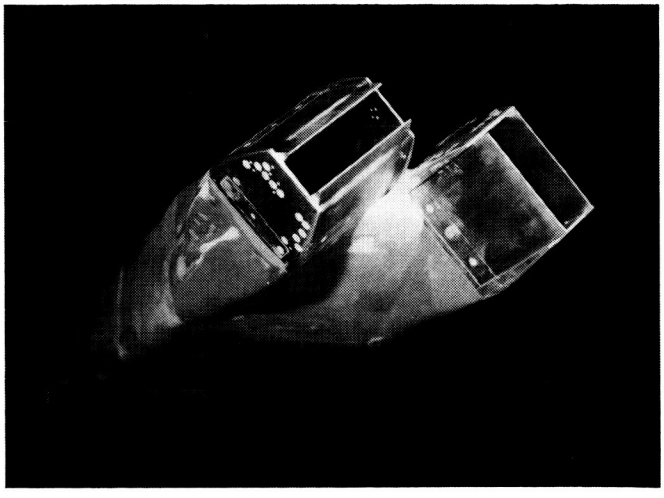

L-86-805

Configuration with canted nozzles.

constant over the entire angle-of-attack range for all Mach numbers tested. No cross-coupling of control forces and moments was found from combined pitch/yaw vectoring. Longitudinal and directional control power from thrust vectoring was greater than that provided by comparable aerodynamic control effectors at low speeds or high angles of attack.

(Francis J. Capone, 2674)

National Transonic Facility

The National Transonic Facility (NTF) is a cryogenic fan-drive transonic wind tunnel designed to provide full-scale Reynolds number simulation in the critical flight regions of most current and planned aircraft. It can operate at Mach numbers from 0.2 to 1.2, stagnation pressures from 1 to 9 atm, and stagnation temperatures from 340 to 80 K. The maximum Reynolds number capability is 120×10^6 at a Mach number of 1.0, based on a reference length of 0.25 m.

Construction of the NTF was completed in September 1982. The tunnel was declared operational in August 1984, and aerodynamic calibration and research and development testing were begun in 1984.

The unique transonic capabilities of the NTF have been used primarily for highly important military programs during the past year. One of these programs involved the study of Reynolds number effects in the wake of a submarine.

Optimization of model instrumentation and wiring

The NTF has been used to evaluate on-board model instrumentation of the Pathfinder I model, which is an advanced transport configuration with a high-aspect-ratio supercritical wing. The initial test entry of this model in the NTF (January 1985) evaluated on-board model instrumentation which included a six-component strain-gauge force balance, six 32-port electronically scanned pressure modules, a three-axis angle-of-attack accelerometer package, an electrolytic bubble, and type-T thermocouples. Most of the instrumentation is located in the nose of the fuselage, and the associated wiring is routed aft across the force balance. Analysis of the data from a second entry in the NTF (November 1985) indicated that at cryogenic temperatures the wires produced significant shifts in axial force measurements.

A series of tests in the cryogenic chamber at the NTF proved that the thickness of the insulation on the wires was primarily responsible for the axial force shifts. By reducing the number, size, and insulation thickness of the wires, the wire bundle was reduced in size by over 50 percent. Force data from a subsequent entry in the NTF (November 1986) confirmed that the new wire bundle produced negligible axial force shifts at cryogenic temperatures.

(Peter F. Jacobs, 2701)

High Reynolds Number Wake Measurements on Submarine Model

A research program sponsored by NASA, the David W. Taylor Naval Ship Research and Development Center, and the Office of Naval Research is being conducted in the NTF to investigate Reynolds number Rn effects over a large range on the complicated flow field around the stern of a submarine model. To extend the current data base for defining the Reynolds number scaling effects, a 20-ft-long submarine model was tested at subsonic speeds to a Reynolds number of 50×10^6 per foot, as shown in the figure. Near the stern of the model, five-hole pitot pressure probes and triaxial hot-film probes were located at 10 different radii from the hull centerline to the maximum hull radius. These probes were rotated 360°, in steps of 1.8°, to map the wake

flow. Additionally, surface pressure and boundary-layer measurements on the hull were obtained.

The data presented are the circumferential mean axial velocity U at each probe distance from the surface r. These preliminary data indicate that the mean velocity flows are significantly affected by Reynolds number.

(Stuart G. Flechner and John B. Peterson, Jr., 2701)

L-86-9456

Model of submarine in NTF.

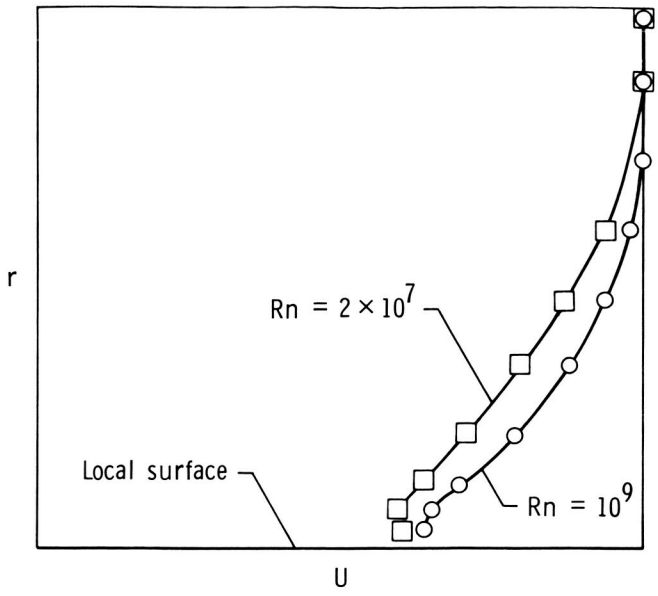

Reynolds number effects on mean axial velocity in wake.

0.3-Meter Transonic Cryogenic Tunnel

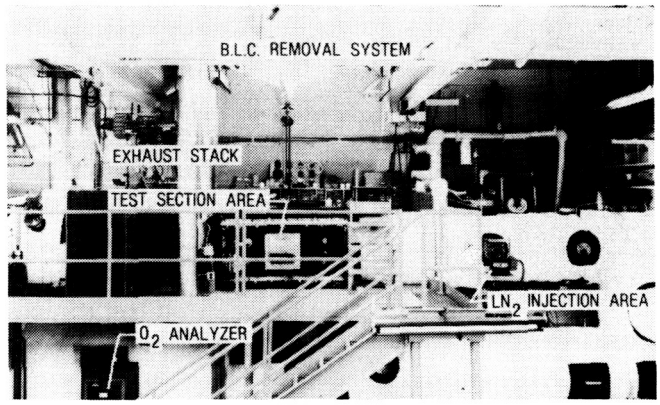

The Langley 0.3-Meter Transonic Cryogenic Tunnel (TCT) is a continuous-flow fan-driven transonic tunnel that uses nitrogen gas as a test medium. It is capable of Mach numbers up to approximately 1.0, stagnation pressures up to 6 atm, and stagnation temperatures from 340 to approximately 80 K. The tunnel has been designed to permit different test sections to be installed in the circuit.

The facility was placed in operation in 1973 as a three-dimensional pilot tunnel to demonstrate the cryogenic wind tunnel concept at transonic speeds. The original test section was octagonal and was designed with a manually driven sting-type model support system. The successful demonstration of the cryogenic concept in the 0.3-Meter TCT played a major role in the decision to build the National Transonic Facility. In 1975, the three-dimensional test section was replaced with an 8- by 24-in. two-dimensional test section with slotted top and bottom walls. The two-dimensional test section has motorized model support turntables and a traversing wake survey probe, both of which are computer controlled. At the maximum test condition with a 6-in. model, a chord Reynolds number of 50×10^6 is possible. In 1985, the 8- by 24-in. test section was replaced with a 13- by 13-in. adaptive wall test section.

Adaptive wall test section

Shakedown tests with the new adaptive wall test section were completed in late 1986. The test section is 55.8 in. long and 13 by 13 in. in cross section at the entrance. All four walls are solid, and the top and bottom walls are flexible. During a typical test, the flexible walls can be computer directed and driven to streamline shapes above and below the model to eliminate or drastically reduce the wall interference. In addition to providing interference-free results, the elimination of wall effects enables the testing of larger chord airfoils, thereby increasing the test Reynolds number capability.

The airfoil mounting system, as shown in the figure, features a turntable system that is

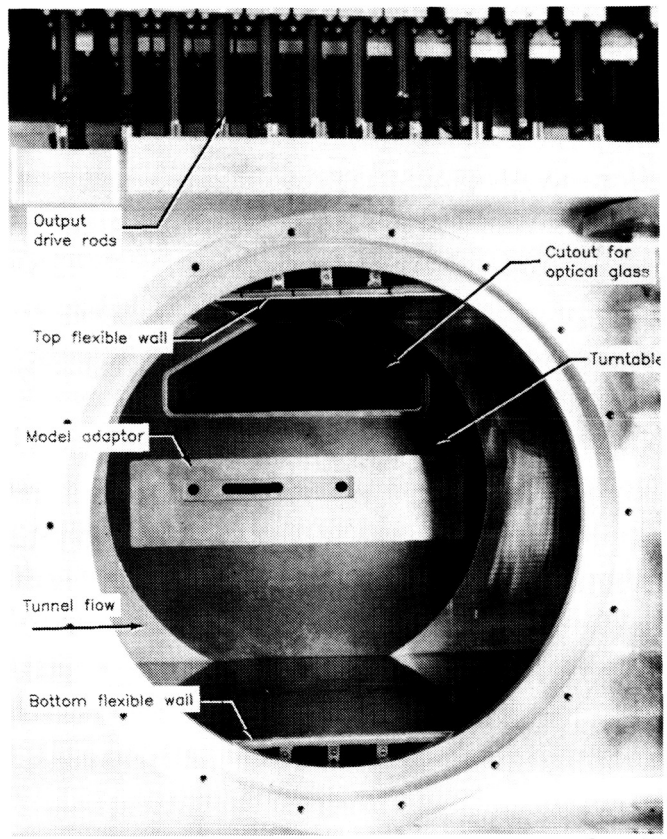

L-86-07

View of test section with pressure wall and nearside turntable removed.

centered 30.7 in. downstream from the test section entrance. Airfoils ranging in chord from 6 to 13 in. have been tested in the unique test section with very promising results. For instance, interference-free, high subsonic results have been obtained at high lifts and chord Reynolds numbers of 70×10^6. These results have indicated the potential for achieving airfoil results at Reynolds numbers up to 100×10^6. Transonic interference-free results have been obtained with a smaller 6-in. airfoil at lift coefficients up to about 1.5. In general, the airfoil investigations conducted thus far have indicated that the 0.3-Meter TCT provides interference-free results at about twice the lift and Reynolds number levels of any other known adaptive-wall test capability.

(Raymond E. Mineck, 4385)

High Reynolds Number Wall Interference

A cooperative program with the Canadian National Aeronautical Establishment (NAE) was initiated in 1984 to develop the technology to correct or eliminate wall interference in transonic two-dimensional airfoil tests. The NAE designed and fabricated a model with the CAST-10 airfoil section and a 9-in. chord. The model was tested in the NAE High Reynolds Number Two-Dimensional Test Facility. The NAE tunnel height to the model chord ratio was 6.7. Data were corrected for top and bottom wall effects using the method by Mokry and Ohman (J. Aircraft, vol. 17, 1980).

Following the NAE tests, the model was installed in the adaptive wall test section of the 0.3-Meter TCT and tested at Mach numbers from 0.3 to 0.8 and chord Reynolds numbers from 6×10^6 to 70×10^6. The tunnel height to the model chord ratio was 1.4. No corrections were applied to the 0.3-Meter TCT data thereby placing a total dependence of the elimination of the wall interference effects on the wall adaptation process.

A comparison of the results from both tunnels is presented in the figure. In this figure, C_n represents normal force coefficient, C_d section drag coefficient, α angle of attack, R Reynolds number, and M Mach number. Results were based on a Mach number of 0.765 and a Reynolds number of 20×10^6. Lift curve slopes are in excellent agreement up to near-stall conditions. The small shift between the curves could be attributable to slight model installation inaccuracies. The drag polars are in reasonable agreement. These results indicate that correction techniques applied to the NAE results and the wall adaptation technique used to position the flexible walls both do a reasonable job in accounting for the interference from the top and bottom tunnel walls.

(Raymond E. Mineck, 4385)

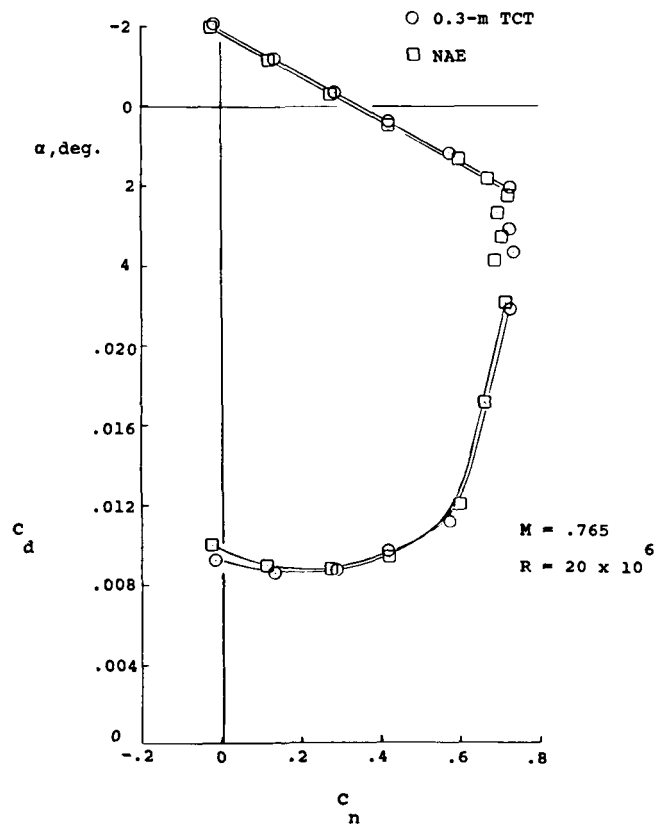

Comparison of results from 0.3-Meter TCT and NAE.

Unitary Plan Wind Tunnel

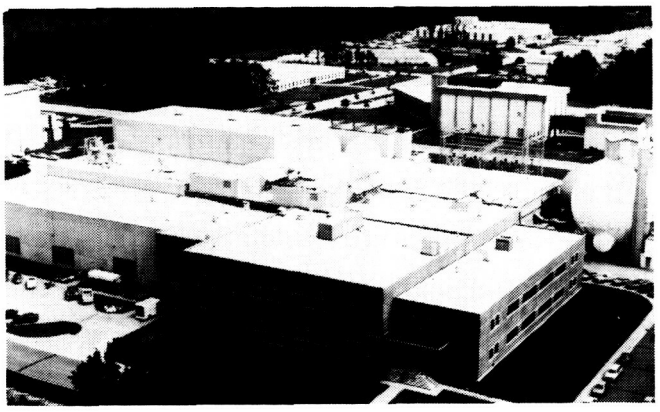

Immediately following World War II, the need for wind tunnel equipment to develop advanced airplanes and missiles was recognized. The military and the National Advisory Committee for Aeronautics (NACA) developed a plan for a series of facilities which was approved by the U.S. Congress in the Unitary Wind Tunnel Plan Act of 1949. This plan included five wind tunnel facilities, three at NACA laboratories and two at the Arnold Engineering Development Center. The Langley Unitary Plan Wind Tunnel (UPWT) was among the three built by NACA. The UPWT is a closed-circuit continuous-flow variable-density tunnel with two 4- by 4- by 7-ft test sections. The low-range test section has a design Mach number range of 1.5 to 2.9, and the high-range section Mach number varies from 2.3 to 4.6. The tunnel has sliding-block-type nozzles that allow continuous variation in Mach number while on-line. The maximum Reynolds number per foot varies from 6×10^6 to 11×10^6 depending on Mach number. The tunnel is used for force and moment, pressure distribution, jet effects, dynamic stability, and heat transfer studies. Flow visualization data, which are available in both test sections, include schlieren, oil flow, and vapor screen.

Reaction Control System Plume/Flow Field Interaction

The first entry flight of the Space Shuttle orbiter *Columbia* revealed that the effect of the interaction between the reaction control system (RCS) rocket plumes and the leeside flow field on the rolling moment of the orbiter was greatly overpredicted. As shown in the figure, there was a large disagreement between the preflight wind tunnel data and the postflight curve. In this figure, $\Delta C_{l,JI}$ represents rolling-moment interaction coefficients, $\dot{m}_j/\dot{m}_\infty$ Mach number ratio, $\dot{m}_j$ Mach number of jet, and $\dot{m}_\infty$ free-stream or flight Mach number. The discrepancy resulted in noticeable excursions in the vehicle attitudes during the first navigation bank maneuver at high altitude. Because of this, an RCS plume flow field interaction technology study has been initiated. The purpose of this study is to establish improved ground-to-flight test correlations and flight prediction techniques applicable to future space vehicles. The Space Shuttle orbiter was chosen to be modeled because of the opportunity to obtain ground and flight data on the same configuration.

An 0.0125-scale model was tested in the UPWT at Mach 2.5, 3.5, and 4.5, and in the Arnold Engineering Development Center (AEDC) Tunnel C at Mach 10. Surface pressure measurements were obtained on the upper surface of the wing, fuselage side, and vertical tail with the model RCS on and off for various test conditions. Preliminary analysis of the tests at Mach 10 indicates that the new wind tunnel data (which are classified) are in better agreement than the original data with flight results taken from on-board inertial measurements. The differences in surface pressures between RCS on and RCS off were integrated over the affected areas to determine the moment increments resulting from the RCS plume/flow field interaction. These data are the first wind tunnel measurements that demonstrate the response of the wing upper surface pressures to the plumes from the RCS yaw thrusters. Preliminary assessment indicates that for a given momentum ratio, the interactions are

insensitive to plume shape or number of thrusters fired. A parallel flight experimental program has been proposed in which additional pressure sensors will be installed on the wing, fuselage, and vertical tail surfaces of *Columbia*. The wind tunnel and flight measurements will be correlated to provide applicable ground-to-flight extrapolation methods. **(William I. Scallion, 3984)**

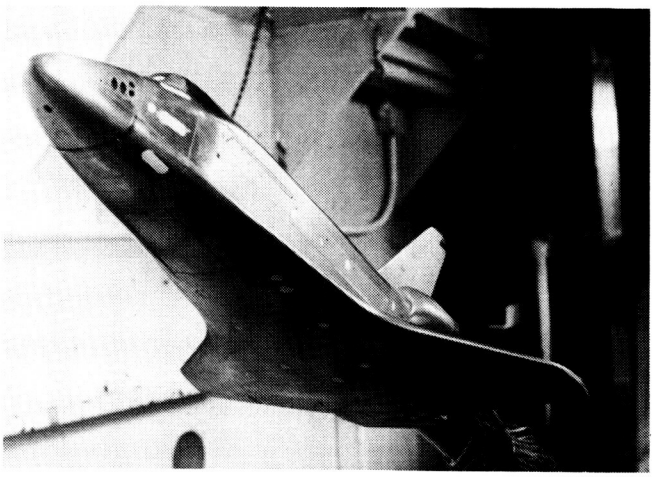

RCS study model installed for tests in AEDC Tunnel C.

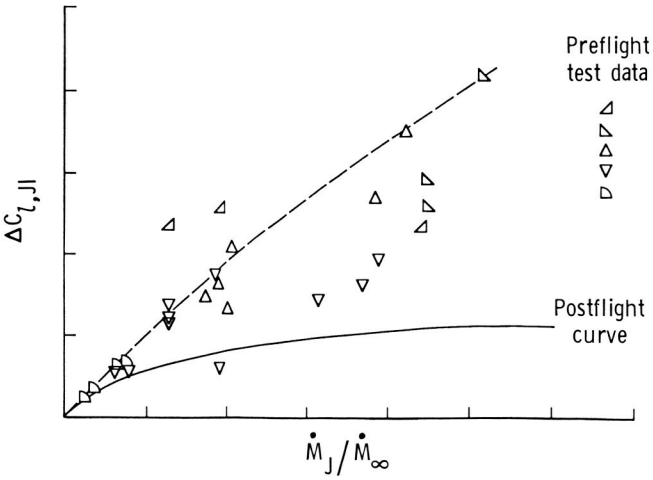

Predicted and postflight rolling-moment interaction coefficients as function of Mach number ratio.

Strake Design Procedure for Low Lift and Supersonic Speeds

The latest generation of American fighter aircraft (such as the F-16's and F-18's) employs strakes to improve maneuver performance at transonic speeds. The next generation of fighter aircraft may have an efficient supersonic cruise requirement in addition to a transonic maneuver capability equivalent to today's standards. An accurate method of designing and/or analyzing strakes for supersonic cruise is therefore required.

A nonlinear, full-potential solver (NCOREL) was used to design a highly swept strake in the presence of a large fighter-type forebody including a canopy. The design procedure relied upon a parametric evaluation of strake camber and thickness to yield a specified target pressure distribution for attached flow at a Mach number of 1.80 and an angle of attack of 4° The target pressure distribution was characterized by the absence of the large flow gradients that are associated with flow separation.

An experimental validation of the strake design procedure was carried out in the UPWT in April 1986. The wind tunnel model was instrumented to obtain force, moment, and surface pressure data. Additionally, oil-flow and vapor-screen data were obtained during the tunnel entry. A cambered strake was tested to obtain a validation of the computational procedure, and an uncambered strake was tested for comparison purposes. The test

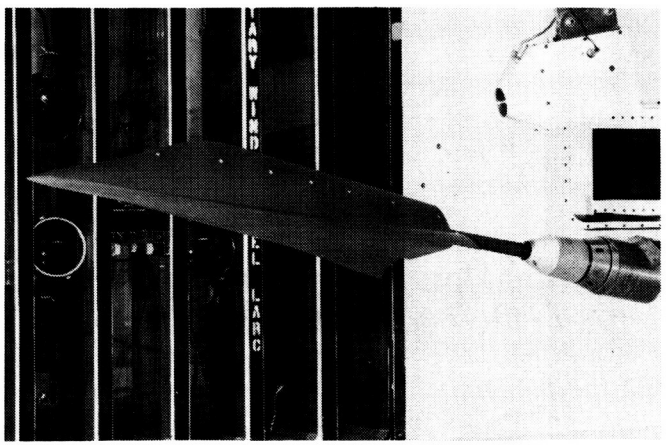

L-86-3885

Generic fighter forebody with cambered strake mounted in UPWT.

Mach numbers were 1.6, 1.8, and 2.0 for a range of angle of attack and sideslip.

A comparison of the experimentally obtained surface-pressure data on the strake with the theoretically predicted pressures showed that the specified target pressure distribution was achieved at the design conditions. Vapor-screen and oil-flow data provided further verification that an attached flow field was obtained on the strake. Additionally, an extensive data base was developed for Euler and Navier-Stokes code validation at high angle of attack and for sideslip conditions.

(James L. Pittman, 4009)

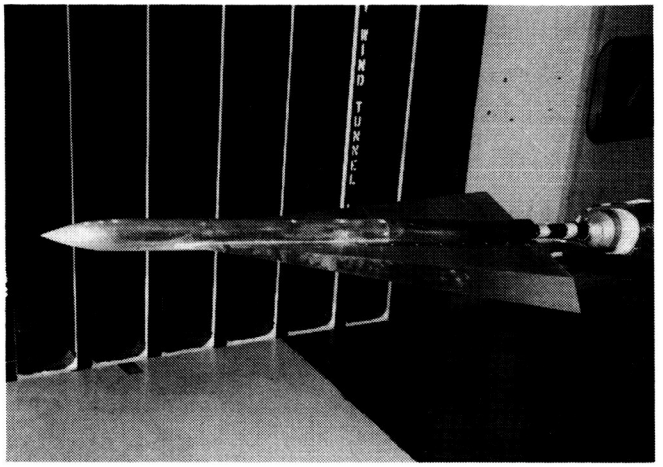

L-86-4376

75° *sweep delta wing with ogive-cylinder forebody.*

Body Effects on Aerodynamic Characteristics of 75° Delta Wing Leading-Edge Flap

A wind tunnel investigation was conducted to determine the effects of a forebody on the aerodynamic characteristics of a 75° sweep delta wing with leading-edge flaps. The forebody has a cylindrical cross section of constant diameter aft of the nose. The wing has a sharp leading edge and a flat upper surface. The constant percent span flaps were tested at streamwise deflections of 0°, 5°, 10°, and 15°.

The tests were conducted at Mach numbers of 1.5, 1.7, 2.0, 2.4, and 2.8 for Reynolds numbers of 10^6 and 2×10^6 per foot. Angles of attack up to 22° and angles of sideslip up to 8° were tested. Force data, upper-surface pressures, and flow visualization pictures were obtained. The tests were completed in May 1986.

Test results have been compared with those from previous tests without the forebody. The upper-surface pressures indicate that the primary effect of the body is to push the leading-edge vortex system closer to the leading edge and increase its strength slightly; however, these effects have very little effect on the overall performance of the wing.

(Peter F. Covell, 4008)

Hypersonic Facilities Complex

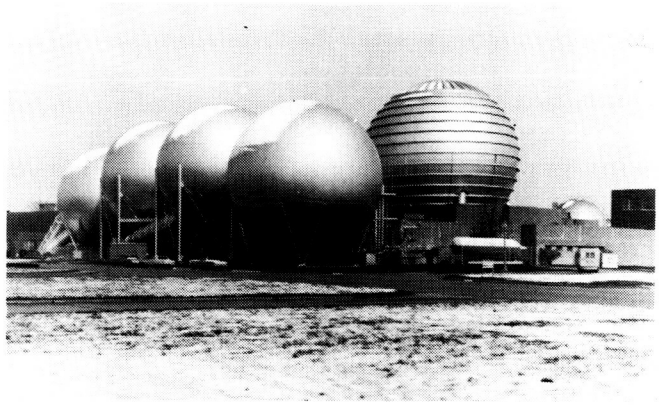

The Hypersonic Facilities Complex consists of several hypersonic wind tunnels located at four Langley sites. They are considered as a complex because these facilities represent a major unique national resource for wind tunnel testing. The complex currently includes the Hypersonic CF_4 (tetrafluoromethane) Tunnel ($M = 6$), the Mach 6 High Reynolds Number Tunnel, the 20-Inch Mach 6 Tunnel, the Mach 8 Variable-Density Tunnel, the 31-Inch Mach 10 Tunnel, the Hypersonic Nitrogen Tunnel ($M = 17$), and the Hypersonic Helium Tunnel and its open jet leg ($M = 20$). These facilities are used to study the aerodynamic and aerothermodynamic phenomena associated with the development of advanced space transportation systems, including future orbital-transfer and launch vehicles; to support the development of advanced military spacecraft capability; to support the development of future planetary entry probes; to support the development of hypersonic missiles and transports; to perform basic fluid mechanics studies, to establish data bases for verification of computer codes, and to develop measurement and testing techniques.

This complex of facilities provides an unparalleled capability at a single installation to study the effects of Mach number, Reynolds number, test gas, and viscous interactions on the hypersonic characteristics of aerospace vehicles. Approximately half the current testing in these facilities is classified, thus restricting the amount and content of test results that can be reported in the open literature.

20-INCH M-6 TUNNEL

$M_\infty = 6$ AIR R_∞ 0.7-9.0x10^6

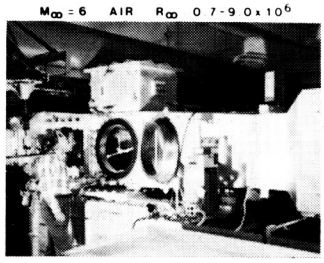

M-8 VAR.-DENS. TUNNEL

$M_\infty = 8$ AIR $R_\infty = 0.1\text{-}10.7 \times 10^6$

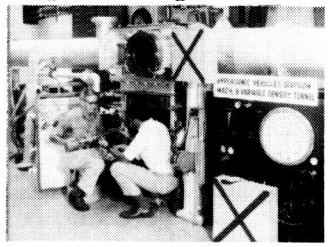

31-INCH M-10 TUNNEL

$M_\infty = 10$ AIR $R_\infty = 0.4\text{-}2.4 \times 10^6$

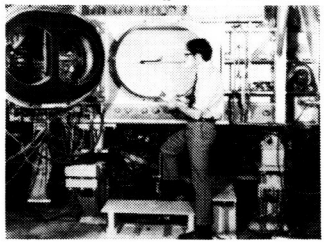

NITROGEN TUNNEL

$M_\infty = 17$ N_2 $R_\infty = 0.35 \times 10^6$

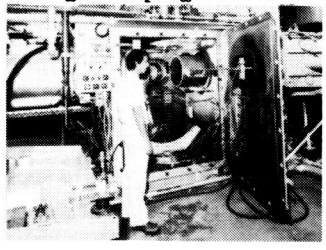

CF_4 TUNNEL

$M_\infty = 6$ CF_4 $R_\infty = 0.25\text{-}0.55 \times 10^6$

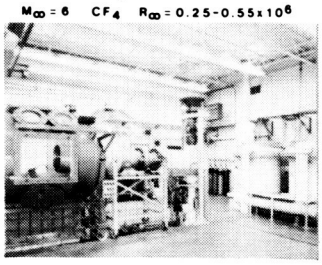

HIGH R_∞ M-6 TUNNEL

$M_\infty = 6$ AIR $R_\infty = 0.8\text{-}42.0 \times 10^6$

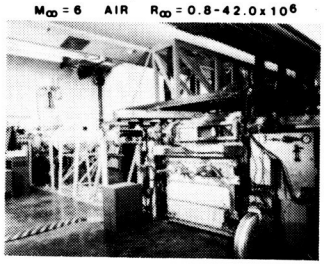

HELIUM TUNNEL

$M_\infty = 19\text{-}21.6$ He $R_\infty = 3.5\text{-}12.5 \times 10^6$

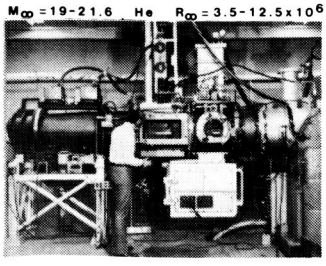

OPEN JET LEG-HE TUNNEL

$M_\infty = 20$ He $R_\infty = 6.0 \times 10^6$

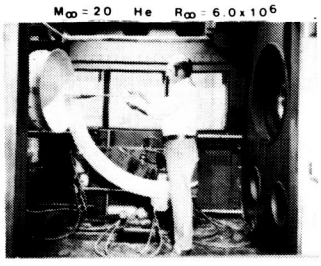

Experimental Investigation of Transatmospheric Vehicle Concept

An experimental aerodynamic study of a transatmospheric vehicle (TAV) generic concept has been performed across the speed range from subsonic ($M = 0.6$) to hypersonic ($M = 20$) speeds. The concept tested was a winged cone configuration representative of one type of TAV design having atmospheric flight capability. The objectives of this study were to: (1) identify potential aerodynamic/aerothermodynamic problem areas for this type of configuration, and (2) establish a timely experimental data base for use in future TAV development and in comparisons with engineering code predictions (such as those obtained with the Hypersonic Arbitrary Body Program). Force-and-moment tests were conducted at the Langley Research Center in the diffuser flow apparatus ($0.6 \leq M \leq 0.95$), the Unitary Plan Wind Tunnel ($1.5 \leq M \leq 4.6$), the 20-Inch Mach 6 Tunnel, the 31-Inch Mach 10 Tunnel, and the Hypersonic Helium Tunnel ($M = 20$).

A steep rise in transonic drag was observed for the configuration and was accompanied by an aftward center of pressure shift of about 10 percent of the length. At hypersonic conditions, the experimental results were in agreement with predictions obtained using the tangent-cone option of the Hypersonic Arbitrary Body Program.

(W. Pelham Phillips, 3984)

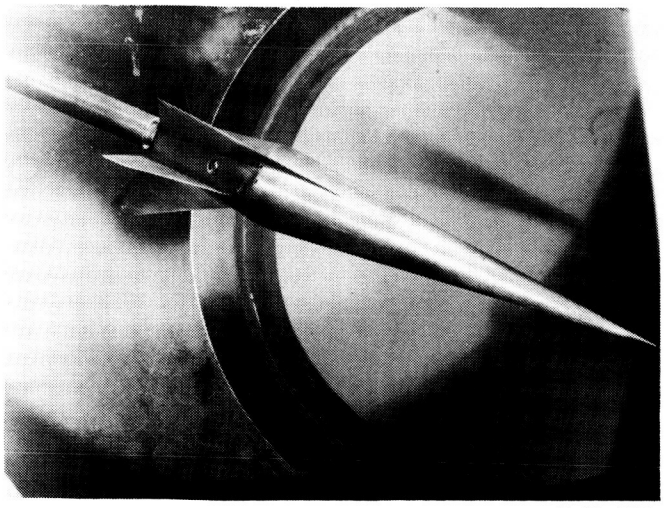

L-86-4898

Transatmospheric model in 20-Inch Mach 6 Tunnel.

AFE Code Validation Study in Hypersonic Continuum Flow

An optimum shape was selected for the proposed Aeroassist Flight Experiment (AFE) vehicle based on results from an earlier parametric study. Determination of the actual flight conditions for the AFE will rely heavily on recently developed computer codes, since ground-based hypersonic facilities do not provide the capability to duplicate and simulate the high-velocity, high-altitude (low-density) trajectory. These facilities, however, can be used to validate recently developed codes over a wide range of hypersonic, continuum-flow conditions.

For code validation studies, the wind tunnel models conform to the numerical model of the computer code, since the inputs for fabrication of the models on numerically operated machines were obtained from the code. Five high-fidelity AFE models were constructed to measure detailed pressure and heat-transfer distributions, aerodynamic forces and moments, shock shapes, thermal maps, and surface-flow directions. Tests in five different hypersonic wind tunnels are under way and include the simulation of the high normal-shock density ratio of a real (dissociated) gas such as occurs in flight. The test matrix includes an angle-of-attack range from $-10°$ to $10°$ at Mach numbers of 6, 10, 18, and 22. Preliminary findings reveal that the aerodynamic characteristics and pressure distributions for this blunt configuration are essentially independent of Mach number and Reynolds number but exhibit a significant dependence on density ratio.

(William L. Wells, 3984)

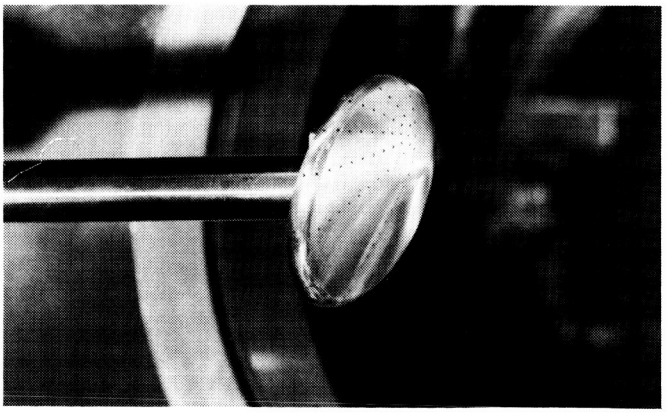

L-86-7123

AFE high-fidelity wind tunnel model. Pressure distribution shown in 20-Inch Mach 6 Tunnel.

Hypersonic Missile Trim Test

An experimental and theoretical study of the maximum trim capability of a Mach 6, surface-launched, airbreathing missile has been conducted in the 20-Inch Mach 6 Tunnel. Minimum turn radius, which is dependent on maximum lift coefficient, was the parameter of primary interest. Because the missile must also be trimmed at angles of attack for maximum lift, the center-of-gravity positions that allowed trim at maximum lift were also of interest.

Force, moment, and flow visualization data were obtained using an 0.0619-scale model of a Johns Hopkins University/Applied Physics Laboratory missile configuration. Two nose geometries were employed; one had six closed-off inlets representing unstarted inlets at high angles of attack, and the other was a simple generic 12°/6° biconic nose. The all-movable tail fins could be positioned in the + or × configuration. Fin size was limited by the size of the launch system box.

Test results show that maximum lift coefficient could not be accurately predicted except when the configuration was in the generic nose +-fin configuration. In addition, pitch-up occurred at high angles of attack on the ×-fin configurations due to local "choking" between the bottom (windward) fins and "shielding" of the top (leeward) fins.

(Edward R. Hartman, 4012 and Patrick J. Johnston, 4004)

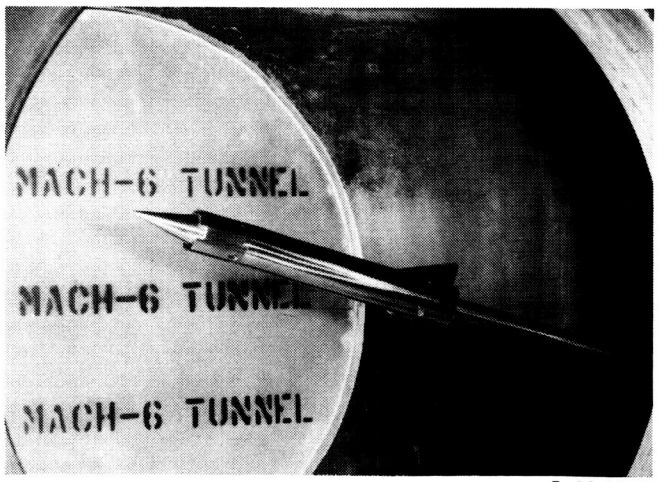

L-86-3618

Inlet nose +-fin configuration model installed in 20-Inch Mach 6 Tunnel.

Scramjet Test Complex

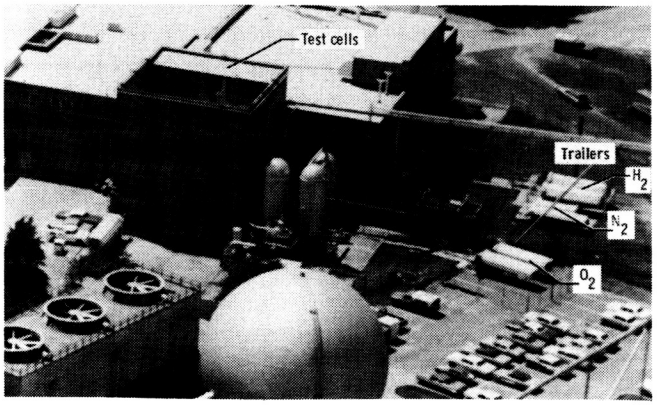

After an almost 15-year lull in interest for hypersonic flight, there is again a strong emphasis on the potential for a number of applications. These applications include the Aero-Space Plane, or transatmospheric vehicle, which would be able to take off from a conventional runway and fly to orbit, as well as a variety of hypersonic airplane concepts for military reconnaissance, strike, or semiglobal transport. Langley has maintained a research team that has been working on basic hypersonics continuously throughout the last several decades. Facilities that played a key role at Langley in developing the present Shuttle configuration have been applied to a wide variety of other aerospace vehicles. Langley, the lead Center in defining Shuttle II, has been the only research organization in the nation to continuously maintain a viable effort in hydrogen-fueled supersonic combustion ramjet propulsion since the 1960's. Ground tests of subscale engines conducted in the Scramjet Test Complex have demonstrated levels of net thrust sufficient to accelerate at Mach 4 and to cruise an airplane at speeds up to Mach 7 and beyond. These results are entirely consistent with the projection of attractive performance up to much higher speeds, even approaching orbital velocity.

SMALL SCALE COMBUSTOR TESTS

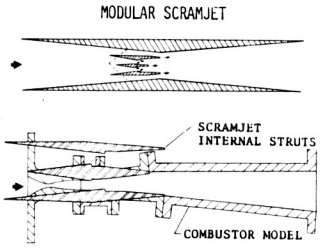

COMBUSTOR MODELING

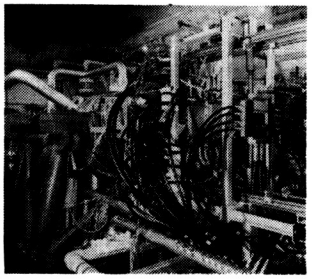

TEST CELL #2

ENGINE MODEL TESTS

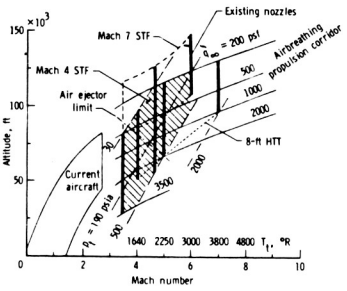

POTENTIAL TEST CAPABILITY

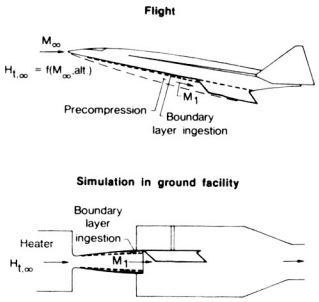

FLIGHT CONDITION SIMULATION

SMALL SCALE INLET TESTS

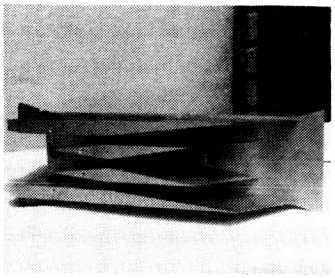

INLET MODEL

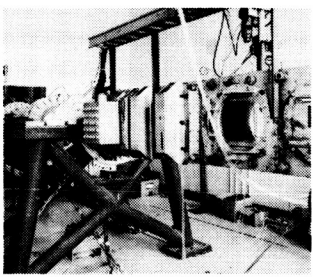

MACH 4 BLOWDOWN TUNNEL

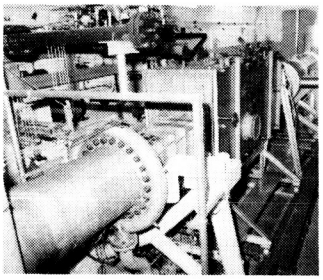

MACH 4 STF TEST CELL #1

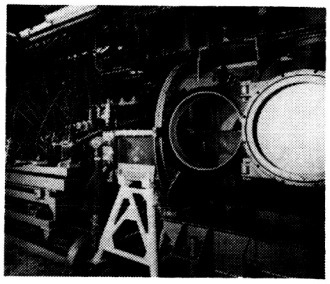

MACH 7 STF

A research program to develop technology for a hydrogen-burning airframe-integrated supersonic combustion ramjet (scramjet) propulsion system has been under way for several years at Langley. The experimental portion of this research consists of tests of engine components (inlets, combustors, and nozzles) and complete, component integration engine models.

Small-scale inlet tests for "screening" potential inlet designs are performed in a 9- by 9-in. Mach 4 Blowdown Tunnel. Larger-scale inlet tests are performed in various other Langley aerodynamic wind tunnels. Small-scale direct-connect combustor tests that simulate a portion of the engine combustor are conducted in Test Cell #2 to provide basic research data on supersonic mixing, ignition, and combustion processes. The hot test gas is supplied to the combustor models by a hydrogen-air-oxygen combustion heater, which maintains 21-percent free oxygen by volume to simulate air with enthalpy levels ranging up to Mach 7 flight speeds. Various facility nozzles produce the desired combustor entrance flow conditions.

Designs from the individual component tests are assembled to form component integration engines so that tests can be conducted to understand any interactions between the various engine components and to determine the overall engine performance. These component integration tests are conducted in engine test facilities. The feature that separates these propulsion facilities from aerodynamic wind tunnels is their capability to produce true-velocity, true-temperature, and true-pressure flow for flight simulation.

The Mach 4 Scramjet Test Facility (Test Cell #1) uses a hydrogen-air-oxygen combustion heater to duplicate Mach 4 flight enthalpy. The test gas is exhausted to the atmosphere with the aid of an air ejector. A Mach 3.5 contoured nozzle with a 13-in.-square exit is presently attached to the heater to yield a free-jet tunnel flow (simulating Mach 4 flight conditions) for subscale engine tests. The Mach 7 Scramjet Test Facility uses an electric-arc heater to produce enthalpy levels corresponding to flight speeds up to Mach 7. The tunnel exhausts into a 100-ft-diameter vacuum sphere. Eleven-in.-square exit nozzles (Mach 4.7 and 6) are used to deliver a free-jet tunnel flow for scramjet engine tests. The same size models (frontal view about 6 by 8 in.) are tested in both these facilities.

By 1989, an oxygen replenishment system and new facility nozzles will be added to the Langley 8-Foot High Temperature Tunnel (HTT), which is presently part of the Aerothermal Loads Complex. This tunnel will then be capable of testing large-scale engines (about 20 by 28 in.), multiple engines, or engines that have full nozzle expansion surfaces at Mach numbers of 4, 5, and 7. In addition, the operational capability of the Mach 4 Scramjet Test Facility is being enhanced by a new test gas heater, a new Mach 4.7 nozzle, and a new vacuum sphere/steam ejector system. Upon completion of these modifications, the 8-Foot HTT, together with the smaller-scale facilities described, will comprise a Scramjet Test Complex at Langley unequaled in the Western world. The potential operational envelope of this complex would extend over a flight Mach number range from 3.5 to 7.

Scramjet inlet tests

In support of the National Aero-Space Plane Program, a multiple-inlet model has been designed to establish the relationship that may exist between scramjet engines flying from low subsonic speeds to near-orbital velocity. The three 1.4-in.-high inlets are a precursor to a 2.5-ft scramjet engine system planned for the oxygen-enriched 8-Foot High-Temperature Structures Tunnel located at Langley Research Center. In addition, the test results will be used to validate complex three-dimensional computational fluid dynamic (CFD) computer codes capable of solving complete vehicle flow problems.

Model geometry variations include inlet contraction ratio, sidewall angle, and cowl position, all of which can be changed during the test. Pneumatically driven pins can close each module in order to determine crossflow effects. The 5.5-in.-long foreplate provides a simulated vehicle boundary layer. The model is currently being tested in the Langley Mach 4 Blowdown Tunnel, which will provide pressure, schlieren, oil-flow, and mass capture data utilizing an instream rectangular flow meter.

(Carl A. Trexler, 2803)

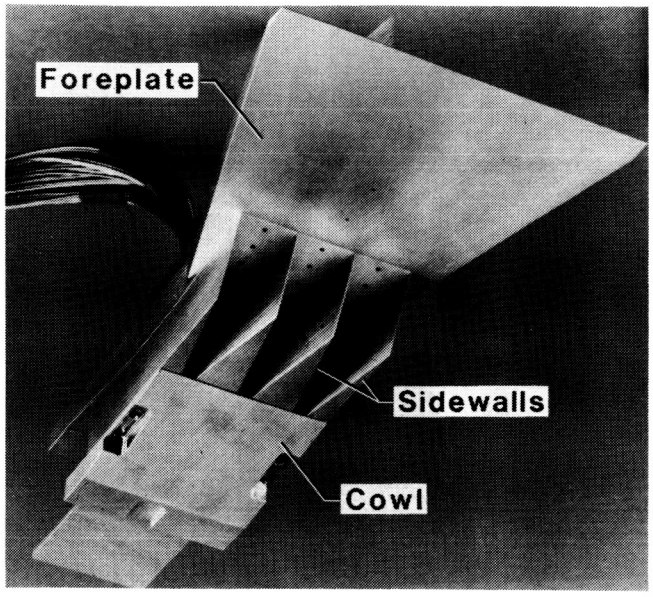

Multiple inlet model.

Plasma Jet Ignitor for Scramjets

A 1 kW plasma torch was developed and tested in conjunction with a novel injector design as an ignitor and flameholder for supersonic combustion. The uncooled torch operated on argon-hydrogen mixtures at power levels of 630 to 2590 W. The injector design incorporated a small upstream pilot fuel flow, a step for recirculation, and primary fuel injectors downstream of the recirculation region (as shown in the first figure). The torch was located in the recirculation region. Both unconfined and ducted tests were conducted in a Mach 2 flow under simulated scramjet combustor conditions. The hydrogen fuel injection was maintained at an equivalence ratio of approximately 0.3. For the ducted tests the argon-hydrogen plasma produced ignition for all temperatures tested. The pressure distributions and the corresponding calculated efficiencies were not affected by changes in the torch parameters. For the lowest burner temperature tested ($T_t = 1400°R$), as shown in the second figure, the flame persisted even when the torch was extinguished. An argon plasma produced ignition for total temperatures greater than 1600°R. Furthermore, the flame ignited by the argon plasma persisted even after the torch was extinguished. A 20-percent silane-hydrogen mixture was found to produce ignition for temperatures in excess of 1780°R. For the silane-hydrogen flows tested, the flow rate of this pilot did not affect the minimum ignition temperature or the combustion efficiency.

From these tests it may be concluded that the combination of the argon-hydrogen torch and the new injector design is a very effective ignitor and flameholder for scramjet combustors, even at power levels of 780 W. At total temperatures below 1600°R, only the argon-hydrogen plasma produced reliable ignition and high combustion efficiency.

(G. Burton Northam, 2803)

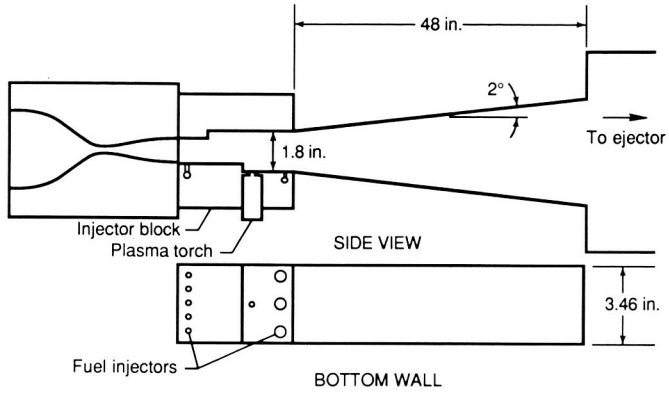

Schematic of ducted model.

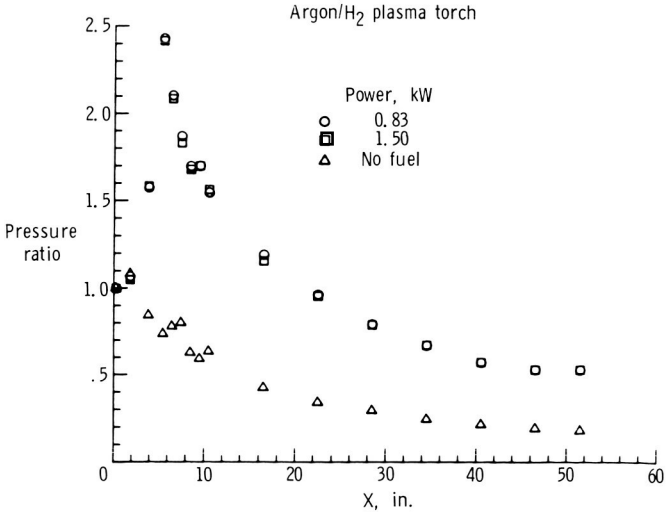

Pressure distributions in ducted model.

Aerothermal Loads Complex

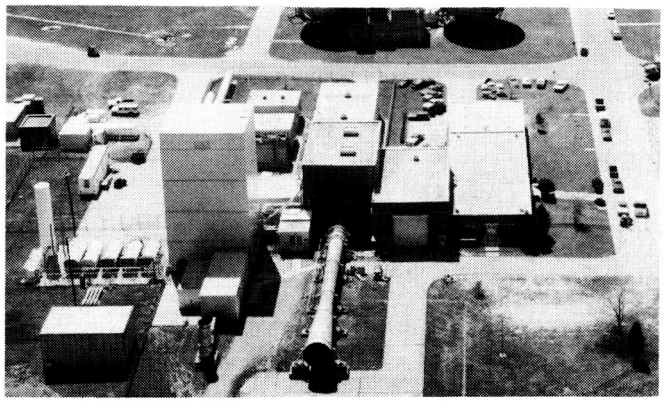

The Aerothermal Loads Complex consists of six facilities that are used to carry out research in aerothermal loads and high-temperature structures and thermal protection systems. The 8-Foot High-Temperature Tunnel (HTT) is a Mach 7 blowdown type facility in which methane is burned in air under pressure and the resulting combustion products are used as the test medium with a maximum stagnation temperature near 3800°R in order to reach the required energy level for flight simulation. The nozzle is an axisymmetrical conical contoured design with an exit diameter of 8 ft. Model mounting is semispan or sting with insertion after the tunnel is started. A single-stage air ejector is used as a downstream pump to permit low-pressure (high-altitude) simulation. The Reynolds number ranges from 0.3 to 2.2 $\times$ 10^6 per foot with a nominal Mach number of 7, and the run time ranges from 20 to 180 sec. The tunnel is used for studying detailed thermal-loads flow phenomena as well as for evaluating the performance of high-speed and entry vehicle structural components. A major effort is under way to provide alternate Mach number capability as well as O_2 enrichment for the test medium. This is being done primarily to allow models that have hypersonic airbreathing propulsion applications to be tested.

The 7-Inch High-Temperature Tunnel is a 1/12-scale version of the 8-Foot HTT with basically the same capabilities as the larger tunnel. It is used primarily as an aid in the design of larger models for the 8-Foot HTT and for aerothermal loads tests on subscale models. The 7-Inch HTT is currently being used to evaluate various new systems for the planned modifications of the 8-Foot HTT.

The 20-MW, 5-MW, and 1-MW Aerothermal Arc Tunnels are used to test models in an environment that simulates the flight reentry envelope for high-speed vehicles such as the Space Shuttle. The amount of energy available to the test medium in these facilities is 9 MW, 2 MW, and 1/2 MW, respectively. The 5-MW is a three-phase AC arc heater and the 20-MW and 1-MW are DC arc heaters. Test conditions such as temperature, flow rate, and enthalpy vary greatly since a variety of nozzles and throats are available and model sizes can range from 3 in. in diameter to 1- by 2-ft panels.

8-FOOT HIGH-TEMPERATURE TUNNEL
M = 7 R_n = 0.3 - 2.2 x 10^6

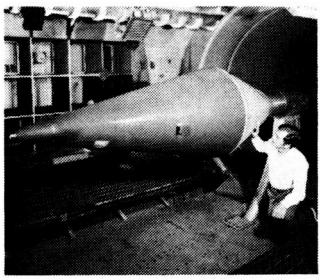

7-INCH HICH-TEMPERATURE TUNNEL
M = 7 R_n = 0.3 - 2.2 x 10^6

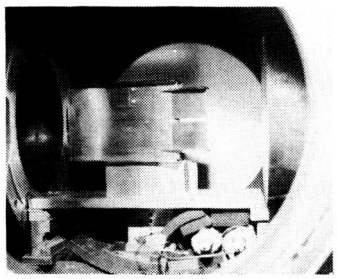

1 x 3 HIGH ENTHALPY AEROTHERMAL TUNNEL
M = 3.5 - 4.7 R_n = 0.3 - 1.4 x 10^6

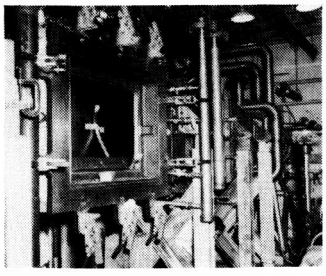

AEROTHERMAL ARC TUNNEL

Actively Cooled Radome Tests in 8-Foot High-Temperature Tunnel

An actively cooled radome was tested in the 8-Foot HTT for the Army Strategic Defense Command (SDC). The cone was tested at Mach 6.8 with a total temperature of 3500°R and plenum total pressure of 2500 psia; radar was active on all tests. Radar signals (with measured attenuation) were transmitted from the model to receiving horns just outside the flow field. The model was cooled by distributed discrete injection (transpiration cooling) of water into the boundary layer at each dielectric wave guide (small white areas on the cone). The front of the cone was fitted with a sharp solid cone covered with plasma-sprayed nickel aluminide and fitted with a double array of spherical boundary-layer trips. Tests at angles of attack of 0°, 10°, and 20° with a thin skin calorimetric cone verified that the boundary layer, which was tripped, became turbulent and provided baseline heating rates with no injection of coolant. The actively cooled cone was then tested at angles of attack of 0° and 20° with the coolant flow varied from much above the analytical design value to the design value.

Favorable test results were found with the radar transmitting as the coolant (deionized water) flow rate approached the design value. These tests were the first demonstration that a cooled radome could function in a high Mach number environment. The radome, however, did overheat near the front of the cone as the coolant flow rate approached the design value. This problem can be resolved by a change in coolant and flow rates. The test and its data provide a valuable data base for the correct design of a full-scale radome capable of surviving high Mach number flight and with continuous radar transmission.

(Richard L. Puster, 3115)

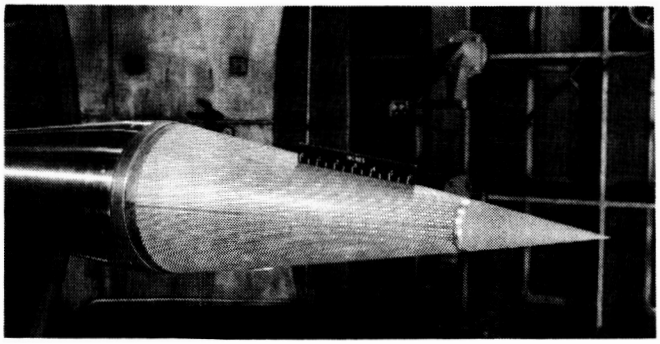

L-86-12,215

Actively cooled radome successfully tested in 8-Foot HTT.

Removal of Protective Shroud at Mach 6.7

The Army SDC is developing viable interceptor weapon systems that must protect forebody radomes during portions of the flight trajectory when the aerothermodynamic loads are most severe and when rain or debris impact is most likely. A simulated forebody protected by a series of shroud petal sets was designed and fabricated by the McDonnell-Douglas Astronautics Company to function in the 8-Foot HTT at a Mach number of 6.7 and a dynamic pressure of 600 lb/ft^2. Six shroud configurations consisting of various petal orientations and release angles were tested with and without insulation inserts designed to suppress shock interaction effects. The forebody was instrumented with 20 high-frequency pressure transducers for high-resolution recording of loads during petal release. High-speed movie and video cameras were used to document petal trajectory.

All six configurations were successfully tested and provided transient pressure data corresponding to selected design variations. A typical shroud petal removal sequence is shown in the figure. Picture frame (1) shows the petal configuration intact prior to release. The subsequent selected frames capture the four petal release with a 5-ms time interval between frames. As the petals open and release, the insulation insert disintegrates and is dispersed to expose the forebody. The sketch in the lower left of the figure illustrates the assumed shock pattern that produces the transient surface pressure histories shown in the lower right. The surface peak pressure loads without foam insulation were up to seven times the steady-state forebody pressure. The peak pressure with foam was reduced in magnitude and duration indicating the effectiveness of insulation to reduce shock loads on the radome.

(Kristopher K. Notestine, 3168 and L. Roane Hunt, 3423)

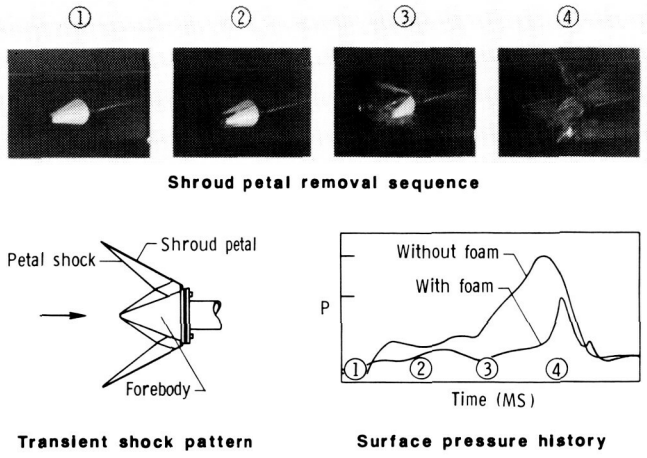

L-86-10,170

Shroud removal system at Mach 6.7 in 8-Foot HTT.

Augmented Heating Rate Measurements by Shock Impingement on Cylindrical Leading Edge

Impinging shock waves interacting with the bow shock of a blunt leading edge produce strongly augmented leading-edge heating rates. The magnitude of the heating augmentation is a function of the flow conditions and the location of the shock interaction with respect to the leading-edge centerline. Several types of shock interaction types are possible, but the most severe is the Type IV interaction (shown in the schematic in the figure) which occurs when the impinging shock interacts with the bow shock in a narrow region below the leading-edge centerline and forms a supersonic jet that conducts high-energy flow directly to the leading-edge surface. Shock interactions that occur above and below this narrow region form shear layers that interact with the cylinder with decreasing severity as the location of the interaction moves away from the critical region. Flow configurations of this type occur on hypersonic engine inlets, where, for engine efficiency, it is desirable to have the forebody compression shock incident on the engine cowl (a condition referred to as "shock-on-lip").

The 8-Foot HTT and the Calspan 48-Inch Shock Tunnel were used to define the heating and pressure loads on a 3-in.-diameter cylindrical leading edge (with a dense population of instrumentation) with an incident shock formed by a wedge shock generator. Detailed measurements were made over a range of Mach numbers, Reynolds numbers, shock strengths, and shock interaction locations. Data for the heating rate distribution (normalized by the no-shock stagnation heating rate) over the surface of the cylinder for Mach 8.0 flow using a 12.5° wedge shock generator with the shock positioned to produce a Type IV interaction are shown at the left of the figure. In this figure, Q_p represents the local peak heat transfer rate, Q_o the undisturbed stagnation point heat transfer rate, and δ the wedge angle. The peak heating rate is a factor of 10 higher than the no-shock case. Also, the locus of peak heating rates for the range of shock interaction locations (including data for a sphere due to Edney [NASA TN-D-7139]) is shown at the right of the figure.

(Allan R. Wieting, 3423)

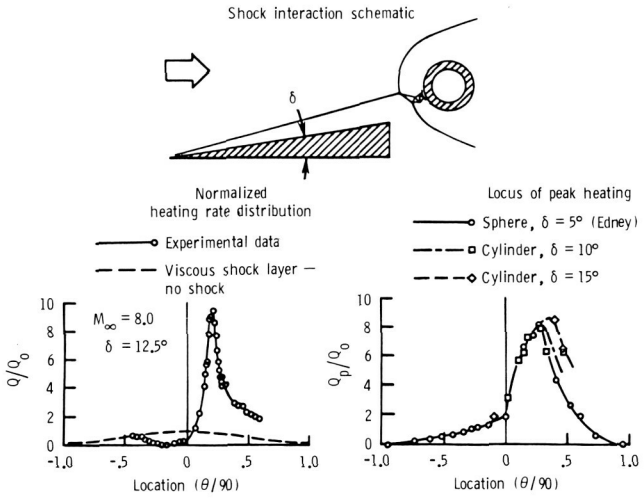

Heat transfer rate distribution for shock interference on leading edge.

Aircraft Noise Reduction Laboratory

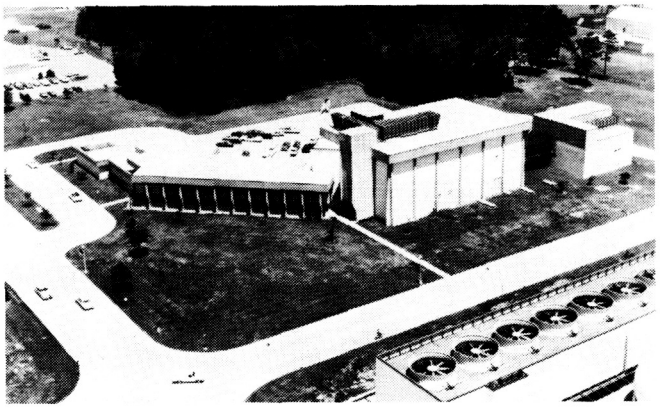

The Langley Aircraft Noise Reduction Laboratory (ANRL) provides the principal focus for acoustics research at Langley Research Center. The ANRL consists of the quiet flow facility, the reverberation chamber, the transmission loss apparatus, and the human-response-to-noise laboratories. The quiet flow facility has a test chamber treated with sound-absorbing wedges and is equipped with a low-turbulence, low-noise test flow to allow aeroacoustic studies of aircraft components and models. The test flow, which is provided by either horizontal high-pressure or vertical low-pressure air systems, varies in Mach number to 0.5. The reverberation chamber is used to diffuse the sound generated by a noise source and provides a means of measuring the total acoustic power spectrum of the source. The transmission loss apparatus has a source and a receiving room, which are joined by a connecting wall. A test specimen such as an aircraft fuselage panel is mounted in the connecting wall for sound transmission loss studies. The human response laboratories consist of the exterior effects room and the anechoic listening room.

Three laboratory companions of the ANRL are the Anechoic Noise Facility, the Jet Noise Laboratory, and the Thermal Acoustic Fatigue Apparatus (TAFA). The Anechoic Noise Facility is equipped with a very high-pressure air supply used primarily for simulating nozzle exhaust flow. The Jet Noise Laboratory has two coannular supersonic jets for studying turbulence evolution in the two interacting shear flows that are typical of high-speed aircraft engines. The TAFA provides the capability to subject flat structural panels to high-level acoustic pressures and high-temperature radiant heating to 1900°F.

Microphone clusters for rotor noise source distributions

A directional array that employs multiple clusters of microphones has been developed which, when coupled with special digital processing techniques, will enable the user to focus on a portion of the total rotor disk area. This development was based on the objective that while a single microphone measures the noise produced by a rotor, it is desirable to have the capability to examine the noise produced by only a portion of the entire rotor.

The array design consists of three clusters of four microphones. Each cluster has a finite spatial resolution that depends on the individual cluster size, distance from the array to the source, and desired frequency of interest. This array can be considered as the main lobe of an acoustic antenna. Just as in radio antennas, side lobes also occur, and it is desirable to have these side lobes pointing away from any noise source. The clusters of the array are selected to focus on a portion of the rotor disk at discrete frequencies. The location of the source area of interest on the rotor disk can be varied by changing the relative time delay between the microphones of a cluster. To maintain a constant source area over a broad range of frequencies, the data from two clusters are blended using a relative weighting. A computer model was created to facilitate array design, and the concepts were examined in laboratory testing in the quiet flow facility. This experiment used a rotating rod as a noise source which would simulate the noise produced by a model rotor. Individual clusters and a prototype directional array were tested, thus permitting examination of cluster spacing and

delay effects, as well as providing a means for checking different data processing techniques. A four-microphone cluster is shown in the figure, in which the cluster is focused at the center of the source and the frequency dependence of the lobe size is seen in the data. Where the main lobe is larger than the noise source, the cluster output, which is the sum of the four individual microphone signals, is 20 log (4) = 12 dB greater than the single microphone output. For higher frequencies, the main lobe decreases in size, pointing at only the center portion of the source, so that the cluster output is attenuated. Finally, side lobe contributions are seen to again increase the cluster output.

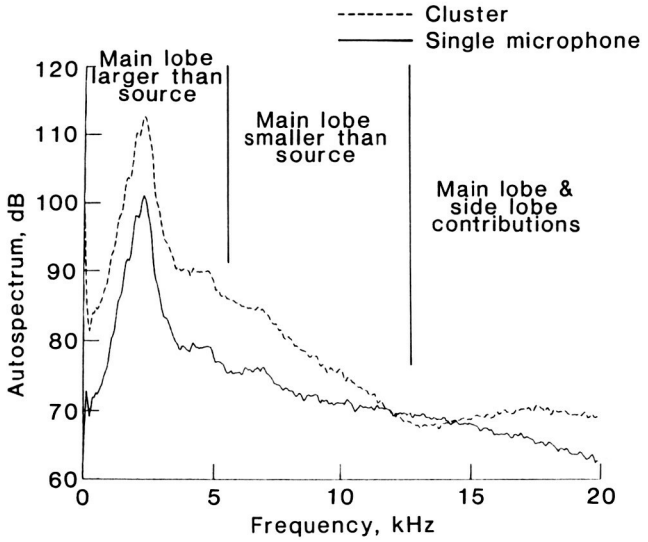

Comparison of cluster and single-microphone spectra.

Results from laboratory testing indicate the validity of the design approach. An array has now been designed for use in a main rotor noise experiment conducted in the Duits-Nederlandse Windtunnel (DNW). Data from this experiment using the array are currently undergoing processing.
(Michael A. Marcolini, 2645)

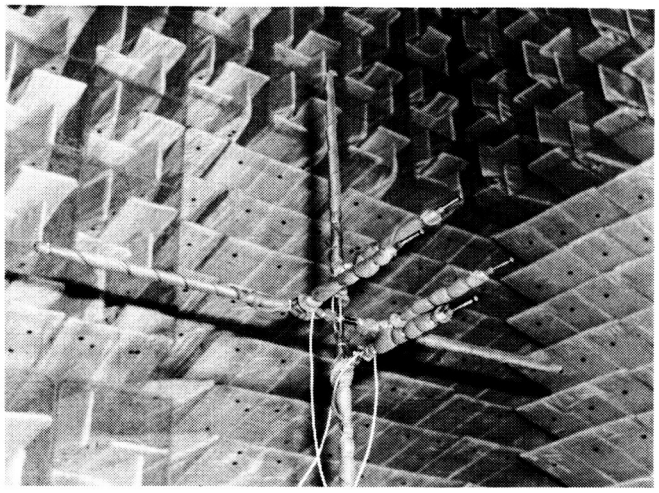

L-85-14,310

Four-microphone cluster in quiet flow facility.

Low-Frequency Sound Propagation in High Winds

The effect of refraction due to wind gradients on low-frequency acoustic signals was experimentally investigated using a wind turbine as the acoustic source. The wind turbine, located at Medicine Bow, Wyoming, generated a l-Hz periodic noise signal rich in harmonics. High-quality acoustic measurements of the wind turbine noise were accomplished through the use of two Langley Research Center ANRL acoustic vans. The vans (one of

Acoustic data acquisition van.

which is shown in the first figure) are equipped with state-of-the-art acoustic measurement instrumentation and have self-contained power and air conditioning systems. The major experimental result was that for downwind propagation the low-frequency wind turbine acoustic signal exhibited cylindrical spreading (a 3-dB reduction in level for every doubling of propagation distance) rather than the expected spherical spreading (a 6-dB reduction with every doubling of propagation distance).

An underwater sound propagation computer code based on the ray theory was adapted for use to the wind turbine measured results by Dr. D. Blackstock of the University of Texas under contract to NASA. Ray theory predicts that beyond a certain range a portion of the wind turbine signal (the part of the signal emitted parallel to the ground) becomes trapped in a two-dimensional channel due to downward refraction and repeated reflections from the ground. An example of a ray theory/data comparison is shown in the second figure for 8 Hz wind turbine data. The sound pressure level for a ground-level observer moving away from the source will initially follow spherical spreading. Between 2 and 3 km an abrupt jump of 10 dB is predicted indicating the onset of trapped acoustic rays and cylindrical spreading. The data closely match these trends, although the onset distance appears to occur closer to the source than predicted. The significance of this measured and predicted trapping of low-frequency acoustic energy is that measured levels at long distances can be much higher than anticipated when wind is present.

(W. L. Willshire, Jr., 4310)

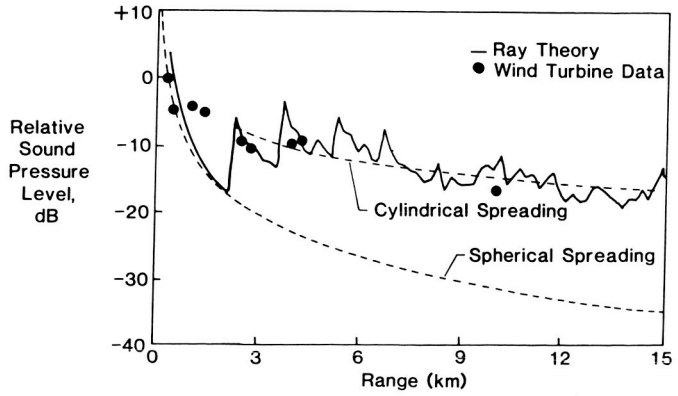

Wind turbine noise data.

Response of Rectangular Panels to Acoustic Loading

A study has been undertaken to assess the accuracy of classical linear acceleration/strain prediction theory for rectangular panels excited by acoustic plane waves. The long-range goal is to produce an analytical model for predicting the stresses and strains that lead to sonic fatigue in composite panels. To provide experimental data for evaluation of theoretical predictions, carefully controlled tests were carried out in a reconfigured transmission loss apparatus. A photograph of the test apparatus and a schematic of test facility used in this study are shown in the figure. The test panels, one aluminum and three graphite/epoxy composites, were excited by plane waves emitted from a horn/speaker. A noise survey performed prior to the acquisition of strain and acceleration data showed that the sound incident on the panels was relatively uniform spatially and spectrally. Each panel was 0.040 in. thick

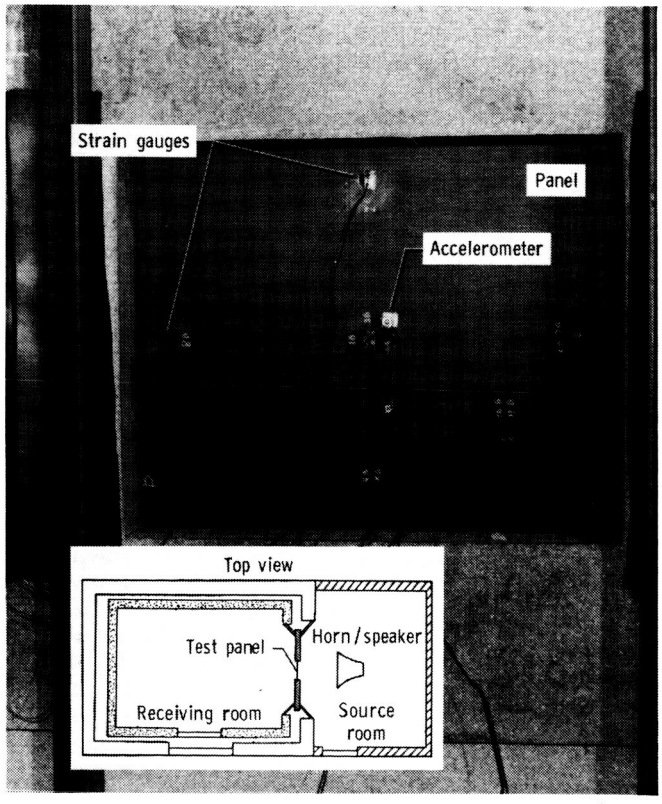

L-86-3857

Experimental setup.

and had a 15- by 12-in. exposed area. Bending strain measurements were acquired at locations perpendicular to the midpoints of the edges and parallel to the edges at the panel centers. Accelerations were measured near the center of each panel. The natural frequencies and damping values for each panel were determined from impact hammer tests.

The model to predict the strains and accelerations of the panels was based on the Ritz technique. The predicted and measured acceleration results agree to within 2 percent. The analysis predicted the distribution of strain over the panel to within 30 percent; however, the magnitudes of the predicted strains were three times those of the measured strains. This difference is presently being investigated. Both theory and test showed that the composite panel layup configuration had a large effect on strain; one layup resulted in twice the strain experienced by another layup.

(Karen H. Lyle, 3561)

Vortex Strength Measurement in Oscillating Airfoil Wake

One prominent helicopter noise source is blade-vortex interaction (BVI), which occurs when a blade tip vortex encounters a rotor blade. The resulting impulsive noise can dominate the noise radiated from the helicopter. Several years ago, a research program was initiated in-house to explore the basic physics of two-dimensional BVI. In this program, performed in the quiet flow facility, the wake from an airfoil oscillating through a prescribed pitch schedule was used as an incident vortex field and allowed to interact with another stationary airfoil representing a blade section. In order to define the input to the interaction study, it was necessary to measure the strength of the incident vortex.

Since the vortex flow field was two-dimensional, there was only one component of vorticity ω. The circulation of the major vortex could be found by integration of the vorticity field. It was necessary to measure the velocity field at a series of survey points along a line perpendicular to the free-stream velocity (the y-direction) as a function of time. This measurement was accomplished using a cross-wire hot-wire probe, which was traversed to the survey points. The velocity data were then differentiated to produce the vorticity field as functions of y/c (spatial dimension across the flow) and time.

The figure shows vorticity data for a portion of the vortex wake containing the major vortices used in the interaction study. The vortices are represented as the peaks of the vorticity in the plot. Integration of the vorticity data shows that the

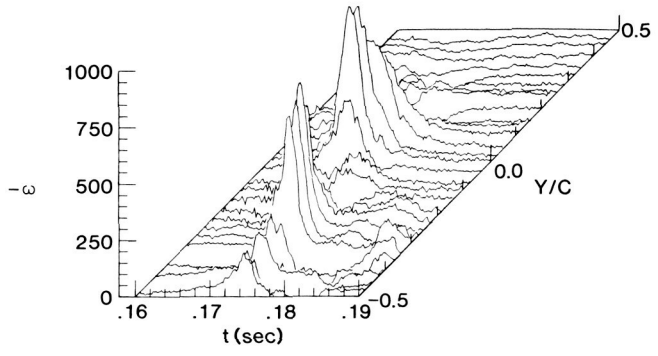

Vorticity field produced by an oscillating airfoil.

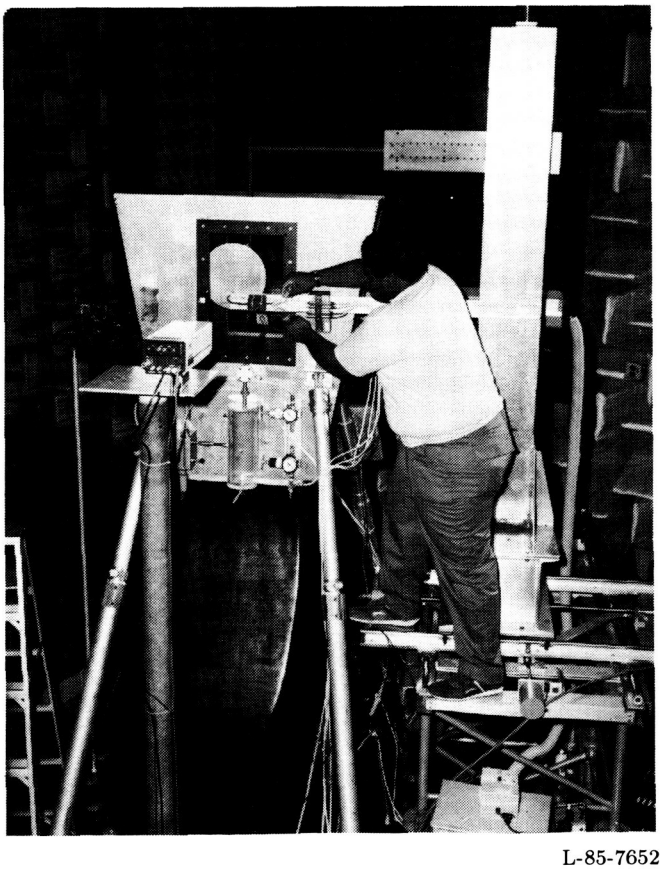

L-85-7652

Test apparatus in the quiet flow facility.

forward peak represents a circulation of 0.6 ft^2/sec while the stronger vortex in the background has a circulation of 4.5 ft^2/sec.

The data from the vortex strength measurement, combined with the data from the interaction study, will be used to test analytical predictions of two-dimensional BVI.

(Earl R. Booth, Jr., 2645)

Supersonic Jet Plume Interaction With Flat Plate

Future supersonic short takeoff and vertical landing (STOVL) aircraft, as well as the National Aero-Space Plane (NASP), call for integrated configurations in which a significant portion of the aft-fuselage is subjected to the severe thermal-acoustic fatigue loads created by the high-temperature, supersonic jet propulsion system. New design criteria and design methods for lightweight, heat-resistant airframe structures for these new vehicle classes are required.

As a first step, a model-scale apparatus has been designed to simulate jet plume interaction with structures. The generic model apparatus utilizes two rectangular nozzles with design exhaust Mach numbers of 1.35 and 2.00. Both nozzles have aspect ratios of 7.6. The plume from the rectangular nozzles is exhausted in a parallel stream over a large instrumented flat plate. The separation distance between the nozzle exit and flat plate is variable. Computer driven movement of the instrumented flat plate permits measurements to be made with high spatial resolution.

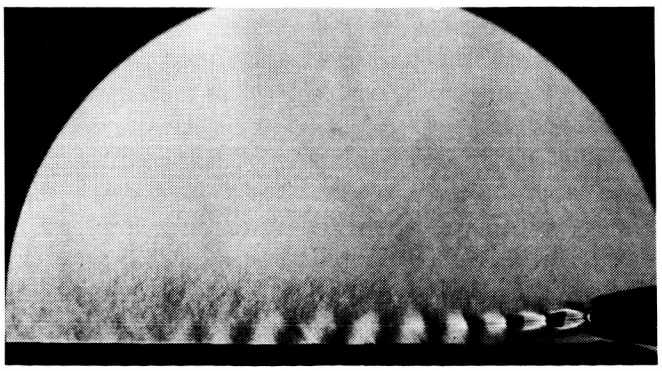

Jet plume structural loads test apparatus.

With initial separation heights of one nozzle exit height or less, the exhaust plume rapidly deflects to interact with the flat plate. The behavior is clearly observable in the nonphased averaged schlieren photograph (first figure) and is due to a loss of entrainment air on the side between the plume and the plate. Dynamic interaction between the jet plume and the plate establishes large-scale wave patterns that produce dynamic pressure loads in excess of 172 dB at frequencies of typical scaled structures as shown in the narrowband pressure spectrum.

Complete mapping of the thermal-acoustic fatigue loads and the measurement of structure responses are planned for further studies using this apparatus.

(John M. Seiner, 2645)

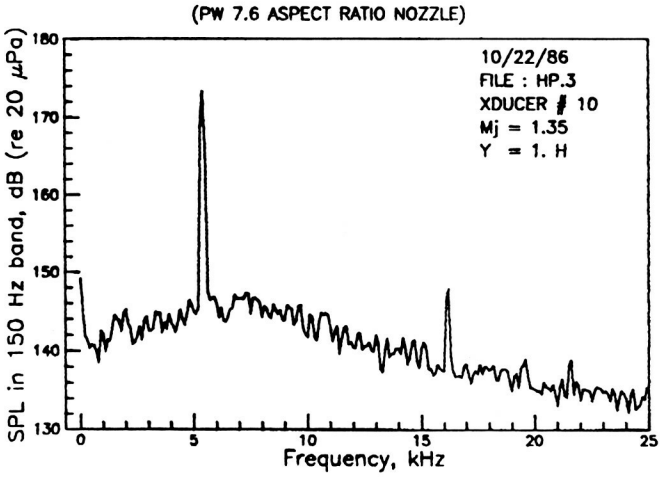

Advanced supersonic takeoff and vertical landing (ASTOVL) loads.

Active Control of Aircraft Cabin Noise

Requirements for low-frequency noise attenuation in advanced turboprop aircraft are exacerbated by the increased noise levels of these propulsion systems. Although supersonic tip speeds make possible a 30-percent or more increase in fuel efficiency, the exterior noise levels are predicted to be more than 30 dB higher than current-generation propeller aircraft. To attain acceptable cabin levels, noise

control treatments must provide up to 70 dB of sound transmission loss across the fuselage sidewall. Current construction techniques alone cannot provide such sound isolation without an unacceptable weight penalty. One alternative technique is active noise control. This technology uses additional interior noise sources to provide control of the cabin acoustic environment.

In order to investigate the application of this technology, a finite-length, thin-walled, elastic cylinder was used to model a fuselage. Plates sealed the ends to minimize sound transmission through this path. Structural and acoustic damping material was used to reduce the effect of end reflections, both to better represent an aircraft structure and to validate an existing theory. Exterior acoustic sources placed on opposite sides of the cylinder forced the cylinder into vibration and produced an interior noise field. The electrical inputs to interior acoustic control sources were optimized in order to minimize the pressure measured over an interior array of microphones.

Good agreement between measurement and theory was obtained for both internal pressure response and overall noise reduction. Attenuations in the source plane greater than 15 dB were recorded along with a uniformly quieted noise environment over the entire length of the experimental model. Results indicate that for extended axial forcing distributions or low shell damping, axial arrays of control sources may be required. For effective control the number of azimuthal control sources must equal twice the highest order azimuthal mode in the primary field.

(Richard J. Silcox, 3561)

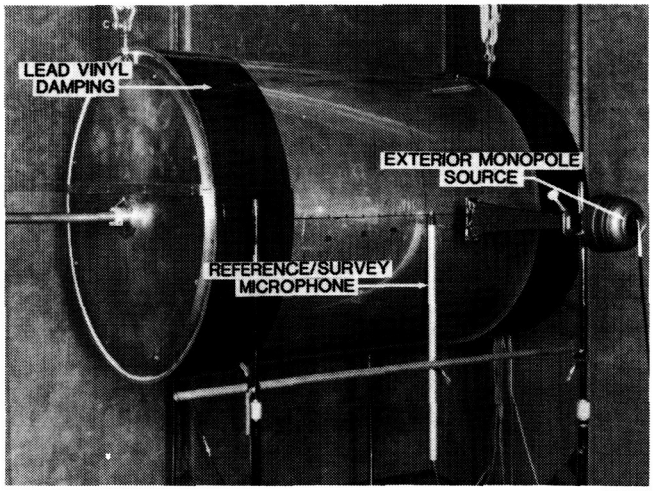

L-86-6793

Finite cylinder experimental configuration.

Noise Penalty Trends for SR Propeller in Pusher Installation

Fuel economy incentives have prompted a major change in large aircraft propulsion concepts from turbofans to propellers. Current propeller noise prediction and control technology needs to be extended considerably to accommodate the new advanced propeller designs and installations.

An experiment designed to examine the noise from a propeller installed as a pusher (behind a pylon, as shown in the figure) was conducted with a model-scale SR-2 propeller in a low-speed anechoic wind tunnel. The wake generated by the pylon produces unsteady loading on the propeller blades which radiates as sound. A detailed mapping of the noise from both pusher and tractor installations was obtained at 10 conditions covering a range of propeller operating conditions. The noise penalty associated with a pusher installation at a given flyover angle θ is defined as the average pusher level minus the average tractor level. The average is taken over all the circumferential measurement angles ϕ.

The figure shows the trends of the noise penalty with propeller power loading, $SHP/d^2/B$, at $\theta = 30°$and $90°$ to the flight direction. The estimated power loading ranges for approach, cruise, and takeoff are given along the abscissa for propeller-driven aircraft that accommodate 15 to 150 passengers. At 90°, which corresponds to the propeller rotational plane, the noise penalty has been found to decrease rapidly with increasing propeller loading so that only the lightly loaded approach conditions show a penalty. However, at 30° to the flight direction, the noise penalty does not decay rapidly with loading indicating large noise penalties (>15 dB) for all operating conditions. Other results from this test show that increased spacing between the pylon and propeller reduces the noise penalty considerably as does judicious choice of the type of pylon-to-nacelle attachment. Because of the large noise penalties toward the direction of

flight ($\theta = 30°$), it is anticipated that on approach a pusher installation will be heard before a tractor installation will be heard and will be audible for a longer period of time.
(P. J. W. Block, 4910)

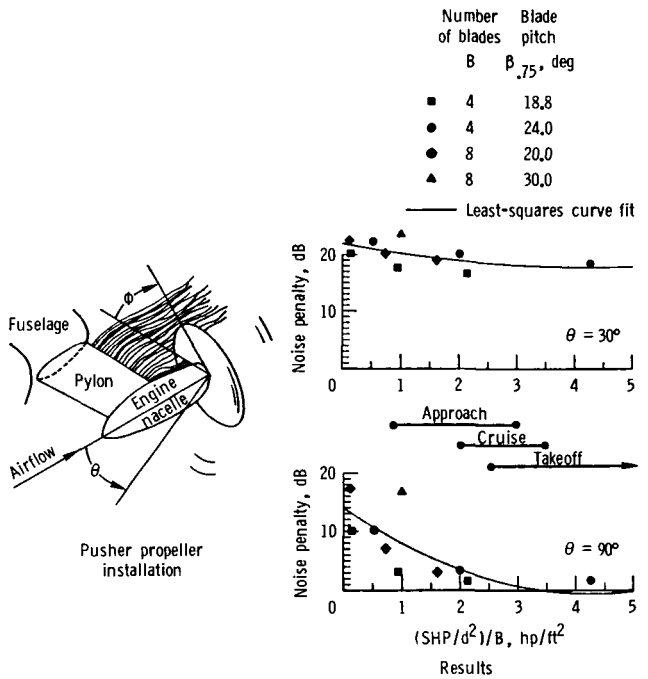

Pusher propeller noise penalty trends.

Avionics Integration Research Laboratory–AIRLAB

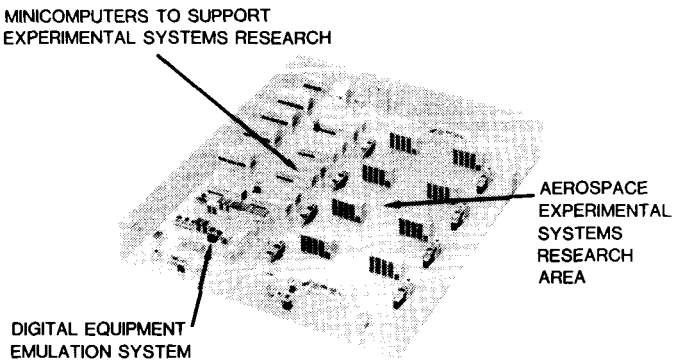

The United States leads the world in the development, design, and production of commercial and military aerospace vehicles. To maintain this leadership role throughout the 1990's and beyond will require the incorporation of the latest advances of digital systems theory and electronics technology into fully integrated aerospace electronic systems. Such efforts will entail the discovery, design, and assessment of systems that can dramatically improve performance, lower production and maintenance costs, and at the same time provide a high, measurable level of safety for passengers and flight crews.

AIRLAB has been established at Langley Research Center to address these issues and to serve as a focal point for U.S. government, industry, and university research personnel to identify and develop methods for systematically validating and evaluating highly reliable, fully integrated digital control and guidance systems for aerospace vehicles. More specifically, AIRLAB provides research resources to address design and validation issues of flight-critical fault-tolerant flight control systems, and in this role, functions much like a "community center" in which researchers with diverse backgrounds can conduct research with common goals.

The increasing complexity of electronic systems entails multiple processors and dynamic configurations. These developments allow for greater operational flexibility for both normal and faulty conditions, thus impacting and compounding the validation process. Whereas a typical reliability requirement for current electronic systems is a probability of failure of less than 10^{-6} at 60 minutes, the requirement for flight-critical electronic controls is for a probability of failure of less than 10^{-9} at 10 hours. Obviously, a new validation process is essential if this significant increase in reliability (four orders of magnitude) is to be achieved and believed.

Validation research in AIRLAB encompasses analytical methods, simulations, and emulations. Analytical studies are conducted to improve the utility and accuracy of advanced reliability models and to evaluate new modeling concepts. Simulation and emulation methods are used to determine latent fault contributions to electronic system reliability and hence aircraft safety. Experimental testing of physical systems is conducted to uncover the latent interface problems of new technologies and to verify analytical methods.

AIRLAB is a 7600-ft^2 environmentally controlled structure located in the high-bay area of Building 1220. There are three rooms within the laboratory. The largest room is the experimental systems research area which is configured into eight research stations and a central control and/or software development station. Each research station is supported by a VAX 11/750 minicomputer system that can be used, for example, to control experiments (fault insertions, performance monitoring, etc.) and retrieve, reduce, and display engineering data. A VAX 11/780 minicomputer system supports the central control and/or software development station. The second largest room contains the VAX minicomputers, disk drives, and tape drives that support the research work stations. The third room contains the Digital Diagnostic Emulator, which is a special minicomputer (Nanodata QM-1B) that communicates by a special high-speed digital data link with one of the VAX 11/750 minicomputers. The QM-1B is a nanocodable host computer with a unique emulation algorithm that allows gate logic level emulation of a target computer at a

very fast rate. The diagnostic emulator provides the capability to experimentally address design issues of new fault-tolerant computer concepts and reliability issues in the fault behavior of fault-tolerant computers. Also included in AIRLAB are three advanced fault-tolerant computer systems, SIFT (software-implemented fault tolerance), FTMP (fault-tolerant multiprocessor), and FTP (fault-tolerant processor) which are designed to explore fault-tolerant techniques for future flight-critical aerospace applications. These computer systems serve as research test beds for validation studies in AIRLAB.

Synthetic workload environment for fault-tolerant computer validation

Validation of fault-tolerant computers requires a comprehensive methodology to organize and direct specific tasks. These tasks in turn require various techniques and tools to facilitate their execution. As part of the fault-free performance validation methodology development conducted by researchers from Carnegie-Mellon University (CMU), a synthetic workload was implemented on the FTMP in AIRLAB.

A synthetic workload is used to model a natural workload. A natural workload is the set of all programs, data, and commands to be executed by a computer. In research situations, the development of natural workloads for test specimens like the FTMP can be very difficult and costly; therefore, a synthetic workload can be used to facilitate research experimentation.

The synthetic workload environment is comprised of four parts, as illustrated in the figure. The workload calculator converts function- and system-level parameters of a natural workload to iteration numbers for the synthetic workload on FTMP. The workload generator is the interface between a user and the FTMP. It takes the outputs of the calculator and uses them to set up the specific workload to be run on the FTMP. It also issues configuration commands to FTMP and sets up the data collection. The synthetic workload is a program that runs on the FTMP to simulate natural workloads. The data analyzer processes data and timer dumps and produces summary statistics and histograms.

This technique has been a valuable contribution to the validation methodology developed by CMU. The synthetic workload environment has been successfully used to measure and analyze various performance parameters of the FTMP. In the future, this environment will be enhanced to allow software-controlled fault insertion in order to investigate fault-handling behavior.

(George B. Finelli, 3681)

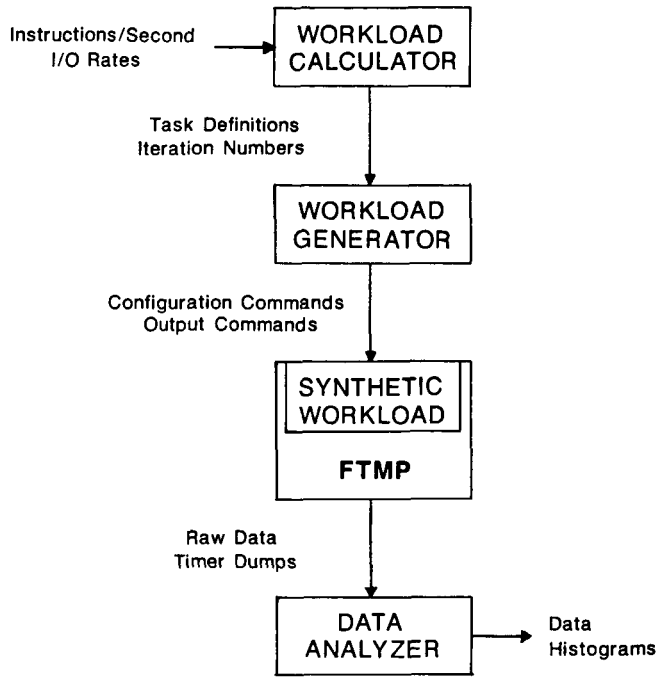

FTMP synthetic workload environment.

In-circuit fault injector

A major requirement of AIRLAB is to support the development of fault-tolerant electronic system validation experiments. Fault-tolerant system validation experiments require the simulation of subsystem failures and the measurement of the system response to those failures for reliability and performance estimates. In general, electronic systems are not designed to facilitate direct electrical fault injections to simulate system failure. Previous methods of injecting electrical faults required the electronic boards or cards to be modified to allow a special fault injection jig to be inserted between the board and the chip. The insertion of the fault injection jig in the signal path considerably slowed down and distorted circuit signals, leading in some cases to subsystem malfunction. A new fault injection method (called in-circuit fault injection) has been developed which permits fault injection through a probe that attaches directly to the pins of the chip mounted

on the board. The new in-circuit fault injection method provides a mechanism for injecting faults in any electronic system without special test fixtures (e.g., sockets), and unlike the previous method, it does not affect the normal operation of the circuit under test.

The feasibility of the new fault injection method was tested by subjecting the complementary metal oxide semiconductor (CMOS) and the transistor-transistor logic (TTL) gates to an in-circuit fault injection for long periods of time. The performance of the gates was measured before and after the fault injection, and the results were compared to determine the injection damage effects, if any, on the gates. Electrical data shown in the figure were taken during these experiments and used to determine the electrical specifications for the design of an in-circuit fault-injector system capable of injecting faults on the most common logic technologies (CMOS and TTL).

The in-circuit fault injector system, developed for conducting fault-injection experiments in AIRLAB, is under automatic control of a DEC VAX minicomputer. The system supports "stuck-at-1," "stuck-at-0," and transient fault models and also provides for injection of variable voltage levels. ("Stuck-at" faults are permanent faults manifested by continuous voltage values at the circuit nodes.)

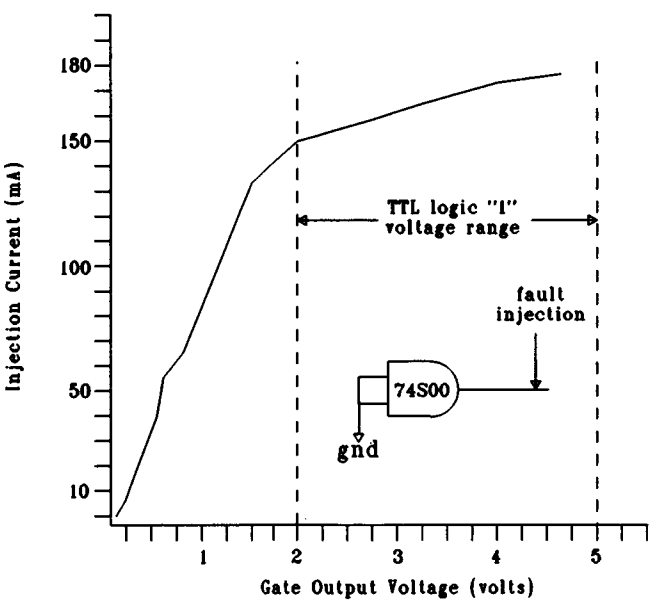

"Stuck-at 1" fault injection current for 74S00 gate.

The variable fault voltage range accommodates various types of circuit technologies in which faults can be injected. The in-circuit fault injector system is an important addition to AIRLAB resources and is being used to inject transient and "stuck-at" faults as part of experiments to characterize the behavior of a fault-tolerant multiprocessor system.
(Peter A. Padilla, 3681)

Effectiveness Measure of Diagnostic Test Vectors

The reliability of a fault-tolerant system is a direct function of the ability of the system to detect and isolate faults and failures. In order to analyze and predict the reliability of such systems one must determine as accurately as possible the probability that the system will detect failures. The AIRLAB Diagnostic Emulation Facility (Nanodata QM-1B) was used by the Research Triangle Institute to conduct a fault injection experiment on the Charles Stark Draper Labs (CSDL) FTP to determine the effectiveness of the processor's diagnostic test sequences. The network modeled on the diagnostic emulator was the communicator/interstage (C/I) function used in the FTP. This function plays a critical role in FTP fault tolerance by providing for input source congruency, error masking, and reconfiguration.

An integral part of the FTP design was the establishment of diagnostic test sequences used to insure that faults occurring in the C/I will be detected within a specified time interval. In the conduct of the experiment, test vectors from the diagnostic test sequences were used as C/I network inputs while the digital logic gates within the C/I network model were faulted. Faulted network model outputs were compared to fault-free network outputs to detect the presence of faults not detected by the test vectors.

As a result of this experiment, the CSDL assumption that a high percentage of data path faults would be detected by certain test vectors was confirmed. Further, over 90 percent of all gate faults were detected with the test vectors used. It was determined that certain faults could not be detected even by modifying the test sequences; the most important of these were faults associated with

gates in the C/I reset signal path. Finally, it was found that most of the faults were detected with approximately 20 percent of the 456 test vectors applied. By repeating these productive vectors more frequently than the less productive vectors, the average time that a C/I fault remains latent can be reduced along with the vulnerability of the system to the faults. The figure shows the individual performance of five of the diagnostic test sequences and the combined performance of all of the test sequences.

(Amy O. Lupton, 3681)

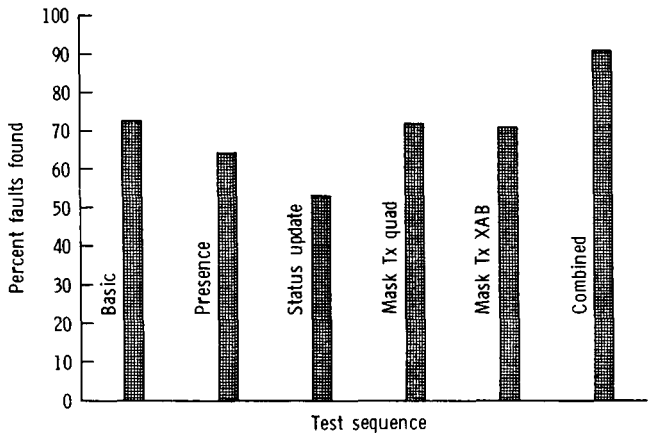

Diagnostic test performance.

Transport Systems Research Vehicle (TSRV) and TSRV Simulator

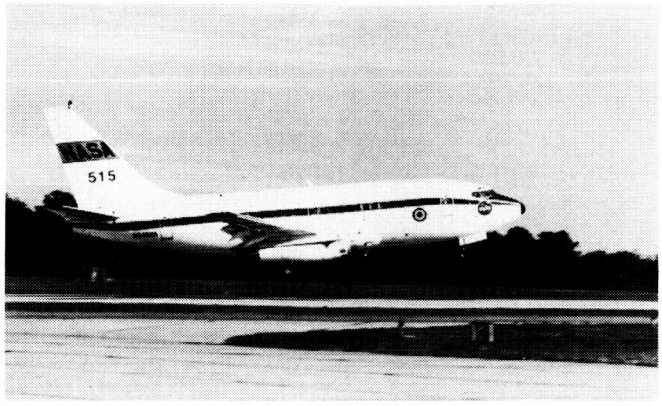

The TSRV and the TSRV simulator are primary research tools used by the Advanced Transport Operating Systems (ATOPS) Program. The goal of the ATOPS Program is the improvement of operational efficiency and safety in the evolving Nation Airspace System (NAS). Specific program objectives are to develop aircraft systems concepts and companion procedures that will permit the use of more airborne capabilities within the evolving NAS to achieve more efficient operations and to improve aircraft capability to cope with external factors such as adverse weather and airspace restrictions. In addition, the TSRV affords NASA the capability to respond to unique flight test opportunities in a timely manner. A joint NASA/FAA runway friction and braking flight test program used the TSRV to evaluate braking performance and assess performance predictions made with various runway friction ground measurement techniques. Tests were conducted over the full speed range under a wide variety of test conditions, including surface textures, grooving, wetness, snow, ice, and slush.

The TSRV is a specially equipped Boeing 737 airplane used to conduct research flight tests. The airplane has a special research flight deck located about 20 ft aft of the standard flight deck. Two research pilots fly the airplane from the aft cockpit during test periods. In order to extend the viability of the TSRV as a research tool for the next decade, an experimental system upgrade has been undertaken. The first phase provides increased computational power and speed, higher-order programming language, and a single global bus (DATAC or Digital Autonomous Terminal Access Communication) in lieu of a multiple-bus architecture, display of real-time engineering data on strip charts and TV terminals, and provisions for reducing engineering units data on 540 channels in 1 day instead of 10 days. The second phase of the upgrade will encompass provisions for an "all-glass" flight deck in the aircraft with eight large color hybrid displays.

The TSRV simulator, which provides the means for ground-based simulation in support of the ATOPS Program, is being modified to duplicate the upgraded aft flight deck located in the TSRV. It allows thorough evaluation of proposed concepts in such areas as guidance and control algorithms, new display techniques, operational procedures, and man/machine interfaces. Promising simulation research results will become the subject of actual flight test research.

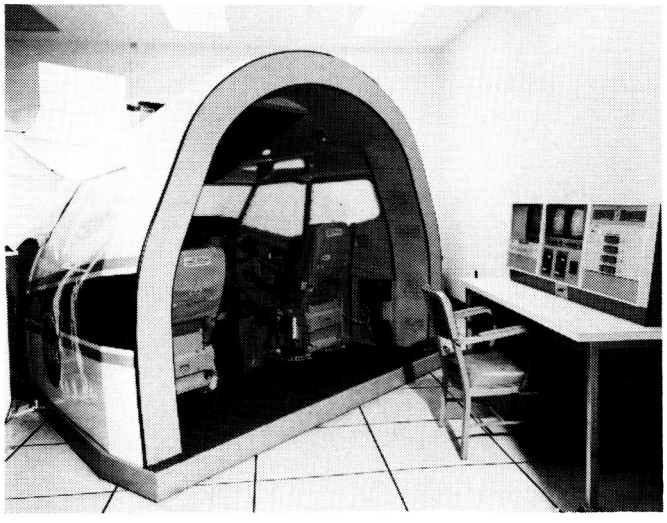

L-81-4715

TSRV simulator cockpit.

Takeoff Performance Monitoring System

A Takeoff Performance Monitoring System (TOPMS), which provides pilots with graphic/numeric information pertinent to their decisions to continue or reject takeoffs, has been developed and evaluated at Langley Research Center using the TSRV. The TOPMS display, as shown in the figure, consists primarily of a runway graphic overlaid with symbolic status, predictive, and advisory information including: (1) current position and airspeed, (2) predicted locations where decision speed ($V1$) and rotation speed (VR) will be reached, (3) balanced field length and the groundroll limit for reaching VR, (4) predicted stop point for a rejected takeoff from current conditions, (5) engine-failure flags, and (6) an overall situation advisory flag, which recommends continuation or rejection of the takeoff.

In this study, over 30 experienced Air Force, airline, industry, and government pilots evaluated the TOPMS display on the TSRV real-time simulator. The pilots used a qualitative pilot rating scale with a range of 1 to 10 (where 1 equals excellent and 10 equals unusable) based on criteria that included clarity, credibility, ease of comprehension, suitability for task, and pilot comments. The simulation tests involved each pilot making approximately 20 runs as the "pilot flying" and then repeating them as the "pilot not flying." The simulated test conditions included: (1) wet, dry, and slushy runway surfaces, (2) a range of winds, ambient temperatures, pressure altitudes, and runway lengths, and (3) degraded acceleration performance (including engine failure).

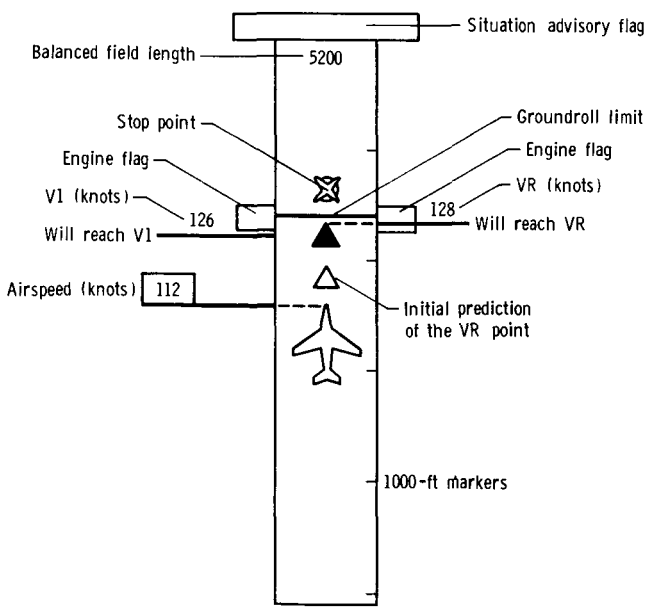

TOPMS display symbology.

The pilots, in this study, gave the display an average overall rating of 2.92 (where 3.0 equals good). In addition to the ratings, the pilots provided comments and suggestions that are being incorporated into a revised display that will be retested on the simulator and then checked out on the TSRV itself.

(David B. Middleton and R. Srivatsan, 3595)

Data Link ATC Message Exchange Tested

Communication clutter on air traffic control (ATC) voice radio channels in many busy terminal areas and the resulting high flight crew workload could possibly be eased by using a two-way digital link to exchange routine ATC messages. An initial concept for exchanging both tactical and noncontrol ATC messages over a simulated Mode S data link has been tested in the TSRV simulator. The objective of the tests was to develop guidelines, from the flight crew's perspective, for implementing data link ATC message exchange in transport aircraft. The test results combined the crew's subjective evaluations, performance, and scanning behavior.

The TSRV simulator's control display unit (CDU), which is the crew's normal interface with the flight management computer, was also used as the crew's data link interface. The figure shows data-linked ATC messages displayed on the CDU located below the moving map display of horizontal situation.

Test results indicated that the data link message exchange was acceptable to the flight crews for routine tactical ATC messages and noncontrol information; however, time-critical messages such as "go around" should be transmitted over the voice radio. Also, in non-time-critical situations the crew

preferred to have all information exchange on the data link. Mixing data link and voice presented data management difficulty in keeping track of and integrating clearances recorded on a note pad. Absence of the partyline effect, i.e., overhearing ATC's communication with other aircraft, was not felt by the crews to be a critical issue for these tests.
(Marvin C. Waller, 3621)

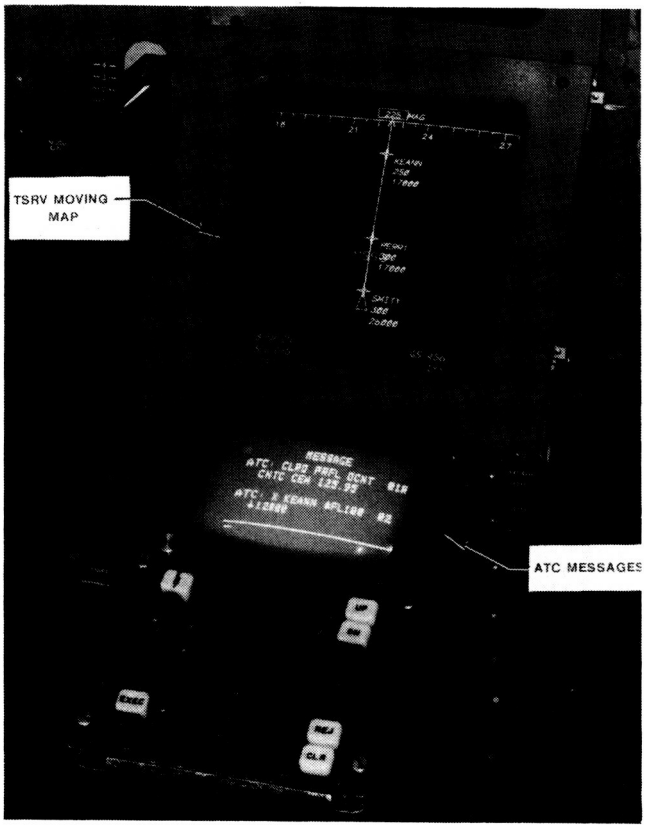

L-86-8062

ATC message examples displayed on CDU.

altimeter and airspeed indicators with electronically generated representations. Several key questions related to the representation of information on moving-tape formats were examined during this study, including tape centering, trend information, and tape orientation. The technical issues related to these parameters are as follows: First, does a significant difference in interpretability exist if, for example, a reference altitude is used as the centering index of the altitude tape versus using the actual altitude as the center? Second, how beneficial would trend information, such as acceleration on an airspeed tape, be to the pilot? Third, is the orientation of the tape critical? (Conventional design criteria require that the larger numbers be at the top of the tape; however, some designers believe that having the smaller numbers at the top of an airspeed instrument would be beneficial.)

All possible combinations of these display configurations resulted in eight test cases. A typical display configuration is shown in the figure.

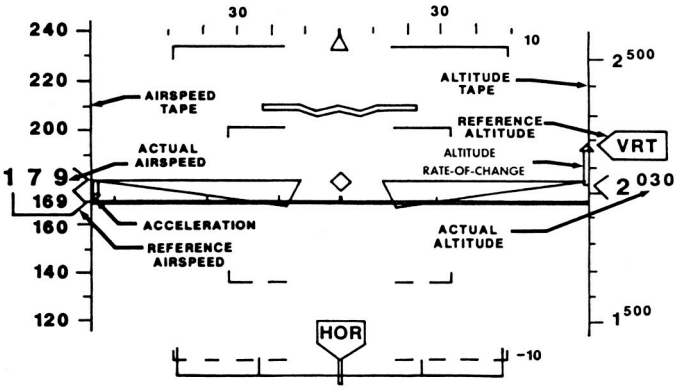

TSRV simulator experimental primary flight display showing one example of altitude/airspeed integration.

Investigation of Altitude and Airspeed Integration on Primary Flight Display

Because of the ever-increasing use of electronic displays in the cockpit, industry has expressed an interest in determining the effect on pilot performance of replacing the electromechanical

Two subjects participated in this study, in which data were collected on 32 trials per subject. A seemingly random, unpredictable guidance task was used. Data collection included objective performance measures, subjective evaluation, and a score from the Subjective Workload Assessment Technique (SWAT). In addition, auditory-evoked-potential data were collected, wherein the subjects were responding to tones presented via headphones.

In general, both pilots gave better ratings to the formats that used actual centering and a higher-numbers-at-the-top (high-to-low) orientation. The actual centered formats resulted in a 52-percent lower altitude root mean square (rms) error relative to reference-centered format. Additionally, greater attention to a secondary task was shown when actual centering was used. Formats with a high-to-low airspeed tape orientation resulted in a 400-percent fewer number of throttle control errors relative to a low-to-high orientation. Formats with trend information absent resulted in the subjects devoting 50 percent more attention to the secondary task.

(Terence S. Abbott, 3917)

Crew Station Systems Research Laboratory (CSSRL)

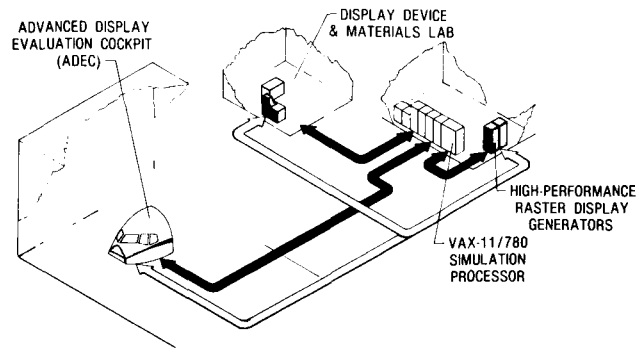

The trend in modern civil cockpits has been to replace electromechanical instruments with electronic control and display devices. The NASA Crew Station Electronics Technology research program is at the forefront of this trend with research and development activities in the areas of advanced display media, display generation techniques, integrated control panels and keyboards, and cockpit systems integration. The experimental devices being developed have unique drive, interface, and systems integration requirements (as opposed to non-cockpit electronics) as well as unique testing facility requirements. The Crew Station Systems Research Laboratory (CSSRL) is being implemented in order to provide for candidate device research in a near-real operational electronic and lighting environment in a timely and effective manner. This laboratory provides a unique civil capability to conduct display materials, device, and photometric characteristics research; establish combined display and graphics generation systems performance; determine synergistic features of integrated systems; and establish a data base on cockpit display systems that utilize emissive and reflective devices which are markedly different from their electromechanical counterparts and may be "washed out" by high ambient light or have poor viewability in darkness.

Major elements of the CSSRL are the Advanced Display Evaluation Cockpit (ADEC), which is a reconfigurable research cab, a simulation host processor, high-performance raster display generators to drive cockpit displays, and a Display Device and Materials Lab. During FY 1985-1986 a variable lighting system has been added for the ADEC to provide the capability of lighting intensities from darkness up to 10,000 footcandles with diffuse through direct-sunlight conditions.

Multifunction Control Interfaces for Transport Aircraft Advanced Caution and Warning System

A simulator evaluation of two multifunction control/display technologies, applied as the interface to an advanced Advisory, Caution and Warning System (ACAWS) for transport aircraft, has recently been completed. This study stems from efforts within the flight management research community to reduce the proliferation of controls (buttons, switches, knobs, and other controls for monitoring and controlling on-board systems) which accompanies the plethora of information now available to the crew of modern aircraft and to focus on the use of multimode, multifunction control/display technologies. ACAWS was incorporated with a large-screen, multiwindow, whole-flight-deck display concept.

Monitoring and controlling of ACAWS were implemented using the multifunction control throttle and stick (MCTAS) and the programmable display pushbutton (PDP) concepts. Both concepts, as well as the whole-flight-deck display concept, were conceived at Langley. The MCTAS concept utilizes a throttle switch and buttons on the hand-controller to activate a cursor-selectable menu choice. Cursor movement and numerical changes to subsystem parameters are commanded through the multiposition thumbwheel switch built into the throttle handle. The PDP concept is based on multifunction switches with programmable legends. The legends on the buttons change to provide the crew with selection of the subsystem display and control of parameters.

Four transport pilots participated in the simulator evaluation of the two multifunction control interfaces to ACAWS. Eight landing approach scenarios were flown by each pilot. Various interactions with ACAWS were required because of subsystem failure alert. Each pilot then completed a formal questionnaire, which contained a rating scale developed by Langley Human Factors researchers, and participated in detailed discussions of their experiences in the study. These subjective evaluations by the pilots have resulted in improved implementations of both concepts. Favorable reactions to both interfaces, to the whole-flight deck display concept, and to the multifunctions control techniques were expressed. The large-screen, multiwindow, whole-flight-deck display concept eliminated the need for multiple (4 to 6) small-screen CRT's for the display of system information. The multifunction control interfaces provided a fivefold reduction in dedicated switches.

(Russell V. Parrish, 4683)

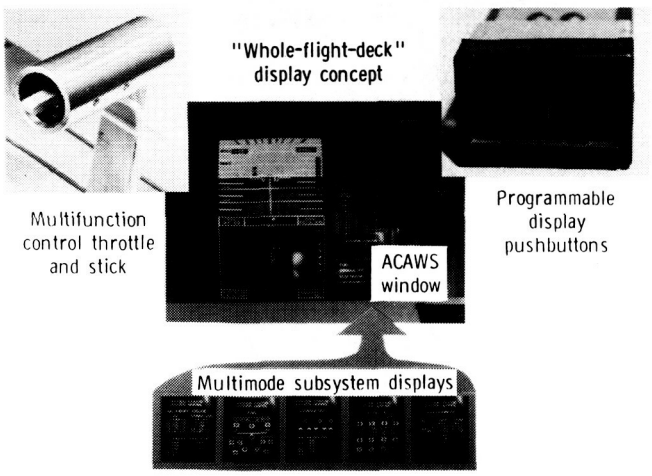

Representation of CSSRL simulator experiment showing multifunction control interfaces, whole-flight-deck display format, and subsystem display formats.

Human Engineering Methods Laboratory

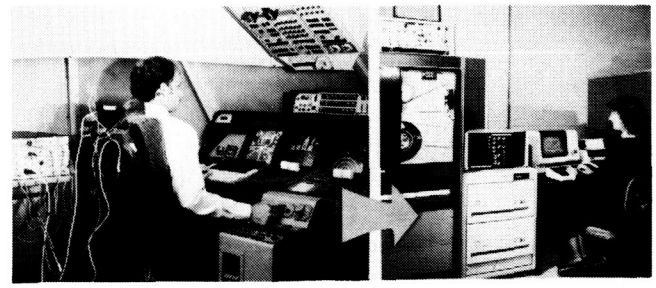

SIMULATOR WITH BIOINSTRUMENTATION DATA ACQUISITION & ANALYSIS

The Human Engineering Methods (HEM) Laboratory has been established to develop measurement technology to assess the effects of advanced crew station concepts on the crew's ability to function without mental overload, excessive stress, or fatigue. The laboratory provides the capability for measurement of behavioral and psychophysiological response of the flight deck crew.

The facility comprises state-of-the-art bioinstrumentation as well as computer-based physiological data acquisition, analysis and display, and experiment control capability. Software has been developed which enables the demonstration of workload effects on the steady-state evoked brain response and transient evoked response signals as well as the monitoring of electrocardiographic (EKG), electromyographic (EMG), skin temperature, respiration, and electrodermal activity.

The Langley-developed oculometer capability has been integrated with the other physiological measurement techniques. Subjective rating and secondary task methods for assessing mental workload have also been implemented. A computer-based criterion task battery is available for preliminary testing (with human subjects) of workload techniques that are being validated prior to evaluation and application in the simulators. Satellite physiological signal conditioning and behavioral response capture stations are located at the simulator sites to provide human response measurement support for flight management and operations research.

Brainwave Measure Applied to Display Evaluation

In 1985, the Human Engineering Methods Laboratory completed the initial development of a brainwave measure that could be used as a workload indicant. In the utilization of the metric, pilots are instructed to fly the simulator and perform a secondary tone-counting task. They are presented low- and high-pitched tones and are instructed to count the number of low-pitched tones. The amplitude of the P300 (i.e., the brainwave at 300 ms after either tone) reflects the amount of attention paid to that tone. The greater the amplitude of the P300, the more attention the pilot is paying to the secondary tone-counting task. Workload levels can be inferred from the data. A decrease in workload would enable the pilot to devote more attention to the secondary task, thereby increasing the P300 amplitude.

A research study in the Transport Systems Research Vehicle (TSRV) simulator compared eight different primary flight displays. These displays varied three aspects (centering, trend, and direction) of moving tape displays from airspeed and altitude information on a primary flight display. For centering, either the actual value or the referenced (desired) value was used as the centering value for the moving tape. For trend information, vectors showing which way and how rapidly the values were moving were either present or absent. For direction, the airspeed scale was oriented either with high or low values at the top of the scale.

A stepwise discriminant analysis was used to select the minimum number of variables capable of perfect prediction of the two extreme display configurations. Of four resulting variables, two were the Subjective Workload Assessment Technique (SWAT) and the P300 measures. A statistically significant correlation (−0.43) existed between SWAT and the P300. The higher the SWAT workload the less attention the pilot devoted to the secondary tone-counting task. The P300 amplitude

was larger when the actual value was at the center of the display, when the trend vectors were present, and when the airspeed numbers were low at the top of the scale. Corroborating evidence (e.g., lower altitude root mean square [rms] error) indicates that the lower workload enabled more attention to be paid to the secondary task. The P300 amplitude results (with the airspeed scale having low numbers at the top) were unexpected. All other measures indicated lower errors/workload with high numbers at the top of the scale. Further research is needed to fully understand this phenomenon.

(Mark Nataupsky and Terence S. Abbott, 3917)

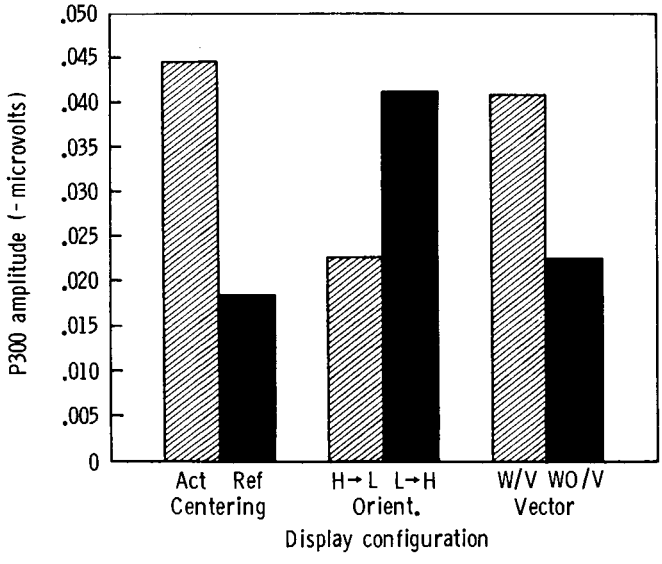

P300 amplitude difference between tones.

Heart Rate Measures Applied to Pilot Workload

Heart rate measurements have been shown by some researchers to be indicative of workload changes during aircraft flight; however, similar results in laboratory tests have not been obtained by other researchers. Therefore, this effort was designed to evaluate whether heart rate measurement would be useful in simulated aircraft operations and to develop the appropriate experimental protocols and analysis techniques that would maximize its effectiveness. The use of heart rate data might provide researchers with a measure of the level of anxiety experienced by pilots under various testing conditions. In particular, when taken in consort with other physiological measures, the data might help pilots to better evaluate the workload associated with various control/display options.

Heart rate data were collected during a simulation project in the Visual Motion Simulator (VMS) which evaluated various Microwave Landing System (MLS) guidance schemes with conventional instruments for approach to landings. Four airline pilots participated in these tests. These data were tape recorded for later playback and analysis. The tests were designed to incorporate various parameters that were expected to affect the workload of the pilot.

Data analysis showed that the difference in heart rate obtained during the period prior to the flight test (baseline), and that obtained during the actual test landing approach, was a significant measurement parameter that was sensitive to some of the experimental test conditions. The incorporation of turbulence in the simulation produced a pronounced increase in the heart rate over baseline. The removal of the flight director (FD) information also resulted in a large increase of the heart rate over baseline.

(Randall L. Harris, Sr., 3917)

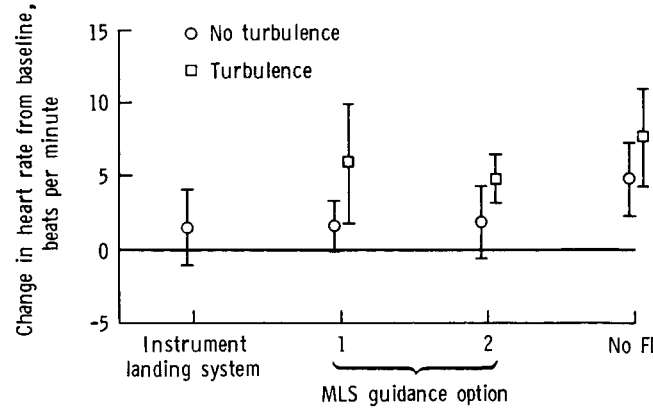

Heart rate changes with pilot workload.

Scan Behavior Using Integrated Display

With the emergence of graphic display devices in the aircraft cockpit, the display designer can now begin to combine information into one display. Consequently, the question arises of when is there too much information in a display for the pilot to assimilate? Most current research concerns the development of separate displays for attitude situation and horizontal situation; however, this study has examined whether these two displays can be combined onto a single graphic display in a manner that will not impair pilot performance.

A series of tests were conducted using four Air Force pilots to measure their scan behavior with separate attitude and horizontal situation displays versus the combined situation display. Each pilot flew seven different flight segments twice with each of the display combinations. Pilot scan behavior was measured with the Human Engineering Methods Laboratory oculometer, and the data were analyzed for dwell percentages, dwell times, and transition percentages for each information area on each instrument. Data resulting from the study are summarized in the figure. This figure shows the dwell percentages and dwell times (both shown inside the instrument boundary represented by rectangles) and transition percentages (shown by the width of the line between two instruments and numerically beside the line) for both of the display combinations.

The combined display did not adversely affect the use of peripheral instruments such as airspeed error, altitude error, and localizer error. The increase in transition percentage to the peripheral instruments was due to a decrease in the total number of transitions. The actual number of transitions to the peripheral instruments was the same. A big difference was found in the dwell time in the center of the display when the attitude and horizontal information was combined in the one display. In fact, the amount of visual time, i.e., time available to take in information from a display, increased with the combined display because of the elimination of time taken in transferring the visual gaze from one display to another (approximately 6 percent of the total flight time). Finally, the flight technical performance was equivalent to the two-display configuration. It would appear therefore that combining attitude and horizontal situation information on one display is advantageous.

(Randall L. Harris, Sr. and Terence S. Abbott, 3917)

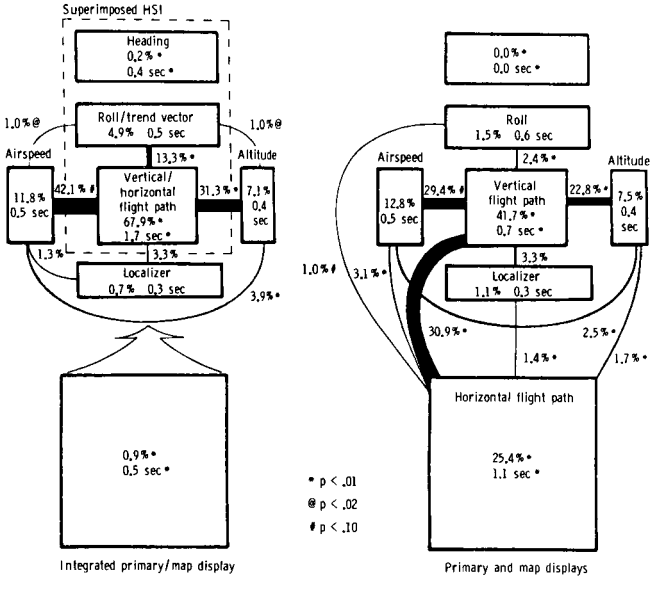

Scan behavior evaluation using two display formats.

General Aviation Simulator

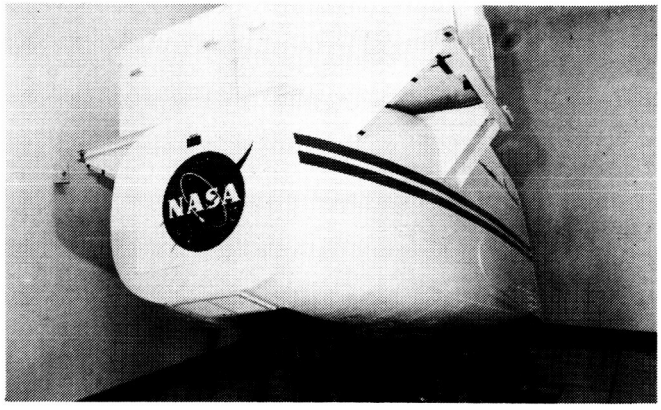

The General Aviation Simulator (GAS) consists of a general-aviation aircraft cockpit mounted on a three-degree-of-freedom motion platform. The cockpit is a reproduction of a twin-engine propeller-driven general-aviation aircraft with a full complement of instruments, controls, and switches, including radio navigation equipment. Programmable control force feel is provided by a "through-the-panel" two-axis controller that can be removed and replaced with a two-axis side-stick controller that can be mounted in the pilot's left-hand, center, or right-hand position. A variable-force-feel system is also provided for the rudder pedals. The pilot's instrument panel can be configured with various combinations of cathode ray tube (CRT) displays and conventional instruments to represent aircraft such as the Cessna 172, Cherokee 180, and Cessna 402B. A collimated-image visual system provides a 60° field-of-view out-the-window color display. The visual system can accept inputs from a terrain model board system and a computer-generated graphics system. The simulator is flown in real time with a CDC CYBER 175 computer to simulate aircraft dynamics.

Research conducted in the GAS on the single-pilot instrument flight rules (SPIFR) has identified the pilot interface with cockpit controls and displays as a critical factor in reducing pilot workload and blunders. The air traffic control (ATC) Mode-S transponder, planned for operational use in the next decade, will add the capability of a digital ground-air-ground data link to the general-aviation (GA) SPIFR cockpit. A research program is under way to evaluate the impact of various levels of data link capability on GA SPIFR operations. The levels tested will vary from uplink only of short ATC messages to uplink and downlink of complex messages. Messages to be considered will include weather data, initial instrument flight rules (IFR) clearances, and ATC tactical instructions. Initial tests will utilize current ATC procedures and conventional aircraft avionics suites. Follow-on tests will consider advanced ATC procedures and the interface of the airborne data link device with flight management system computers for execution of ATC clearances. Another research application using the GAS is the investigation of flight control problems encountered in recovering a twin-engine GA aircraft to normal flight after one engine fails.

Advanced Control Systems for General-Aviation Airplanes

Research on an automatic engine-out trim system has been extended to the consideration of irreversible control systems on the primary control surfaces and a throttle control. The purpose of this work is to explore the benefits of a multipurpose automatic control system for general-aviation airplanes. In addition to the very effective automatic engine-out trim system, the multipurpose automatic control system would incorporate features to prevent stalls, smooth the ride in turbulence for improved ride comfort, and decouple the longitudinal control to improve utility and safety. Such a system would be much more acceptable to the industry because it would make the airplane more comfortable to fly in and easier to maneuver while providing the less popular safety functions of stall deterrence and engine-out control.

The decoupled (easy-to-fly) control system has been developed, and initial test results indicate a decrease in pilot workload and an increase in precision of air speed and flight path angle control. The ride-smoothing system and stall deterrent system are presently being integrated with the decoupled control system and the engine-out trim system.

(Eric C. Stewart, 3274)

Mission Oriented Terminal Area Simulation (MOTAS)

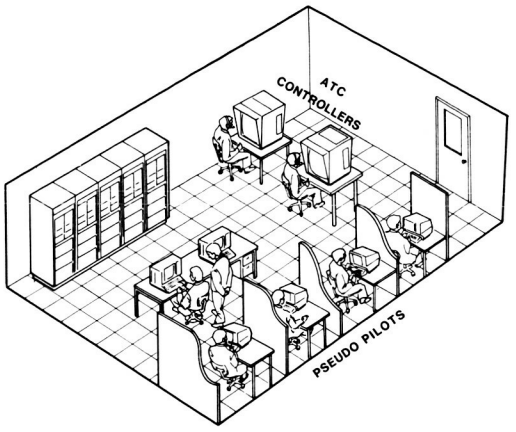

The Mission Oriented Terminal Area Simulation (MOTAS) facility is an advanced simulation capability that provides an environment in which flight management and flight operations research studies can be conducted with a high degree of realism. This facility provides a flexible and comprehensive simulation of the airborne, ground-based, and communications aspects of the airport terminal area environment. The major elements are an airport terminal area environment model, several aircraft simulators, pseudo pilot stations, air traffic controller stations, and a realistic air-ground communications network. The airport terminal area represents today's Denver Stapleton International Airport and surrounding area with either an advanced automated air traffic control (ATC) system or a present-day vectoring ATC system using air traffic controllers.

The MOTAS facility combines the use of several aircraft simulators and pseudo pilot stations to fly aircraft in the airport terminal area. The facility is presently operational with the Transport Systems Research Vehicle (TSRV) Simulator, the DC-9 Full-Workload Simulator, and the General Aviation Simulator. The Advanced Concepts Simulator will be interfaced to the facility once it becomes operational for research studies. These aircraft simulators allow full crews to fly realistic missions in the airport terminal area. The remaining aircraft flying in the airport terminal area are flown through the use of the pseudo pilot stations. The operators of these stations can control five to eight aircraft at a time by inputting commands to change airspeed, altitude, and direction. The final major components of the facility are the air traffic controller stations, which are presently configured to display and control the two arrival sectors, the final approach sector, and the tower and/or departure sectors.

Because of its flexibility in reconfiguring according to research requirements, the MOTAS facility can support a variety of flight vehicle and/or air traffic control system research studies that would not be possible in the real world due to safety, economic, and repeatability considerations. Two aircraft/ATC data link message transfer studies (one addressing civil transports and the other addressing general aviation) are examples of studies that are under way. In both cases, operational issues and experimental equipment involved in the data link transfer of ATC information and advisories are being studied. Examples of studies under development are a baseline controller study to obtain data on manual ATC operations to be used for comparison with results from advanced automated ATC systems, and development of a tieline from the Wallops Flight Center (WFC) to Langley Research Center (LaRC) to allow the Transport Systems Research Vehicle to be flown at WFC as one of the aircraft in the simulated ATC environment at LaRC.

Controller Considerations in Aircraft/ATC Data Link Message Transfer

A simulation study was performed to evaluate a baseline aircraft/ATC data link message transfer concept for the exchange of ATC tactical and certain noncontrol messages between the air traffic services and airborne flight crews. The real-time simulation study used MOTAS as the ATC facility and TSRV as the primary data link aircraft in the

ATC environment. To create a total operational environment, other aircraft were simulated through the use of pseudo-pilot stations. Under the concept, all tactical messages were exchanged on data link with voice communication maintained as a backup. Emphasis was on the airborne interface and operational issues in the flight deck. An evaluation was also made, however, of the controller aspects of an ATC data link environment. The objective was to determine how the controller operates in a mixed voice/data link environment and explore controller-related interface considerations (such as information requirements and display content/format) for implementing an ATC message exchange data link capability.

The initial study has resulted in several important conclusions related to the controller interface with, and acceptance of, a data link for aircraft/ATC message exchange. The overall consequence of the reduced voice communication was a less hurried working atmosphere, which has several implications on the way the controller operates and the associated problems. Specifically, there are fewer transpose errors (errors of transposing numbers or words) due to the reduced voice activity. However, the delayed reply, due in part to the simulated two-way Mode-S data link (up to 8 or 12 s), was a problem when the controller was busy or needed an immediate confirmation of a clearance. Data link was most advantageous for long messages. It reduced the time necessary for message transmission, thereby allowing more time for other tasks. Two major factors in controller acceptance and for safety were the availability and corresponding verification of the voice backup. This work will continue with an emphasis on developing a data base to be used in defining a controller interface for ATC data link operations.

(Hugh P. Bergeron, 3621)

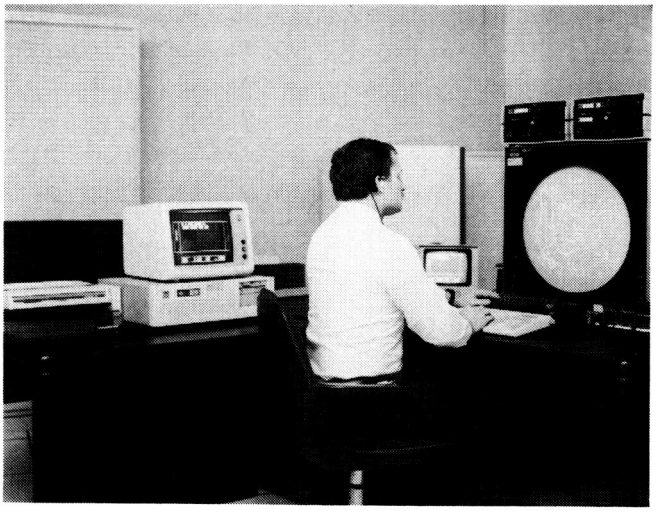

L-86-11,513

ATC controller station.

Differential Maneuvering Simulator

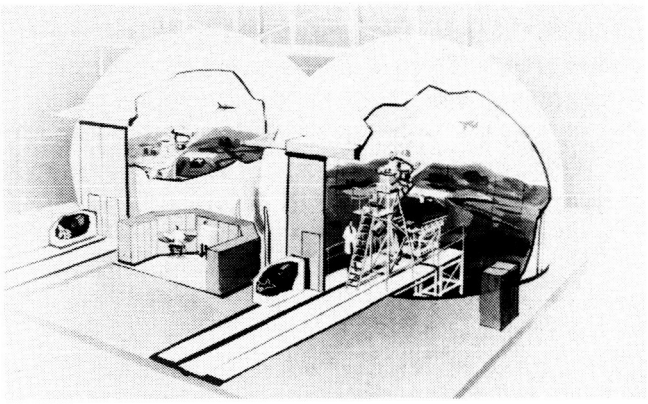

The Langley Differential Maneuvering Simulator (DMS) provides a means of simulating two piloted aircraft operating in a differential mode with a realistic cockpit environment and a wide-angle external visual scene for each of the two pilots. The system consists of two identical fixed-based cockpits and projection systems, each based in a 12.2-m-diameter (40 ft) projection sphere. Each projection system consists of a sky-Earth projector to provide a horizon reference and a system for target image generation and projection. The internal sky-Earth scene provides reference in all three rotational degrees of freedom in a manner that allows unrestricted aircraft motions. The present sky-Earth scene has no translational motion. The internal visual scene also provides continuous rotational and bounded (300 to 45,000 ft) translational reference to a second (target) vehicle in six degrees of freedom. The target image presented to each pilot represents the aircraft being flown by the other pilot in this dual simulator. Each cockpit provides three color displays with a 6.5-in. square viewing area and a wide-angle head-up display. Kinesthetic cues in the form of a g-suit pressurization system, helmet loader system, g-seat system, cockpit buffet, and programmable control forces are provided to the pilots consistent with the motions of their aircraft. Other controls include a side arm controller, dual throttles, and a rotorcraft collective. Research applications include studies of high-angle-of-attack flight control laws, evaluation of evasive maneuvers for various aircraft and rotorcraft, and evaluations of the effect of parameter changes on the performance of several baseline aircraft.

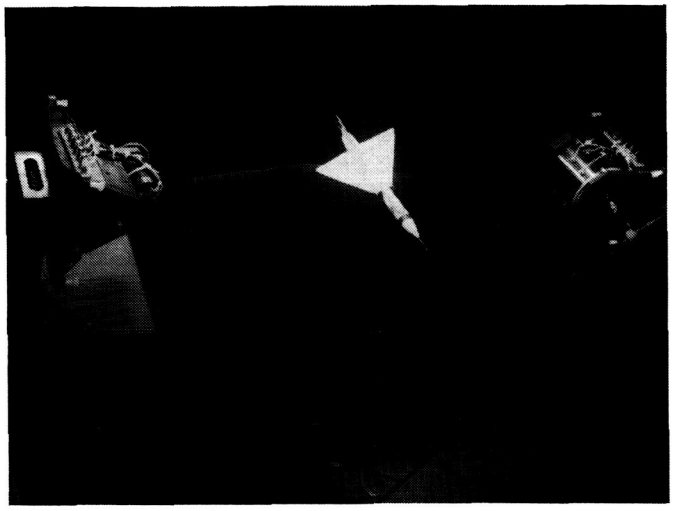

L-71-2579

Target model.

F-18 With Multi-Axis Thrust Vectoring Controls

The importance of providing future fighter aircraft with high levels of ability and maneuverability throughout the flight envelope has been demonstrated by recent air combat studies. Development of many of the technologies that will allow realization of this capability is under way. A key element is the concept of vectoring the engine thrust to produce control moments in pitch and yaw. An earlier simulation of an advanced thrust vectoring fighter configuration explored the improvements in low-speed high-angle-of-attack controllability and maneuverability and the resulting impact on air com-

bat effectiveness. This simulation also identified preliminary design requirements that must be met to maximize these benefits.

To build on and extend these results, a simulation study was conducted on the DMS to study the application of multi-axis thrust vectoring controls to an F-18 airplane. The primary objectives were to derive requirements and design approaches that could be used to develop a thrust vectoring control system for a test F-18 airplane.

An existing full-envelope F-18 simulation was modified to incorporate detailed models of the complete propulsion system including the mechanisms for turning the exhaust jets to produce the desired moments. Control laws were developed to properly integrate the propulsive and aerodynamic controls and to provide desired flying qualities over an expanded maneuvering envelope. The results of the study have shown that a practical thrust vectoring control system can be developed for the F-18 airplane which will significantly improve its maneuverability and enhance its capabilities as a high-angle-of-attack test bed.

(Marilyn E. Ogburn, 2184)

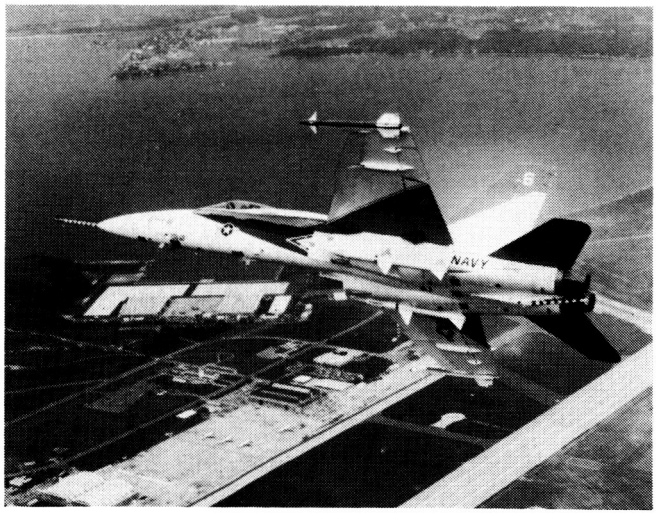

L-80-7960

F-18 high-angle-of-attack research airplane.

Visual/Motion Simulator

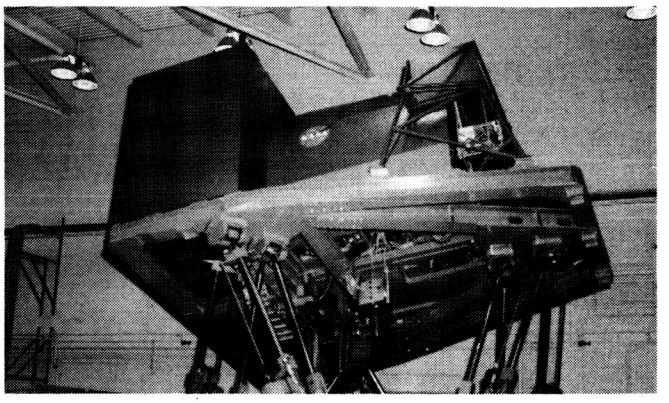

The Visual/Motion Simulator (VMS) is a general-purpose simulator consisting of a two-man cockpit mounted on a six-degree-of-freedom synergistic motion base. A collimated visual display provides a 60° out-the-window color display for both left and right seats. The visual display can accept inputs from several sources of image generation. A programmable hydraulic-control loading system is provided for column, wheel, and rudder in the left seat. A second programmable hydraulic-control loading system for the right seat provides roll and pitch controls for either a fighter-type control stick or a helicopter cyclic controller. Right-side rudder control is an extension of the left-side rudder control system. A friction-type collective control is provided for both the left and the right seats. An observer's seat was installed in 1986 to allow a third person to be in the cockpit during motion operation.

A realistic center control stand was installed in 1983 which, in addition to providing transport-type control features, provides auto-throttle capability for both the forward and reverse thrust modes. Motion cues are provided in the simulator by the relative extension or retraction of the six hydraulic actuators of the motion base. Washout techniques are used to return the motion base to the neutral point once the onset motion cues have been commanded. In addition, a *g*-seat is provided which can be interchanged between the left and right seats to augment the motion cues from the base.

Research applications have included studies for transport, fighter, and helicopter aircraft. These studies addressed problems associated with wake vortices, high-speed turnoffs, microwave landing systems, energy management, multibody transports, and maneuvering stability flight characteristics. Numerous simulation technology studies have also been conducted to evaluate the generation and usefulness of motion cues.

Defined Electro-Mechanical Instrumentation Requirements for Flying Complex Paths With Microwave Landing System

One research objective of the joint FAA/NASA Microwave Landing System (MLS) Advanced Applications Program has been to determine the guidance requirements for flying jet-transport type airplanes equipped with electro-mechanical flight instrumentation along complex, curved paths. A real-time piloted simulation conducted in the VMS was used to evaluate the requirements for flight director steering commands and for various path geometries. Airplane state, navigation, and control activity data; pilot comments; and pilot physiological data were collected on test runs along three complex, curved paths and along a standard Instrument Landing System (ILS) approach path so that an assessment of changes in workload and navigation accuracies could be made.

Analysis of all data parameters (including path tracking errors shown in the figure) clearly shows that flight director steering commands were required for flying a jet-transport airplane on complex, curved precision approach paths when conven-

tional electro-mechanical flight instrumentation was used. Final approach path lengths of 3 and 2 nmi were easily flyable. Finals of 1/2 nmi in length were more difficult but acceptable for category 1 landing minimums (200-ft ceiling and 1/2-mi visibility) approaches. The data also showed that although the workload was slightly higher for the complex, curved paths compared to the ILS path, it was acceptable for normal airline operations.

The results of these tests show that airplanes equipped with electro-mechanical instrumentation can be used to fly on complex, curved paths within the MLS signal environment. This ability will result in more airplanes attaining the benefits of curved paths resulting, in turn, in increased airport capacity, safety, and noise abatement capabilities.
(Charles E. Knox, 3621)

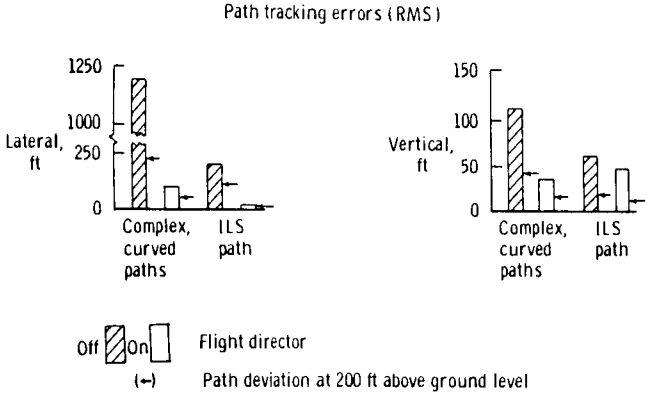

Effects of using flight director steering commands.

Piloted Simulation Tests of Ground-Based Time-Metering Air Traffic Control Algorithm

NASA and ONERA/CERT (Office National d'Etudes et de Recherches Aérospatiales/Centre d'Etudes et de Recherches de Toulouse) conducted a study of a ground-based time guidance algorithm that can enhance aircraft sequencing and improve fuel savings at busy terminal areas. The guidance algorithm computed airspeed and heading commands based on nulling a time error for airplanes to cross a metering fix at preassigned times. A real-time, piloted simulation conducted in the VMS was used to study and evaluate the effects that various operational constraints had on time-control capability of the guidance algorithm.

Test runs along the path, without initial time errors or wind-modeling inaccuracy, showed that use of the time guidance resulted in a mean time error and standard deviation at the metering fix of 1 s and 17 s, respectively. Tests showed that the guidance algorithm could accommodate maximum initial time errors of 72 s late and 76 s early at the beginning of the path. The 250-kn airspeed limit imposed by air traffic control reduced the maximum initial time error that could be nulled by the algorithm to 39 s late. A 10-kn wind bias error resulted in mean time errors at the metering fix of between 28 and 36 s. The subject pilots reported the speed and heading commands generated by the time guidance algorithm were easy to follow and did not increase their workload above normal levels.

The results of these simulation tests have shown that the ground-computed time guidance concept can significantly reduce time errors at the metering fix. This reduction of time error should increase airport throughput and increase fuel savings.
(Charles E. Knox, 3621)

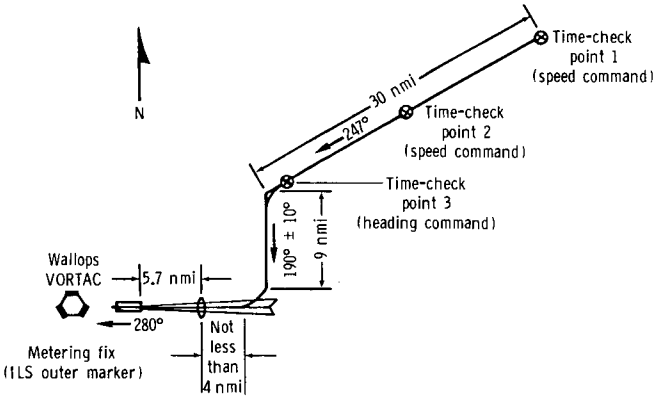

Simulation test path of ground-based time-metering air traffic control algorithm.

Comparison of In-Flight and Ground-Based Simulator-Derived Flying Qualities and Pilot Performance for Approach and Landing Tasks

An obvious void of information exists which allows the flight controls/flying qualities engineer to determine and estimate the incremental flying qualities and/or pilot performance differences that may be expected between results obtained via ground-based simulation and flight tests. To this end, pilot opinion and performance parameters, derived from the VMS and the U.S. Air Force Total In-Flight Simulator (TIFS), have been compared for a jet transport aircraft (with conventional cockpit controllers and displays) for 31 different longitudinal dynamic response characteristics. The primary piloting tasks were the approach and landing, with emphasis on the flared landing.

The results suggest that the ground-based simulator was adequate for determining the flying qualities of the various transport configurations simulated, insofar as determining the level of flying qualities to be expected, 81 percent of the time (25 of the 31 configurations evaluated). Also, the VMS predicted the Cooper-Harper Rating (CHR) to within ±2, 87 percent of the time (27 of 31 configurations). However, the CHR was predicted to within ±1 only 58 percent of the time (18 of 31 configurations). Example results are shown in the figure. In regard to the prediction of pilot performance, the ground-based simulator may be said to be inadequate. For example, the average rate of sink at touchdown was 1.7 ft/s and 5.1 ft/s on the TIFS and VMS, respectively.

Although these results indicate that a ground-based simulator is not an "exact" predictor of aircraft flying qualities and pilot performance for the flared-landing pilot task, such a simulator is a valuable tool to qualitatively assess these characteristics.

(William D. Grantham, 2132)

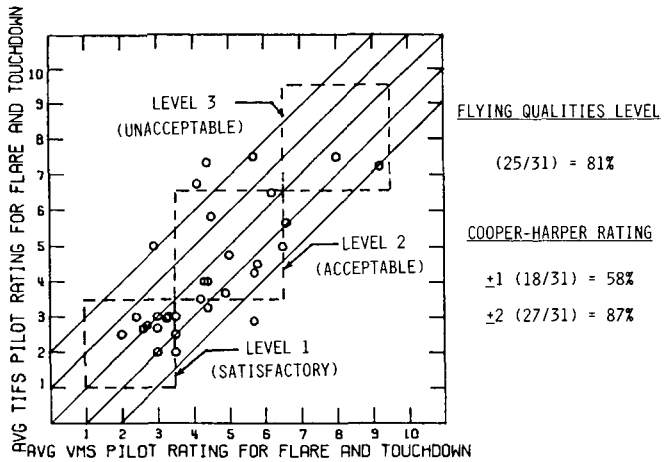

Comparison of pilot opinion of flying qualities obtained on six-degree of freedom (DOF) ground-based simulator and six-DOF in-flight simulator.

Space Simulation Facility

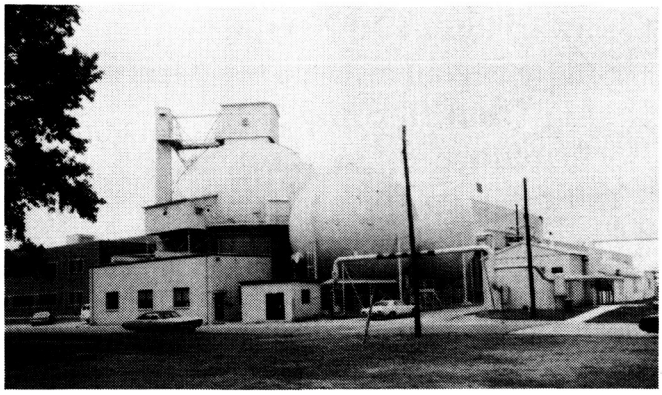

The 60-ft-diameter Space Simulation Facility can simulate an altitude of 320,000 ft (2×10^{-4} mm Hg). This vacuum level is attainable in 7 hours with a three-stage pumping system. The carbon steel sphere is accessible through a personnel door, a 12-ft-diameter specimen door, and a 4-ft maintenance door at the top. A 2-ton hoist located at the top enhances specimen handling inside the sphere. Sight ports are located both at the top and at the equator. Two closed-circuit television cameras, a video cassette recorder, and an oscillograph are available. Firing circuitry and a programmer are available for the use of pyrotechnics, and a system of flood lights is installed in the sphere to facilitate high-speed photography. The sphere is used primarily for dynamic testing of aerospace components and models at near-space environment.

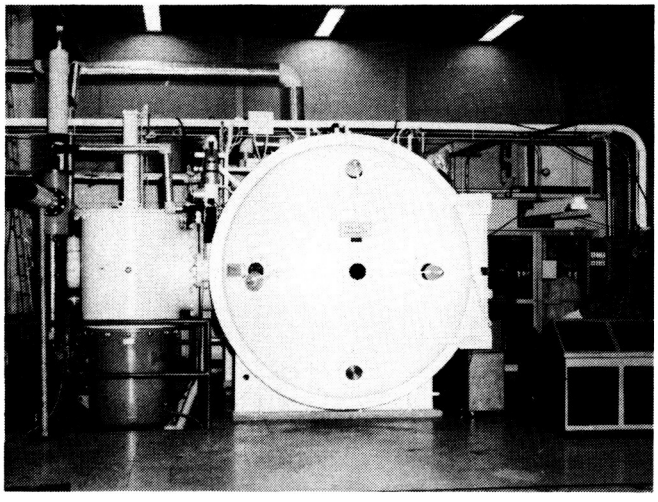

L-82-9,672

8- by 15-Foot Thermal-Vacuum Chamber.

Thermal vacuum testing has long been a prerequisite to the active deployment of space experiments. A series of experiments that optically sense characteristics of the Earth's atmosphere from outer space necessitated the creation of an ultrahigh-cleanliness thermal facility. The optical components of these experiments would be severely degraded by contamination by oils or other vaporous materials commonly found in thermal chambers and vacuum pumping systems. Langley Research Center created the 8- by 15-Foot Thermal-Vacuum Chamber facility by repeated vacuum bakeout and solvent wipedown of a previously used chamber. Two 35-in. cryogenic pumps were installed, and cold traps were inserted in the roughing pump lines to eliminate back contamination from the pumps. The chamber is capable of $-300°$F to $+1000°$F temperatures and has glass ports for solar illumination simulation. A one-unit flux solar simulator is installed with the chamber.

Halogen Occultation Experiment Thermal Balance Test

The Halogen Occultation Experiment (HALOE) is an optical remote sensor designed to globally monitor the vertical distribution of key gases in the ozone chemistry from space. Pointing accuracies of 30.0 arcsec are required under all conditions, including temperature variation, ground-to-orbit alignment, and electronic lifetime considerations. The objectives of the HALOE thermal balance test were to validate the instrument thermal design and to qualify the instrument for flight

by demonstrating acceptable performance under exposure to simulated flight environmental extremes.

The test was conducted in the 8- by 15-Foot Thermal-Vacuum Chamber, in which a vacuum of 3.5×10^{-5} torr or less and wall temperatures of $-320°F$ were used to simulate deep space. HALOE active thermal control and survival heaters were used in conjunction with the chamber quartz lamps to control the instrument temperature levels and gradients. Temperature data were recorded continuously by thermistors mounted on the instrument, and HALOE radiometric performance was checked at each operational plateau.

Initial conclusions from these tests indicate that the instrument is capable of making all the required measurements under orbital conditions. After additional testing, HALOE will begin a refurbishment cycle to replace limited life components prior to final environmental testing and shipment for integration on the Upper Atmosphere Research Satellite.

HALOE requires an infrared light source called a blackbody radiance source for in-flight calibration. This component is required to undergo three tests, called flight qualification tests, in order to verify its ability to operate in the rugged space flight environment. This instrument has successfully completed the first two tests, which verified its ability to operate in a high vacuum and to survive 1.4 times the expected launch loads. The final test will be a 2-year operation of the blackbody in a vacuum to verify its long-term performance over the duration of the HALOE flight. To facilitate this test, a new test facility has been installed with a dual-chamber vacuum system and a personal-computer-based data acquisition system. This new system will permit four instruments to be tested simultaneously and provide very accurate data with on-site data analysis.

(Richard A. Foss, 4508 and Jeffrey A. Jones, 4571)

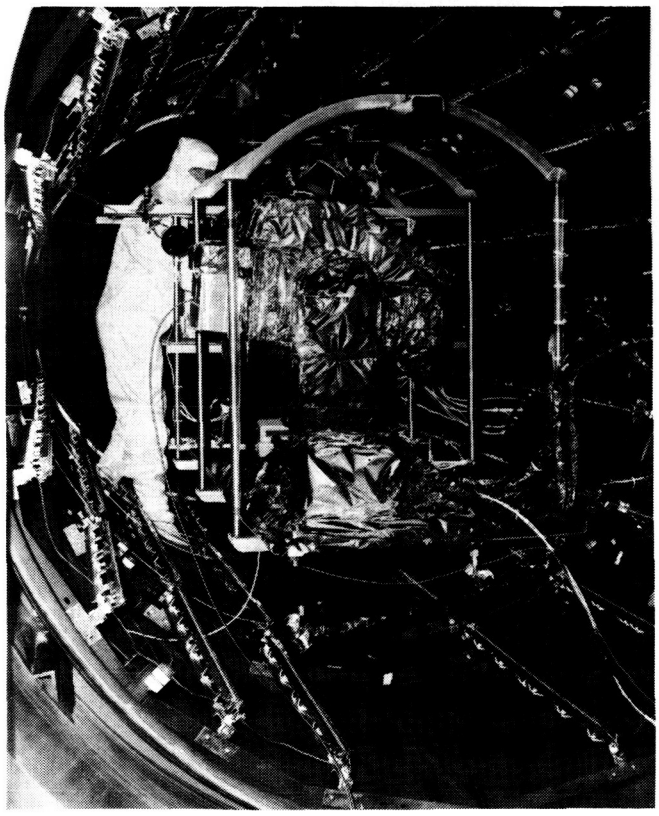

L-86-8005

HALOE instrument undergoing final inspection before thermal balance testing.

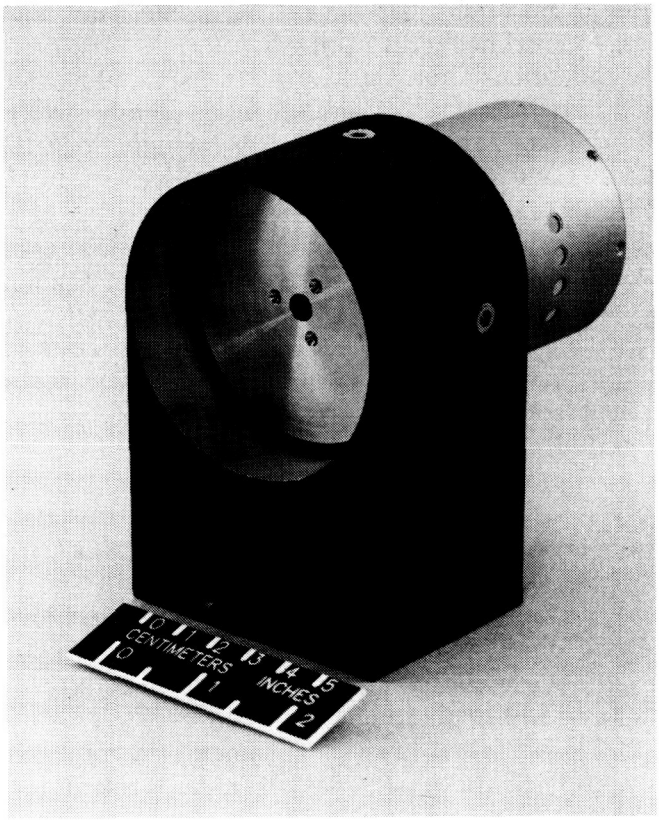

L-86-6721

Blackbody radiance source.

Structural Dynamics Research Laboratory

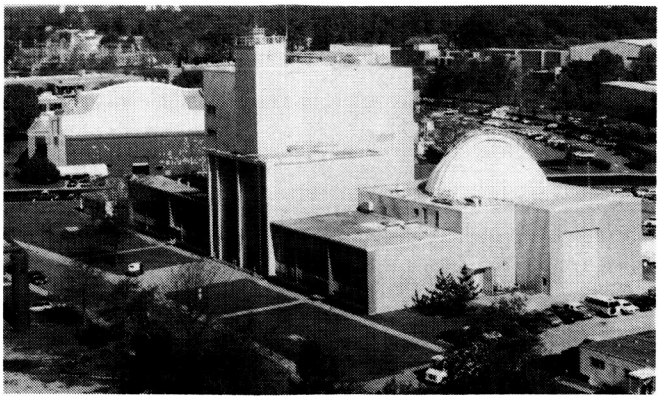

The Structural Dynamics Research Laboratory is designed for the conduct of research on the dynamic behavior of spacecraft and aircraft structures, equipment, and materials. It offers a variety of environmental simulation capabilities, including acceleration, vacuum, and thermal radiation.

A main feature of the laboratory is a 55-ft-diameter thermal-vacuum chamber with a removable 5-ton crane, flat floor, 64-ft dome peak, and large centrifuge or rotating platform. Access is by an airlock door and an 18-ft high, 20-ft-wide test specimen door. There are 10 randomly spaced 10-in.-diameter view ports. A vacuum level of 10 torr can be achieved in 120 minutes and, with diffusion pumps, 10^{-4} torr in 160 minutes. A centrifuge attached to the floor of the chamber is rated at 100 g, with a 50,000-lb capacity and a maximum allowable specimen weight of 2000 lb. Six-ft test specimen mounting faces are available at 16.5-ft or 20.5-ft radius. A temperature range of $\pm 50°F$ is obtained from 250 ft^2 of portable radiant heaters and liquid-nitrogen-cooled plates.

The other predominant feature of the laboratory is a 38-ft-high backstop of I-beam construction. Test areas available around this facility are 15 ft by 35 ft by 38 ft high and 12 ft by 12 ft by 95 ft high. Available excitation equipment includes several types of small shakers. The largest is a hydraulic shaker with a 1200-lb capacity, a 6-in. stroke, and a 0- to 170-Hz range.

Closed-circuit television cameras monitor all tests areas. Both the vacuum chamber and the backstop test areas are hard-wire connected to a central data acquisition and processing room. This room contains signal conditioning equipment and analog and digital data recording capability for up to 220 channels of data. The Hewlett-Packard 5451C and GenRad 2515 digital signal processing systems are available along with a VAX 11-780/EAI 2000 hybrid computer system for simulation and on-line test control. A variety of auxiliary data logging and signal processing equipment is also available.

Effects of Atmosphere on Slewing Control of Flexible Structure

A 3.9-m-long flexible panel, which has a cross section of 0.64 m by 0.33 cm, has been used for laboratory experiments in air and vacuum to assess the effects of atmosphere on the slewing controller design. The first figure shows the test model, which is cantilevered in a vertical plane and rotated 30° in the horizontal plane by an electric gear motor. Transient response data are shown in the second figure for a controlled maneuver in air and vacuum, respectively. The solid lines represent simulated data, whereas the dashed lines represent experimental data. The predicted in vacuo first-mode frequency and damping are within 5 percent of the measured values. Including air effects, the predicted frequencies are within 8 percent of the experimental values, but damping differed by almost 40 percent. Thus, although the curves show very similar trends, the damping discrepancy resulted in an underestimation of the peak strain values. The gear train backlash and deadband effects contribute significantly to the increase of the peak strain value when air opposes the slew maneuver. The discrepancy is also attributed to errors in modeling the drag forces.

A residual motion at the end of the maneuver

was caused by circulating air currents in the laboratory. The magnitude of air damping effects depends on the controller design; the smoother the control command, the lower the effects of air. It is concluded that the effects of atmosphere can be systematically included in the equations for slewing maneuvers of a flexible panel to determine damping trends; however, improvement is still needed to determine absolute damping magnitudes.
(J.-N. Juang, 2881)

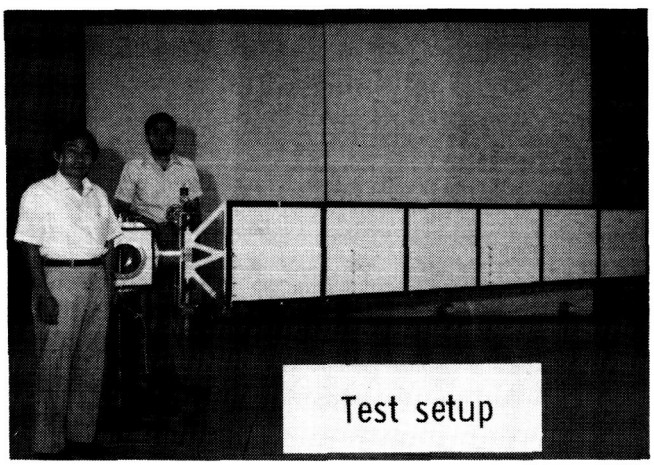

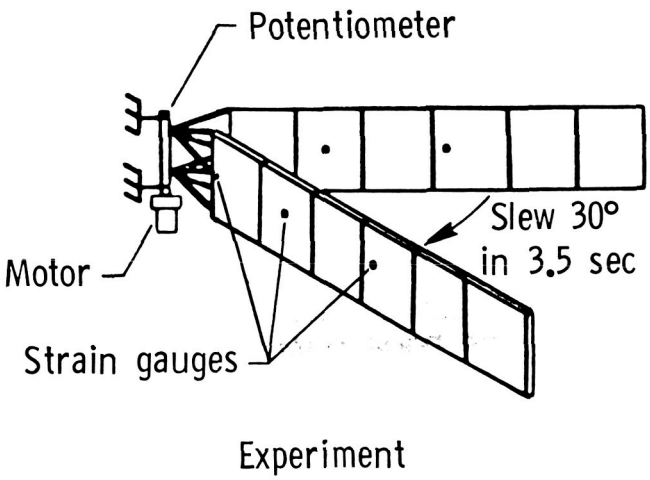

Slewing experiment setup.

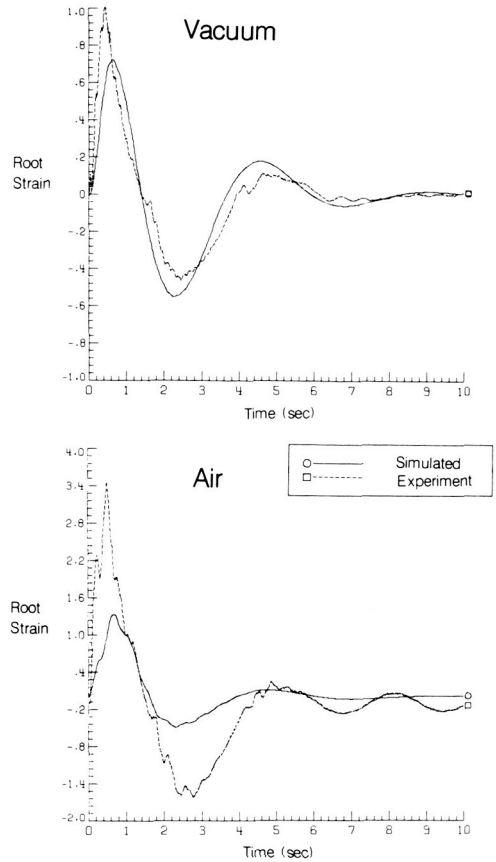

Slewing experiment results.

Completion of Hoop/Column Antenna Dynamic Tests

To achieve close surface tolerances with lightweight, deployable antennas, concepts are being developed which use tension cables for stiffening. New methods for analyzing tension-stiffened structures must be verified by test data. In particular, vibration tests and analysis must be performed to assess the degree to which structural vibrations degrade the surface accuracy and antenna point stability. An advanced tension-stiffened concept, called the 15-m-diameter (approximately 50 ft) hoop/column antenna, was vibration tested in the Langley 55-Foot Vacuum Chamber. In parallel with the vibration tests, an analytical study was performed for comparison.

Modal vibration tests were performed by applying small vibratory forces to the structure and mea-

suring the response. The 15-m antenna was tested in two ways: mounted on a tripod support system, as shown in the figure, and suspended in pendulum fashion. The vibratory response was found to be dominated by column-bending and hoop-rocking motion, which can adversely affect antenna pointing accuracy. However, because of the many

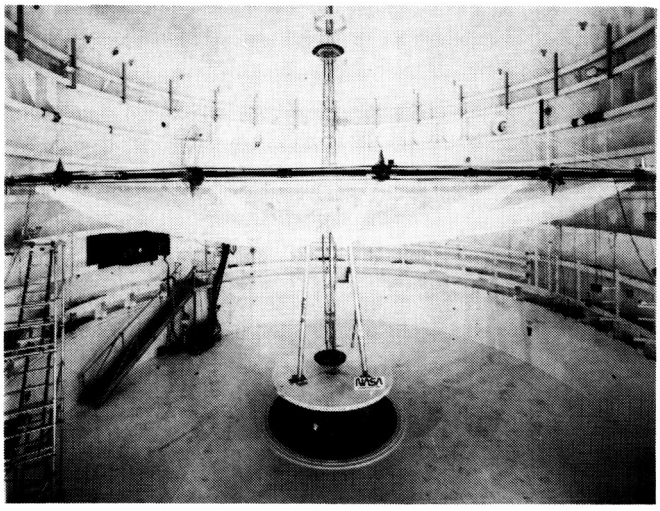

L-85-13,262

Dynamic analysis improved by vibration tests of 15-m hoop/column antenna.

structural joints in the hoop/column concept, the vibrations decay relatively rapidly. In addition, the reflective surface of gold-plated molybdenum wire mesh was found to have modal damping of approximately 10 percent of critical damping. This relatively high damping will help reduce the surface distortions that result from structural vibrations.

The original analytical model predicted frequencies 30 percent higher than those measured in the test. However, after the structural properties and effective joint stiffnesses in the analytical model were updated by static test data, predicted frequencies of the first four vibration modes were within 5 percent of the measured frequencies. Such agreement verifies that finite-element modeling can be used to predict the vibrations of large tension-stiffened antennas. Because the original analytical model contained nearly 10,000 degrees of freedom, it could not be used efficiently to study design changes. Thus, advanced continuum modeling assumptions were applied to reduce the model to below 1000 degrees of freedom. The reduced model accurately predicts the vibration frequencies of interest and permits parametric design changes to be assessed economically.

(W. K. Belvin, 2446)

Mode	Pre-test Analysis F(Hz)	Test		Post-test Analysis F(Hz)
		Vacuum F(Hz)	Air F(Hz)	
1	0.092	0.077	0.076	0.077
2(2)	1.60	0.704	0.700	0.697
3(2)	2.80	1.76	1.75	1.73
4	3.20	3.06	3.10	3.18

Antenna dynamic analysis improved by test.

NDE Research Laboratory

The reliability and safety of materials and structures is of paramount importance to NASA. The assurance of reliability must be based on a quantitative measurement science capability that is nondestructive. The Langley Research Center NDE Research Laboratory has as its prime focus the development of new measurement technologies that can be directly applied to ensuring material integrity. Furthermore, the laboratory activity is strongly directed towards developing relationships between measurable physical properties and the necessary engineering properties required for structural performance.

The Langley NDE Research Laboratory is a combination of research facilities providing advanced nondestructive evaluation (NDE) capabilities for NASA and is an important resource for government and industry technology transfer. The laboratory is the Agency's focal point for NDE and combines basic research with technology development and transfer. The activity concentrates on NDE materials measurement science for composites, metal fatigue, applied and residual stress, and structural NDE.

The facility is a state-of-the-science measurement lab linking 16 separate operations to a central computer consisting of a VAX-750 with 10 megabytes of internal memory and over 500 megabytes of fast storage. The system interfaces with a real-time video input-output so that NDE images can be obtained, processed, and analyzed on line. The major laboratory operations include a 100-KIP load system for stress/fatigue NDE research, a magnetics laboratory for residual stress, three computer-controlled ultrasonic scanners for imaging material properties, a technology transfer laboratory, an electromagnet impedance characterization laboratory for composite fiber integrity, a composite cure monitoring laboratory for process control sensor development, a nonlinear acoustics laboratory for advanced NDE research, a laser modulation applications laboratory for remote strain sensing, a pressure and temperature derivative laboratory for higher order elastic constant measurements, a thermal NDE laboratory, and a signal processing laboratory for improved image resolution and information transfer.

New assessment technique for impact damage in graphite/epoxy composite panels

The quantitative nondestructive evaluation of graphite/epoxy composites using ultrasonics is difficult due to the inherent inhomogenity of the material. An examination technique must discriminate between the inherent scattering centers in an undamaged region and the scattering centers due to defects or damage. An approach under continuing development in our laboratory is the digital signal analysis of the digitized backscattered wave from composite materials. The digital signal analysis projects out the response of the material to the probing ultrasonic energy as a function of depth. This material response signal contains information about the scatterers distributed through the thickness of the material. To improve the detection of scatterers in the interior of a sample, a signal analysis step involving use of the analytic function has been included. The magnitude of the analytic signal is equivalent to the rate of arrival of energy at the receiver. Thus, the energy backscattered from a discontinuity can be compared for undamaged and damaged regions. The magnitude of the function is a well-resolved and unipolar signal allowing statistical analysis for

the distribution of scatterers for any depth in the material.

Results are excellent for imaging impact damage as a function of depth in composites. The data may be examined dynamically as a flight through the composite where each frame in a movie represents the amplitude of scatter at a particular depth in the material. The figure shows a comparison between the ultrasonically determined damage and the result from a destructive deply analysis at the same depth.

(Eric I. Madaras, 3036)

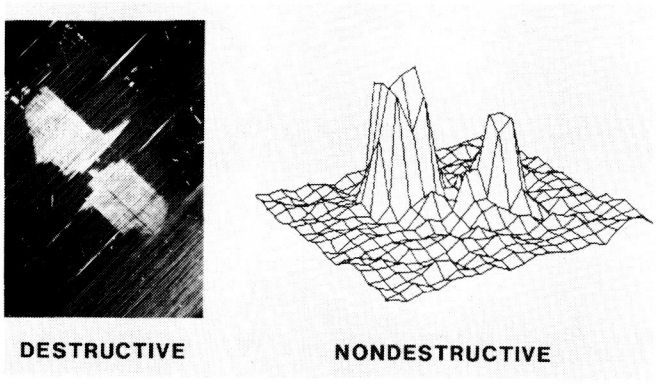

Correlation and assessment of impact damage in graphite/epoxy composites.

NDE detection of temper embrittlement in HY-80 steels

A magneto-ultrasonic technique has been developed in the NDE Research Laboratory to detect the effects of temper embrittlement in HY-80 steel alloy castings. The technique works in the following way: The material under test is subjected to a low-frequency (60 Hz) AC magnetizing field. An ultrasonic transducer (with a frequency range of 100 kHz to 300 kHz) "listens" to the noise generated by the domain wall motion within the sample. When the rate-change of the magnetic field in the sample reaches its maximum value, the noise pulse height from the transducer is measured. After a large number of such measurements have been taken, a distribution of the pulse heights is determined for each sample. A function was made by subtracting each distribution from the (reference) distribution of a sample that was not embrittled. It was found that the functions vary in a way that correlates with the state of embrittlement of the HY-80 steel casting, as measured by the Charpy V-notch Test.

A typical set of results is shown in the figure. The x-axis represents the recorded pulse heights and the y-axis represents the function, which is the difference between the number of counts in corresponding pulse height intervals between a sample under test and the reference sample. The first diagram shows the function of an unembrittled sample. The second diagram shows the function of an embrittled sample. It is seen that the function of the embrittled sample shows a substantial difference in its noise pulse height distribution than does the unembrittled sample, especially among the low-voltage pulse heights. This technique leads to a definite evaluation of the state of embrittlement.

(S. G. Allison, 3036)

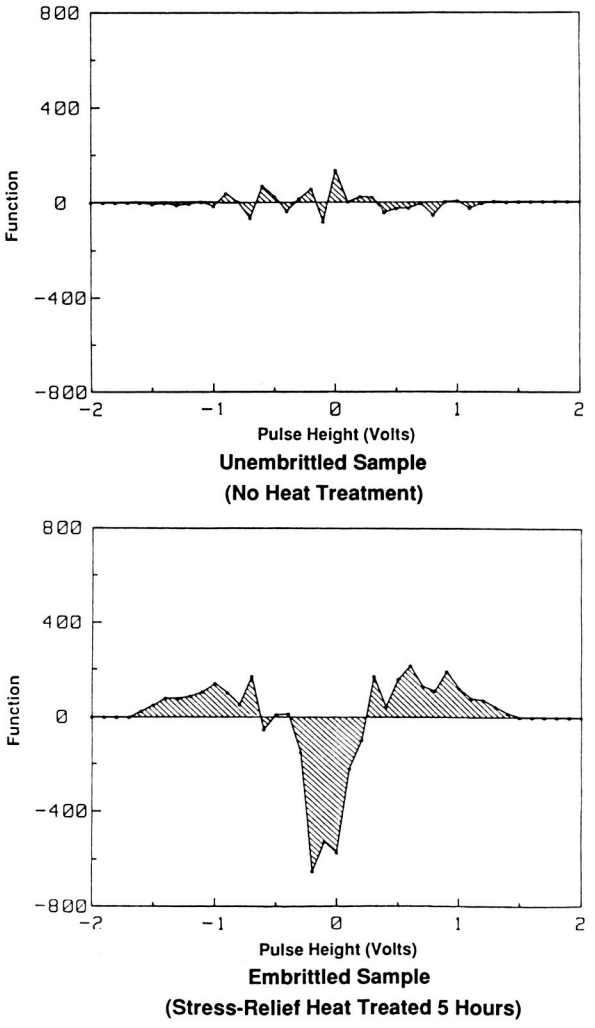

Unembrittled and embrittled samples.

Application of Ultrasonic Digital Data Analysis Techniques to X-29 Aircraft

The experimental X-29 aircraft employs a variety of state-of-the-art technologies, the most obvious of which is the forward-swept wing. Recently, during a routine safety inspection at NASA Dryden Test Flight Facility, a delamination was discovered in a noncritical edge region of the graphite/epoxy composite wing of the X-29. Although the flaw did not represent an immediate mission hazard, growth of the delamination into the more critical wing areas would pose a threat to the safety of the aircraft. The flaw was repaired by Grumman Aerospace Corporation engineers, and the NDE Research Laboratory at Langley Research Center was asked to assist in monitoring the status of the repair.

A quantitative digital ultrasonic measurement system was employed along with a mechanical template that allowed reproducible mechanical positioning of the ultrasonic probe. Data acquired with this system at Dryden were stored on magnetic media for analysis at Langley. Two advanced digital processing techniques, digital pulse shaping and analytic signal analysis, were used to remove measurement system-dependent effects and maximize resolution of the repair and potential crack growth.

Baseline measurements were obtained just following the repair. Measurements were subsequently obtained following 5 hours and approximately 25 hours of flight. Quantitative comparison of these results with the baseline results and with each other showed that the delamination had not grown beyond the repaired region, and that the integrity of the repair was maintained during those periods of flight. Reproducible mechanical positioning, digitized ultrasonic signals, and advanced digital techniques to remove system-dependence and improve resolution all combined to allow quantitative comparison of data sets and to assure that any future measurements of the repaired delamination can be accurately interpreted with regard to growth of the delamination or failure of the repair.

(Patrick H. Johnston, 3036)

L-86-8186

Delamination evaluation in X-29 aircraft wing.

Acoustic Characterization of Glass Transition Temperature

The development of tough high-temperature thermoplastics for composites has led to stricter constraints on the manufacturing process. Obtaining a viable product with conventional techniques requires a reproducibility in materials which is difficult to obtain with current manufacturing operations. To achieve materials that have predictable properties, the manufacturing process needs to be based on a sensor technology to characterize the materials as they evolve during the cure. A real-time characterization of the materials during processing provides information for a process controller which can tailor a process to manufacture a part with the highest quality.

A technique has been developed in the NDE Research Laboratory for determining the glass transition temperature of a thermoplastic from the temperature dependence of its acoustic velocity. The temperature dependence of the acoustic velocity is shown in the figure. Acoustic velocity of the glass was measured as glass temperature was increased using a hot press (with the glass sandwiched between two hot plates). An analytical expression has been found which accurately fits the shape of the data and has a maximum in its derivative at the glass transition temperature. The glass transition temperature is an important processing parameter for determining the temperature and pressure required to fabricate a composite. The acoustic glass transition temperature agrees with values found from traditional techniques to within 1°C. The measurement technique, however, differs

from these traditional techniques in that it can implement in an autoclave environment and perform the characterization during materials processing.
(W. P. Winfree, 4928)

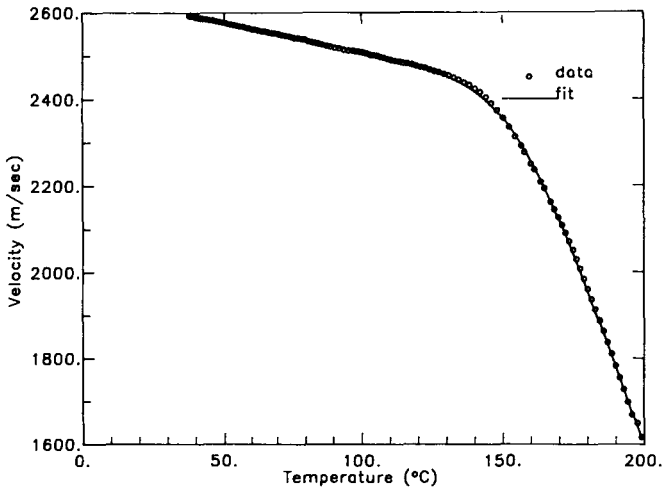

Acoustic velocity of poly(arylene ether) as function of temperature fit by a function that gives glass transition temperature of polymer.

Joining NDE and Fracture Mechanics to Predict Composite Solid Rocket Motor Strength

Filament wound casings, which are used for solid rocket motors, can sustain internal damage from impact with no visible evidence of damage at the surface. Fracture mechanic models have been developed for predicting the failure strength of thick composites that have been impacted. These models require specific information about the damage which is difficult to obtain, especially when the damage is internal. To circumvent this problem, an algorithm was developed which estimated the characteristics of the damage from quantitative ultrasonic attenuation and velocity measurements made in transmission. The ultrasonic response of the samples was modelled depending on good composite material and an effective damaged composite material. If the ultrasonic attenuation and velocity values for both the good and the effective damaged composites are known, then values for the dimensions of the damaged region can be calculated. This information can then be combined with a fracture mechanics model to predict the ultimate strength of a thick composite sample under tensile load.

The combined system that uses principles of NDE and fracture mechanics was tested on impact damaged filament wound casing materials. The samples, which displayed no visible surface damage, were ultrasonically tested and then loaded in tension until failure using the NDE Research Laboratory fatigue machine. The system was able to predict the strength of the damaged samples reasonably well as shown in the figure. The results scatter about the unity correlation line, with 80 percent of the points within a few percent of this line. Variances were typical of those of material variances.
(Eric I. Madaras, 3249)

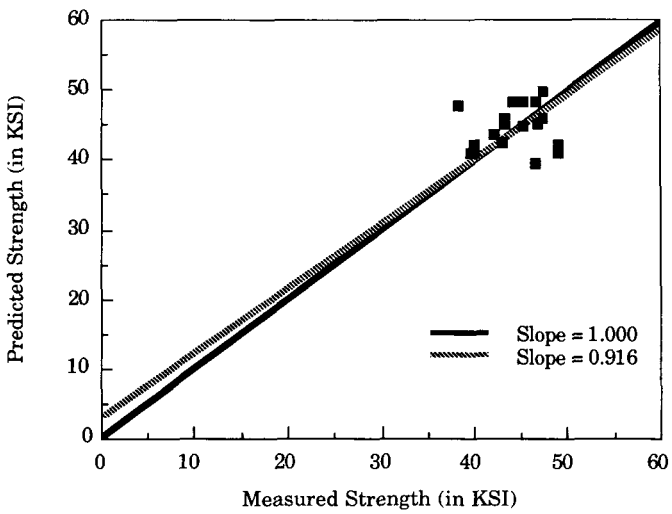

Ability of ultrasonics NDE to predict remaining composite strength.

Vehicle Antenna Test Facility

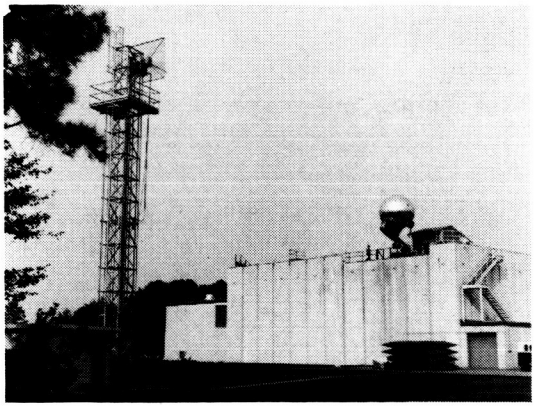

The Vehicle Antenna Test Facility (VATF) is a research facility used to obtain data for new antenna performance and electromagnetic scattering data in support of various research programs. The VATF consists of two indoor radio frequency anechoic test chambers and an outdoor antenna range system. The anechoic chambers provide simulated free-space conditions for measurements from 100 MHz to greater than 40 GHz. The anechoic chambers, which are shaped like pyramidal horns to reduce specular reflections of the walls, are over 100 ft long and have test area cross sections approximately 30 by 30 ft.

A spherical near-field (SNF) measurement capability was added to the low-frequency chamber. A precision antenna positioning system, antenna source tower, and optical alignment system designed for SNF measurements were installed in the low-frequency chamber, and the capability now exists for automatic performance of precision SNF measurements up to at least 18 GHz. Antennas with diameters up to 12 ft can be measured if their electrical size is no greater than 100 wavelengths (i.e., diameter/wavelength $\leq$ 100). This limitation is imposed by the SNF system software, which transforms the near-field data to obtain the desired far-field data. Measured data stored on disc can be processed to provide antenna directivity, polar or rectangular plots of the radiation patterns, and three-dimensional contour plots of the antenna radiation characteristics.

The high-frequency anechoic chamber was used to establish a Compact Range Facility. The compact range is an electromagnetic measurement system used to simulate a plane wave illuminating an antenna or scattering body. The plane wave is necessary to represent the actual use of the antenna or scattering from a target in a real-world situation. The compact range utilizes an offset-fed parabolic reflector to create the simulated plane wave test conditions. The standard commercially available compact range is limited to the measurement of antennas or models with maximum dimensions of 4 ft over the frequency range of 4 to 100 GHz.

The outdoor antenna range system is available for use when the antenna or test model size or frequency precludes the use of the anechoic chambers. The outdoor range consists of two remote transmitting towers that are spaced 150 and 350 ft from the test positioner mounted on the VATF roof. The VATF has several electronic laboratories with the extensive measurement capability needed to support the design of unique antennas prior to their evaluation in the antenna chambers or on the outdoor antenna range system.

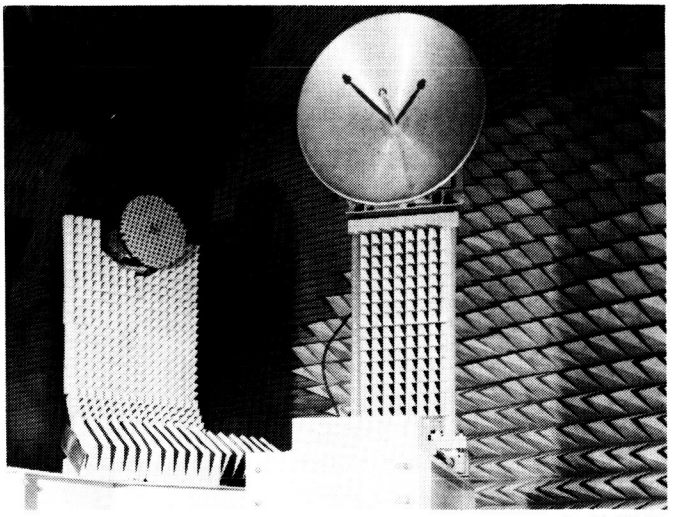

L-85-2143

Spherical near-field equipment.

Development of standard electromagnetic test body

Test bodies are required for evaluating the performance of electromagnetic scattering facilities. There are many electromagnetic scattering measurement facilities in use, and experience has shown that it is extremely difficult to obtain repeatable measurements, even on the same range. It becomes even more difficult to achieve these measurements when different test facilities are used and different operating conditions exist. This makes it extremely important to have a standard test body that can be used for range calibration if data from different facilities are to be compared.

Langley Research Center has been involved in the development of a new class of standard electromagnetic test bodies. One of these bodies, the almond (so-called because of its resemblance to the shape of the kernel of the nut), was measured in the VATF compact range. The radar cross section (RCS) data presented are for a precision 1-m aluminum test body measured at 11.6 GHz. There has been considerable interest by several organizations in obtaining one of these standard electromagnetic test bodies for evaluation on their ranges. A cooperative effort is currently under way in which test bodies will be provided by Langley Research Center in exchange for copies of all test data obtained during the test body evaluation.

(M. C. Gilreath, 3631)

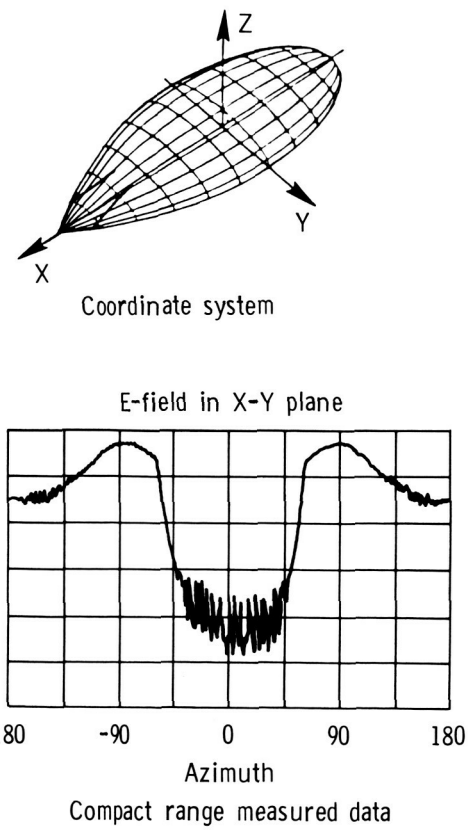

Standard electromagnetic test body.

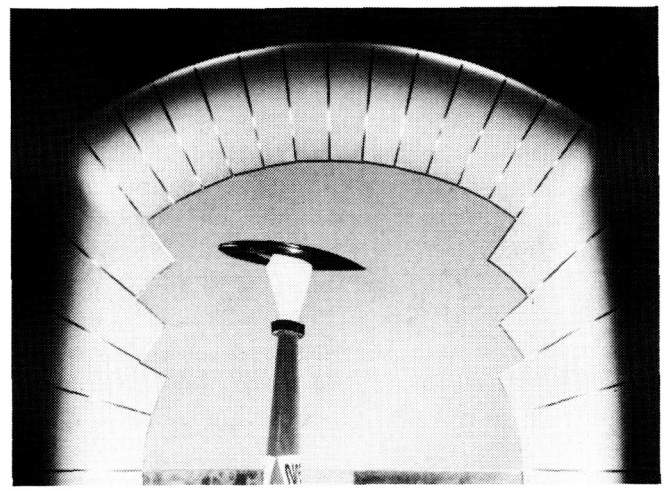

L-85-2139

Test body during evaluation on compact range.

Space Station Antenna Volumetric Pattern Analysis

Antenna pattern coverage for communications and tracking antennas mounted on the Space Station (SS) and the effects of scattering from the SS structure must be accurately known. Conventional techniques, which use scale-model antenna pattern measurements in an anechoic chamber, are limited because of the time and expense required to evaluate the many antenna systems to be employed on the SS. To overcome this limitation, analytical computer codes are being developed to accurately predict the performance of the SS antennas.

An efficient, faster-running version of the Numerical Electromagnetic Code-Basic Scattering Code (NEC-BSC) has been developed for SS application. These codes can determine the near- and

far-zone patterns of antennas in the presence of simulated SS scattering structures. The BSC uses the Uniform Geometric Theory of Diffraction technique for modeling scattering from large structures. This technique and the NEC are very useful for accurately predicting the performance of antennas on a complex structure environment.

Before the new version of the NEC-BSC can be released for general use, the accuracy of computed patterns must be evaluated against those measured in an anechoic chamber using scale models. A preliminary evaluation, using a 1/13-scale model of a position of the upper boom of the Space

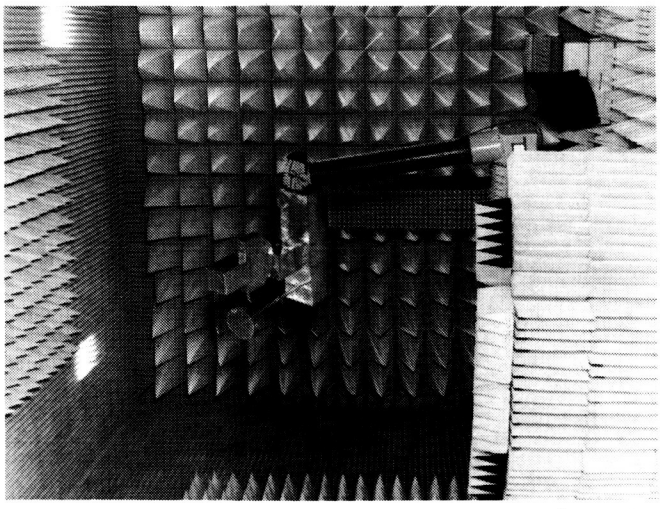

L-86-9474

1/13-scale model of Space Station upper boom mounted in VATF anechoic chamber.

Station, has been conducted. Antenna pattern measurements were made in the VATF at 15.8 GHz for a Global Positioning System (GPS) antenna, which operates at 1.2 GHz. A similar set of patterns was calculated using the NEC-BSC. The calculated patterns show very good agreement with the measured patterns as seen in the figure. Using the NEC-BSC pattern prediction codes along with the previously developed and released obscuration program (SHADOW), an antenna designer can now evaluate the performance of antennas mounted on the Space Station.

(E. M. Bracalente, 3631)

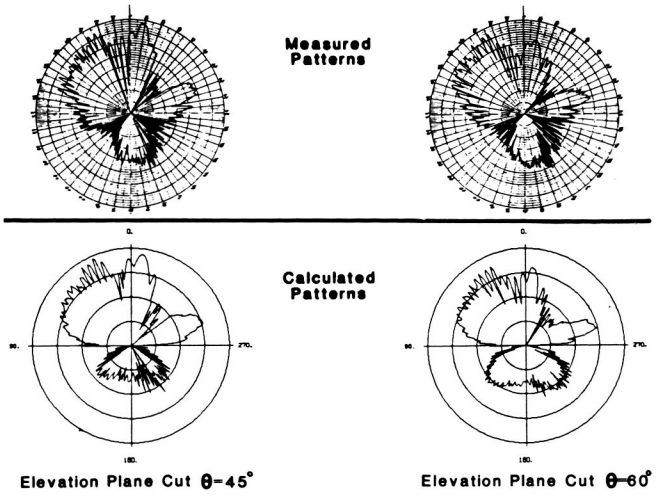

GPS antenna patterns with Space Station structure located on upper boom near Tracking and Data Relay Satellite antenna support boom.

Impact Dynamics Research Facility

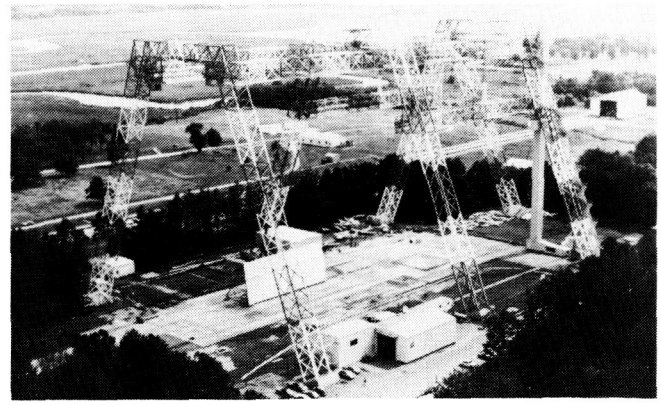

This facility, which was originally used by the astronauts during the Apollo Program for simulation of lunar landings, has been modified to simulate crashes of full-scale aircraft under controlled conditions. The aircraft are swung by cables, pendulum-style, into the concrete impact runway from an A-frame structure approximately 400 ft long and 230 ft high. The impact runway can be modified to simulate other ground crash environments, such as packed dirt with trees. In the past the impact runway has been modified with soil to meet a specific test requirement.

The aircraft is suspended by swing cables from two pivot points 217 ft off the ground. It is then pulled back along an arc to a predetermined height by a pullback cable from a movable bridge on top of the A-frame, released from the pullback cable, and allowed to swing, pendulum-style, into the ground. An instant before impact, the swing cables are separated from the aircraft by pyrotechnics. The length of the swing cables regulates the aircraft impact angle from 0° (level) to approximately 60°. Impact velocity can be varied up to approximately 65 mph (governed by the pullback height) and to 90 mph with rocket assist. Variations of aircraft pitch, roll, and yaw can be obtained by changes in the aircraft suspension harness attached to the swing cables. Onboard instrumentation data are obtained through an umbilical cable attached to the top of the A-frame. Data are transmitted by hard wire to the control room at the base of the A-frame. Photographic data are obtained by ground cameras and cameras mounted on top of the A-frame. Maximum allowable weight of the aircraft is 30,000 lb.

Impact Tests Conducted on Composite Fuselage Frames

Three tests were performed on 6-ft-diameter Z-cross-section graphite/epoxy fuselage frames to determine the global response and failure characteristics of generic composite structural components to typical crash loadings. These complete circular frames were fabricated from four 90° segments, and 10 lb masses were attached on the left and right sides of the frame 90° up from the bottom. A lightweight cable or aluminum tube was used to join the two masses and to simulate the restraint of a fuselage floor on the frame. After 25- to 27 ft/s impacts, the frames failed at one or two locations near the impact point. Although the frames were instrumented with strain gauges around the complete circumference of the frames, high strains causing failure were recorded only in areas below the masses. Because the measured strains were so low and no visible damage was apparent in the upper half of the frames, additional tests using the upper halves were conducted.

The upper halves of the original test frames were re-tested with a 100-lb mass addition, consisting of a bar that extended through the center of the frame and served as a floor beam. These tests were conducted at an impact velocity of approximately 20 ft/s. The impact damage sustained by these frames was much more severe than that of the earlier frames (as shown in the figure). Upon impact the frames failed near the impact point then subsequently failed on the left and right sides of the frame approximately 30° below the simulated floor. Measured floor-level acceleration peaks of approximately 15 g were confirmed by high-speed-film

motion analysis of the test. Floor-level pulse peaks of approximately 60 g were recorded in earlier tests conducted at 25 to 27 ft/s with 20 lb of attached mass. These crash pulses are used to assess the potential crash resistance of composite aircraft and to examine the predictive capabilities of the DYCAST (DYnamic Crash Analysis of STructures) computer code.

(Richard Boitnott, 3795)

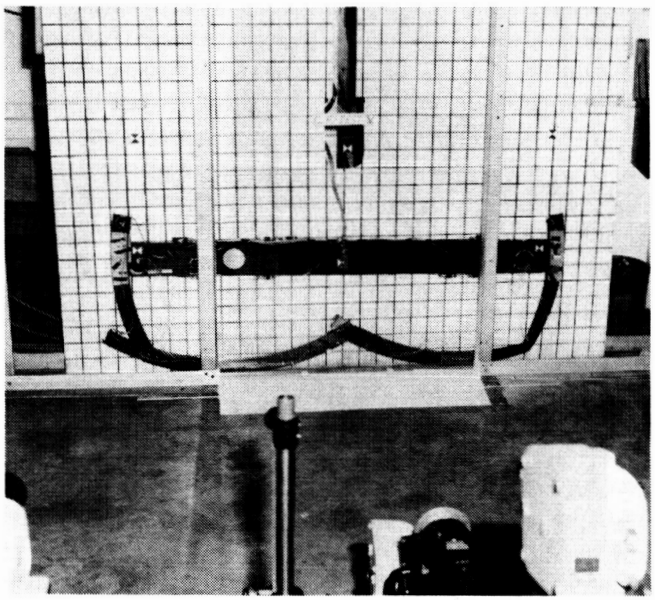

Graphite/epoxy frame with simulated floor mass after 20-ft/s impact.

Structural Analysis of Jet Transport Controlled Impact Demonstration

An extensive research and development program was initiated by the Impact Dynamics Branch and the Federal Aviation Administration (FAA) to quantitatively assess jet transport airplane crash dynamics using nonlinear dynamic finite-element computer codes. The FAA/NASA Controlled Impact Demonstration (CID) of a remotely piloted Boeing 720 jet transport instrumented with over 350 crash sensors provided experimental data for the final modeling effort.

In cooperation with Boeing Commercial Airplane Company, a hybrid finite-element airplane crash model was developed with the nonlinear computer code DYCAST (developed by Grumman under NASA contract) to evaluate pre-CID impact scenarios and to simulate the actual CID test. Three transport fuselage section vertical-drop tests (performed at the Impact Dynamics Research Facility at Langley Research Center) at impact velocity of 20 ft/s were modeled and analyzed using DYCAST to provide nonlinear subfloor crush springs for the hybrid CID model.

Although a symmetric impact for CID was planned, the left-wing outboard engine impacted first with the airplane rolled and yawed 13°. Model predictions begin at fuselage contact with the ground and continue for 0.15 s. Initial conditions used in the analysis are 12 ft/s vertical sink rate at the center of gravity, −0.1 rad/s pitch rate, and initial pitch of −2.5° at fuselage impact. Yaw and roll conditions are not included. The figure shows a schematic of the symmetric CID airplane model and comparisons of predicted vertical floor acceleration peaks with experimental peaks measured along the floor from nose ($X = 0$) to tail. Predictions of the acceleration levels from the model agree well with data from the CID experiment.

The building-block analysis approach of using results from detailed models of substructure to form hybrid elements for input to more complex structures (i.e., full airplane models) has been successfully used. Good agreements between the DYCAST model results and the CID experimental data demonstrate the validity of this approach as a useful method for assessing crash dynamics of large transport aircraft.

(Edwin L. Fasanella, 3796)

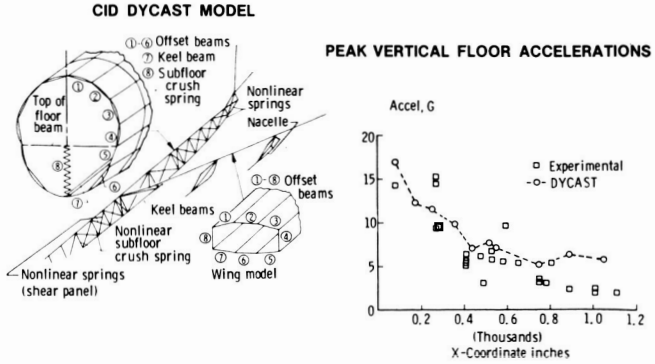

Comparisons of DYCAST-predicted peak vertical floor accelerations with CID experimental data.

Aircraft Landing Dynamics Facility

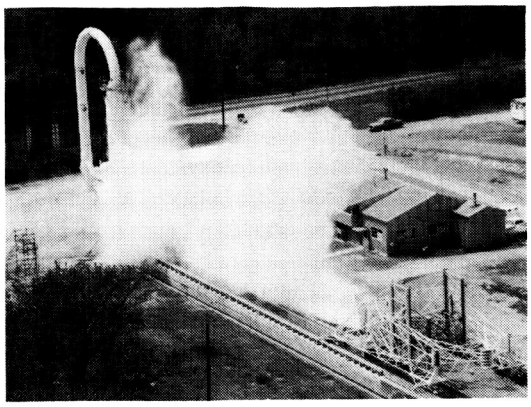

Langley Research Center has recently updated the landing loads track to the Aircraft Landing Dynamics Facility (ALDF) to improve the capability of low-cost testing of wheels, tires, and advanced landing systems. The main features of the updated facility are the propulsion system, the arresting gear system, the high-speed carriage, and the track extension.

The ALDF uses a high-pressure water jet system to propel the test carriage along the 2800-ft track. The propulsion system consists of an L-shaped vessel that holds 28,000 gallons of water pressurized to 3150 psi by an air supply system. A timed, quick-opening shutter valve is mounted on the end of the "L" vessel and releases a high-energy water jet, which catapults the carriage to the desired speed. The propulsion system produces a thrust of 2×10^6 lb at maximum pressure, which is capable of accelerating the 108,550-lb test carriage to 220 knots within 400 ft. This thrust creates a peak acceleration of approximately 20 g. The carriage coasts through an 1800-ft test section and decelerates to a velocity of 175 knots or less when it intercepts the five arresting cables that stretch across the track. The arresting system brings the test carriage to a stop in 600 ft or less. Essentially any landing gear can be mounted on the test carriage, including those exhibiting new concepts, and any runway surface and weather condition can be duplicated on the track. Research on slush drag, hydroplaning, tire braking, steering performance, and runway grooving has been conducted in the past.

Future research programs include the Space Shuttle orbiter main and nose gear tire spin-up wear characteristics and cornering force measurements at high speeds as well as frictional properties of radial and H-type aircraft tires for comparison with conventional bias ply tires. A surface traction program to study the effect of different runway surface textures and various runway grooving patterns on the stopping and steering characteristics of aircraft tires will be conducted. Finally, tests associated with the National Tire Modeling Program will also be conducted.

Space Shuttle Orbiter Main Gear Tire Behavior Modeled

High-speed tests to provide data used to develop mathematical models of Space Shuttle orbiter main-tire wear and cornering characteristics have been conducted. Tests at the ALDF are able to simulate the tire loads and crosswind conditions observed during flight operations at the Shuttle Landing Facility at Kennedy Space Center.

Parametric studies showed that yawed rolling of the tires causes a spin-up patch with exposed cord to grow quickly both in area and depth. This wear phenomenon was expressed as a function of the work produced by the tire during cornering. Tests with the tire plane tilted to the local runway surface showed that shoulder wear of flight tires could be expressed as a function of the tilt angle distance history. Development of these mathematical tools enabled duplication of flight conditions at the ALDF and provided the capability to predict tire wear in crosswind conditions not previously experienced in flight. Low-speed testing was conducted to define the cornering characteristics of the main gear tire at loads up to 120,000 lb. This load represents the main tire loads observed in flight as the nose gear of

the Space Shuttle orbiter touches down. The models of the tire wear and cornering behavior are included in the Space Shuttle orbiter rollout simulators to provide an accurate representation of the handling qualities and tire wear likely to be seen on actual missions.

(Robert H. Daugherty and Sandy M. Stubbs, 2796)

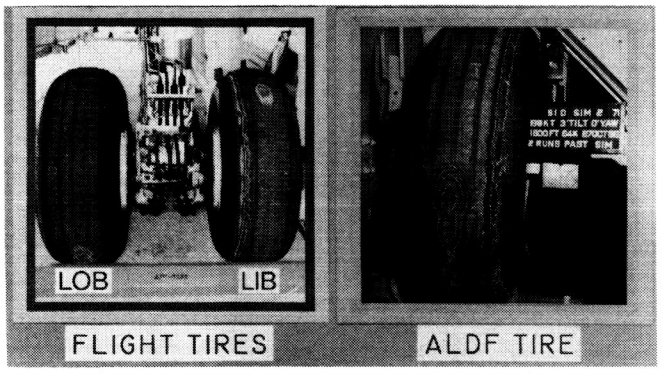

Mission 51D tire wear comparison.

Basic Aerodynamics Research Tunnel

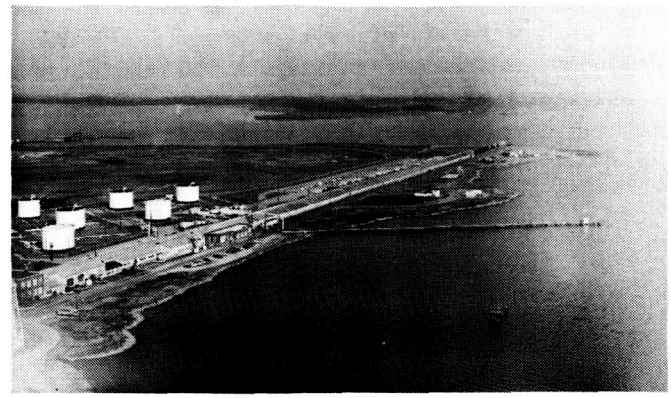

Computational methods are progressing rapidly toward the prediction of the three-dimensional flow field about complex geometries at high angles of attack. These computational methods require a large number of grid points to adequately model the flow field, and they produce large amounts of information. To validate these methods, detailed experimental flow field measurements are required. The Basic Aerodynamics Research Tunnel (BART) is a flow diagnostic facility dedicated to the task of acquiring the detailed data required for code validation and investigating the fundamental character of complex flow fields.

The BART is an open-return wind tunnel with a closed test section 28 in. high, 40 in. wide, and 10 ft long. The maximum test section velocity is 220 ft/s, which yields a Reynolds number per ft of 1.4×10^6. The airflow entering the test section is conditioned by a honeycomb, four antiturbulence screens, and an 11 to 1 contraction ratio. These flow manipulators, coupled with an excellent speed controller, provide a low-turbulence, uniform flow in the test section. The level of the longitudinal component of turbulence intensity ranges from 0.05 percent at low speeds to 0.08 percent at a test section dynamic pressure of 45 lb/ft^2.

The timely acquisition of the detailed data required for code validation dictates the use of a highly integrated and fully automated Data Acquisition and Control System (DACS). The BART DACS consists of a computer system that monitors and controls all test instrumentation. BART instrumentation includes a three-dimensional probe traverse system, an electronic scanning pressure system, a three-component hot wire, and a three-component laser Doppler velocimeter.

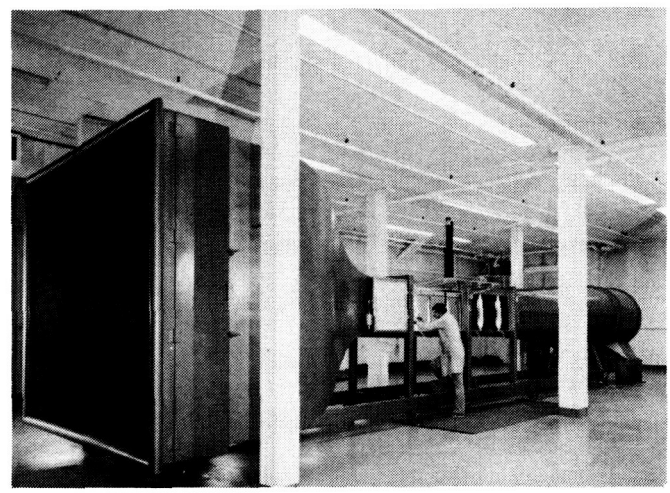

L-85-3069

Forward view of BART.

Investigation of Flow Over 75° Swept Delta Wing

Modern high-performance aircraft generate a substantial amount of nonlinear lift from the vortex flows generated at sharp leading edges and leading-edge extensions. Computational methods are progressing toward the prediction of these highly complex, vortex-dominated flow fields. A detailed investigation of the flow over a 75° swept delta wing at an angle of attack of 20.5° has been conducted in the BART to obtain a detailed data base for code validation. Another important aspect of this investigation was to determine the effects

of Reynolds number R_n on the flow field over the delta wing. The data acquired include surface and flow field visualization at a Reynolds number range from 0.5 to 2×10^6 in increments of 250,000. Presented in the figure is the flow field above the 75° swept delta wing at an angle of attack of 20.5°. The "simultaneous" light sheets are formed by reflecting an argon-ion laser light off mirrors mounted on galvanometers. Pitot pressure surveys were made at five longitudinal stations at $R_n = 0.5$, 1.0, and 1.5×10^6. Flow velocity and angularity surveys were made with a five-hole probe at three longitudinal stations at the same R_n. Each survey plane typically contains 3000 data points above the wing.

The results indicate that Reynolds number has only a minor effect on the global structure of the flow field in the range of R_n that was investigated. The boundary layer transitions from laminar to turbulent at the trailing edge of the wing at a Reynolds number of 1×10^6 and moves forward to 40 percent of the root chord at a Reynolds number of 2×10^6. The positions of the primary vortex cores are insensitive to Reynolds number in this range; however, the lateral position of the secondary vortex core moves outboard aft of the region where the boundary layer transitions from laminar to turbulent.

(Scott O. Kjelgaard, 2543)

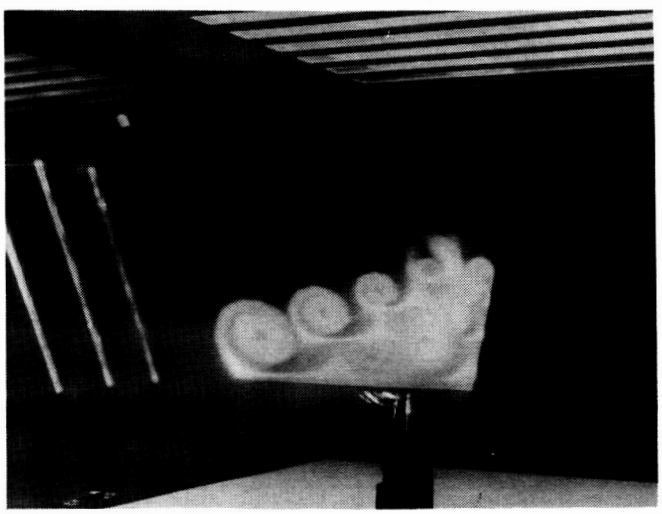

L-86-11,890

Multiple laser light sheet flow visualization.

Pitot Pressure Surveys Over F-18 Fighter Configuration

In an effort to supply an experimental data base for code validation, pitot pressure measurements over an F-18 configuration have been conducted in the BART. This flow field is highly complex and is dominated by vortex flows emanating from the forebody, leading-edge extension, and sharp wing leading edges. The flow field surveys were conducted at an angle of attack of 23° and Reynolds number of 400,000 based on mean aerodynamic chord measured. A pitot pressure probe 0.01 in. high by 0.02 in. wide was traversed above the model at seven streamwise stations. The number of data points acquired for each station ranged from 3000 over the nose to 5800 over the wing. Presented in the figure are six of the pitot pressure surveys, color contoured (although shown here in black and white), and superimposed on a geometrical representation of the F-18. The pitot pressures were scaled into 20 bands of color with black representing the minimum pitot pressure deficit and white a maximum pitot pressure deficit.

Pitot pressure results concur with laser-light sheet flow visualization on the vortex burst position of approximately 25 percent of the wing root chord. The vortex burst is indicated in the pitot pressure surveys by the reduction in the pitot pressure deficit from the fifth to the sixth survey plane.

(Scott O. Kjelgaard, 2543)

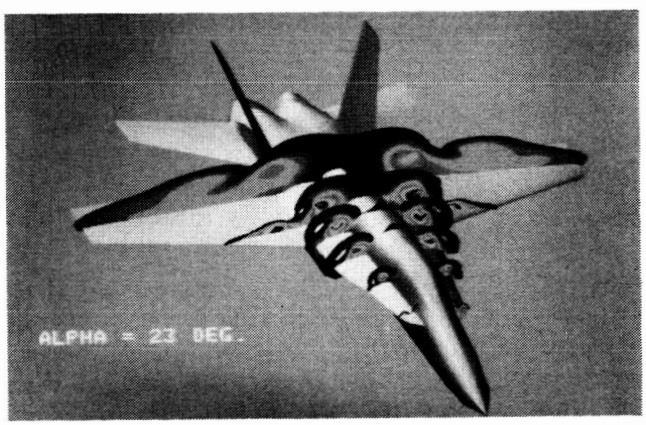

Pitot pressure contours superimposed on geometrical representation of F-18.

Image Processing Laboratory

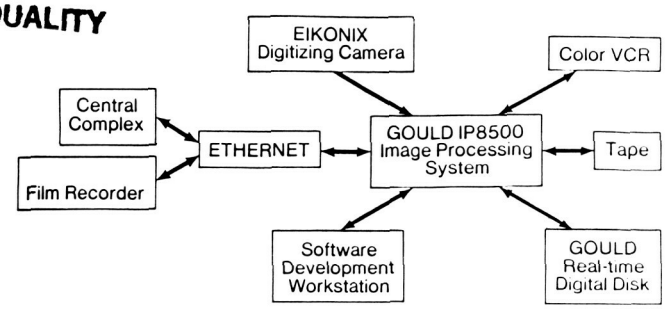

The Image Processing Laboratory (IPL) is a versatile, stand-alone image processing system that allows researchers to enhance and analyze digital images. These images arise from a wide range of applications including wind tunnel flow field experiments, computational fluid dynamics solutions obtained on the VPS-32 supercomputer, nonintrusive aerodynamic heat-transfer measurements, and modeling of satellite imaging systems. Because such images often have very low contrast or spatial resolution, the usual manual methods of analysis and publication of results are time consuming and inaccurate, if not impossible. The IPL provides researchers new analysis tools that allow enhanced images and accurate results to be generated in minutes rather than days.

The IPL is based on a Gould IP8500 image processing system, featuring a digital video processor that is specifically designed to process large arrays of image data fast enough to support interactive work. The system is supported by a number of input/output peripherals in the laboratory. For instance, images on photographic media are input to the IP8500 using the Eikonix digitizing camera, which converts visual information into a digital array of numbers (digital image) that can be quantitatively processed by the system. Also, digital images generated on any computer in Langley Research Center's local area network can be transferred to the system via an Ethernet connection, and a nine-track magnetic tape unit can read digital images created at remote locations. The digital images are then analyzed and interactively enhanced on the IP8500 and subsequently transmitted over the Ethernet connection to either a Dicomed or CELCO film recorder. Both of these devices convert the enhanced digital images into photographic media for a hard copy of results. A sequence of images and individual frames on videotape can be input to the system using the color video tape recorder. Images can be placed on the real-time disk, which is capable of reading and writing a sequence of digital images at video rates, thus allowing dynamic enhancement of a sequence of images (i.e., wind tunnel tests) recorded on videotape and previewing of computer-generated movies. Enhanced sequences of images can then be recorded back onto videotape or used to produce a sequence of photographic images.

The IPL provides researchers with enhanced images that increase their ability to accurately interpret image data in a wide variety of applications. The interactive nature of the system allows researchers to use their experience and judgment to quickly analyze and process their image data.

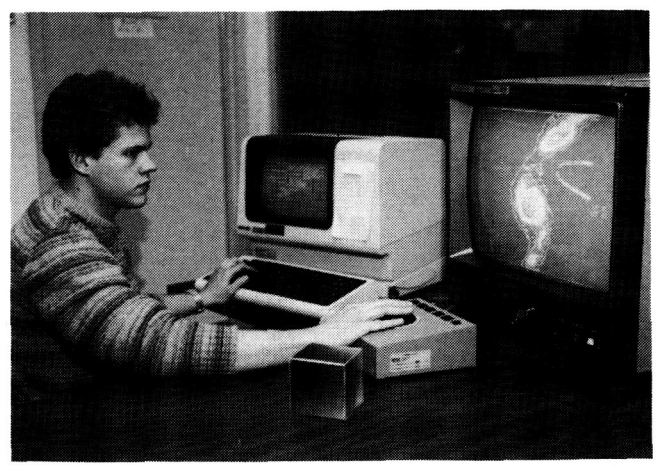

L-86-2268

Track ball used for interactive enhancement of flow field images.

The enhanced images provide an effective means of presenting research results for analysis, publication, and presentation. IPL provides a practical and interactive environment for users to process image data quickly and to obtain a variety of outputs to meet their needs.

Digital Enhancement of Flow Field Images

Significantly enhanced flow visualization has been achieved at Langley Research Center by the application of digital image processing techniques to photographs of wind tunnel experiments. The photographs are typically low contrast, and smoke is used to highlight the flow field features. Of particular interest are the size, shape, and location of vortex cores before and after they interact with an airfoil.

The photographs are taken with a 70-mm-film camera and then digitized into a 2048 × 2048 pixel image with a Eikonix 78/99 digitizing camera, which has an eight-bit gray-level resolution per pixel. Digitization takes several minutes per photograph. The digital images are then processed with a variety of enhancement techniques to fulfill the objectives of improving the contrast, highlighting key vortex structural features, and producing useful publication-quality images. Contrast is improved by the application of linear contrast stretching to use the full range of possible gray levels. Low-pass filtering is used to suppress noise and graininess induced by the digitization process. Selective gray-level regions are then mapped to black to produce a contouring effect and to highlight structural features within the vortices. Enhanced images can also be displayed as black-on-white contour plots or as pseudocolor images.

Previous methods of analyzing this type of data by hand and with a digitizing tablet and visual estimation of gray-level boundaries were slow and inaccurate given the low contrast of the original images. In contrast, the digital enhancement technique is performed interactively in minutes with a Gould IP8500 image processing system and special software written by Langley Research Center personnel. Input and output images can be in the form of negatives, positives, or videotape.

(Robert A. Kudlinski, 3434)

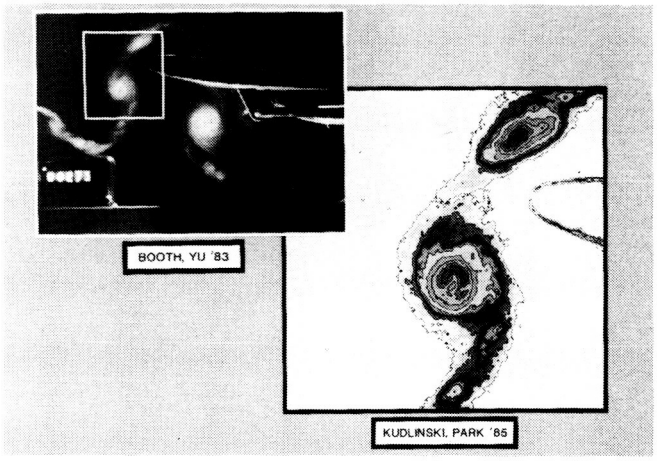

L-85-9441

Vortex details evident through enhancement of 1983 wind tunnel photograph.

Multiple Vortices Above F-106B Wing During Flight

The effects of Reynolds number, Mach number, and angle of attack on the leading-edge shed vortex system above a delta wing airplane in flight have been examined. A vapor-screen technique was used on an airplane of sufficient sweep so that leading-edge vortices were generated and visualized in flight. The vapor-screen technique involved three systems: a seed particle generator to produce the trace material needed to provide a definition of the vortices, a light-sheet generator to illuminate the particles in the vortices, and a video system to record the seeded flow above the wing. Only test data taken for angles of attack between 17° and 23° showed any appreciable vortex activity. Flights were conducted at night in order to obtain the appropriate contrast with ambient light. Reynolds number variations were generally accomplished by flying a l-g deceleration manuever at different altitudes at a Mach number of approximately 0.4.

During flight testing at 1 g and subsonic speeds, large-scaled multiple vortices were recorded via a black-and-white video camera. Through IPL image enhancement and false color assignment, the visual information was made clear. Typical results are detailed in the figure and show two vortices with the same sense of rotation above the left-wing panel.

The occurrence of multiple vortices at most test points was the rule rather than the exception (as shown in the figure by the images for angles of attack of 17° and 20°). The occurrence of multiple vortices differed from anticipated results of only a single leading-edge vortex. Single leading-edge vortices were found at high test angles of attack and were a function of altitude (Reynolds number) in that they appeared at the higher altitudes (lower Reynolds numbers) first.

This study was the first observation in flight of large-scaled multiple vortices having the same rotational sense and comparable size; this occurrence has not been reported in any of the wing solutions made with the computational fluid dynamics codes. The origin of these multiple vortices will be probed in an upcoming flight program. A rotating light sheet (part of the vapor-screen system), mounted on top of the F-106B fuselage, will enable most of the upper surface of the wing to be illuminated and viewed by the video camera.

(John E. Lamar, 2601)

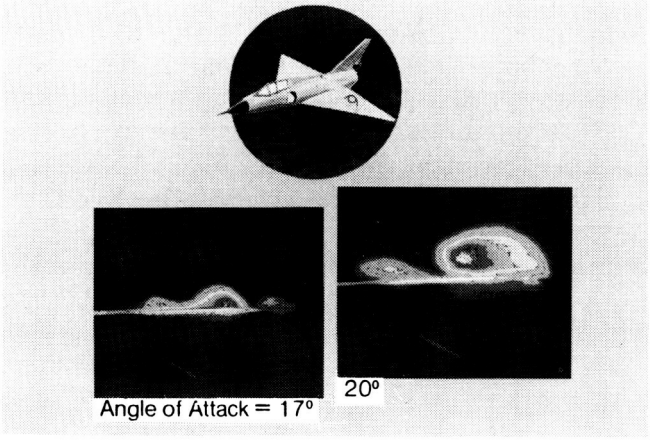

L-87-126

Multiple vortices above F-106B wing at angles of attack of 17° *and* 20°, *Mach number of 0.4, altitude of 25,000 ft, and Reynolds number of* 33×10^6.

Flight Research Facility

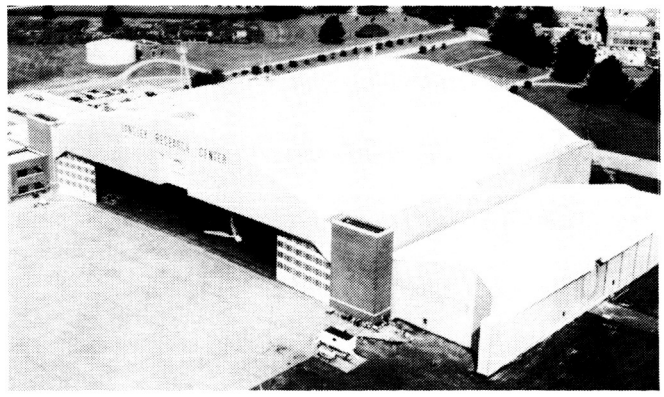

The truss-supported roof of the huge hangar of the Flight Research Facility provides a clear floor space with nearly 300 ft in each direction (over 87,000 ft^2).

Door dimensions will allow entry of a Boeing 747. Features such as floor air and electrical power services, radiant floor heating to eliminate corrosion-causing moisture, a modern deluge fire suppression system, energy-saving lighting, modern maintenance spaces, and entry doors and taxiways on either side of the building make this structure equal or superior to any hangar in the country. Extensive and modern maintenance equipment makes it possible to maintain, repair, and modify aircraft ranging in sophistication from modern metal and composite airliners, fighters, and helicopters to fabric-covered light airplanes. Surrounding the hangar are ramp areas with load-bearing capacity sufficient to handle the largest current wide-body jet. The high-power turnup area can also handle a wide variety of aircraft.

The present array of research and research support aircraft includes an airliner, military fighters, trainers, experimental one-of-a-kind designs, helicopters, and single- and multi-engine light airplanes. This variety enables research to be carried out over a wide range of flight conditions, from hover to Mach 2 and from the surface to 60,000 ft. Research pilot currency in this wide spectrum of aircraft is important in conducting credible in-flight experiments as well as in-flight simulator assessments. A variety of research can be conducted in such areas as terminal traffic flow, Microwave Landing System (MLS) approach optimization, airfoil properties, single-pilot instrument flight rules (IFR), engine noise, turbulence research, natural laminar flow, winglet studies, stall/spin, and severe storm hazards.

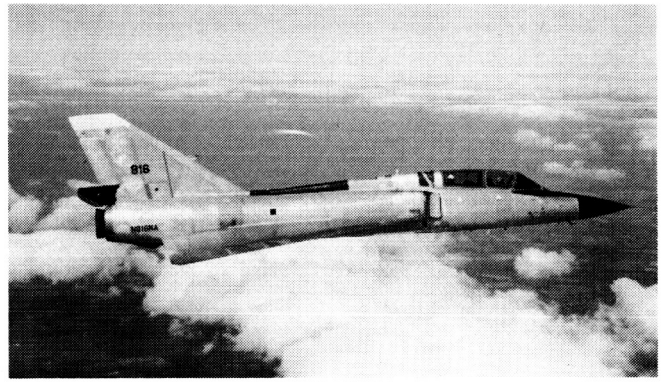

L-83-2747

Convair F-106B configured for Storm Hazards Program.

One of the support helicopters is used to drop unpowered remotely controlled models of high-performance airplanes to study high-angle-of-attack control characteristics. The Radio-Controlled Drop Model Facility is used to study the low-speed flight dynamic behavior of aerospace vehicles with particular emphasis on high-angle-of-attack characteristics of combat aircraft. The technique consists of launching an unpowered, dynamically scaled, radio-controlled model into gliding flight from the support helicopter, controlling the flight of the model from the ground, and recovering the model with a parachute. The models are constructed primarily of molded fiberglass and are typically about 10-ft long with weights in the range of 200 to 300 lb. A comprehensive on-board instrumentation system provides measurements of key flight dynamics parameters that are transmitted to the ground via telemetry and recorded for analysis. The model control loop involves a combination of ground-based and on-board equipment and the required com-

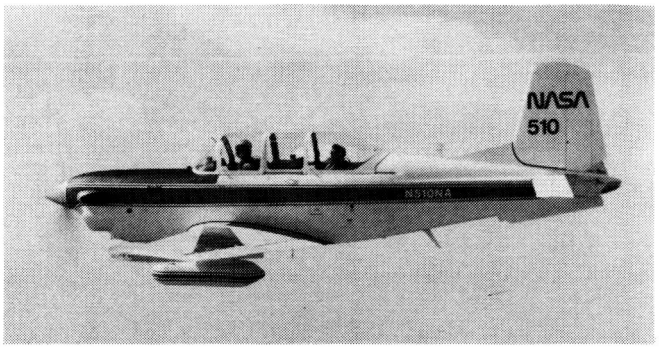

L-80-3923

Beech T34C used for flight support.

L-76-6425

Bell 204B configured for model drop mission.

munication links. The heart of the system is a ground-based digital computer into which the control laws are programmed. The processor accepts downlinked feedback signals from the model and commands from the pilot and computes the control surface commands that are then transmitted to the model. Very-high bandwidth electromechanical servo-actuators are used to drive the model control surfaces. The pilot flies the model from a ground station that provides the required information on a number of displays. These displays include a high-resolution video image of the model, a map display showing model ground track, and conventional analog instruments presenting key parameters such as angle of attack and airspeed.

The tests are conducted at the Plum Tree Test Site located approximately 5 miles from Langley Research Center. The test site is a marsh approximately 2 miles long and 1 mile wide.

L-83-11,167

Radio-Controlled Drop Model Facility.

Liquid crystals for boundary-layer flow visualization

A new method for boundary-layer flow visualization in aerodynamic and hydrodynamic testing has been developed. The technique is based on the ability of liquid crystals to change color in response to changes in shear stress and temperature. Although the liquid crystals appear as oily liquids, they have certain mechanical properties that are analogous to solid crystals. In particular, liquid crystals scatter light very selectively. Thus, when the liquid crystals are subjected to certain physical influences (primarily shear stress and temperature), the wavelength of reflected light changes accordingly. Since the fundamental chemical structure is unaffected by these changes, a liquid-crystal coating will respond quickly and repeatedly to the physical changes.

A liquid-crystal coating is formulated for a particular application to change colors in response to differences in relative shear stress within the temperature environment of the test article. These formulations can be made to respond at test conditions as low as −22°F and up to 480°F.

Liquid crystals have been used to visualize the boundary layer in flight at speeds up to Mach 0.8 and altitudes up to 48,000 ft using a Lear 28/29. The figure shows the boundary-layer transition location on the winglet as a change from dark to light. The higher shear stresses associated with the turbulent boundary layer downstream of transition produced the brighter colors (color figure available from author). Liquid crystals have also been used in wind tunnels at dynamic pressures as low as 5 lb/ft^2. Another successful application of the liquid-crystal technique has been on surfaces tested under water. In addition to visualization of boundary-layer transition location and modes, liquid crystals have been used to observe other aerodynamic phenomena such as shock locations, laminar separation bubbles, and separated flows. **(Clifford J. Obara, 3274)**

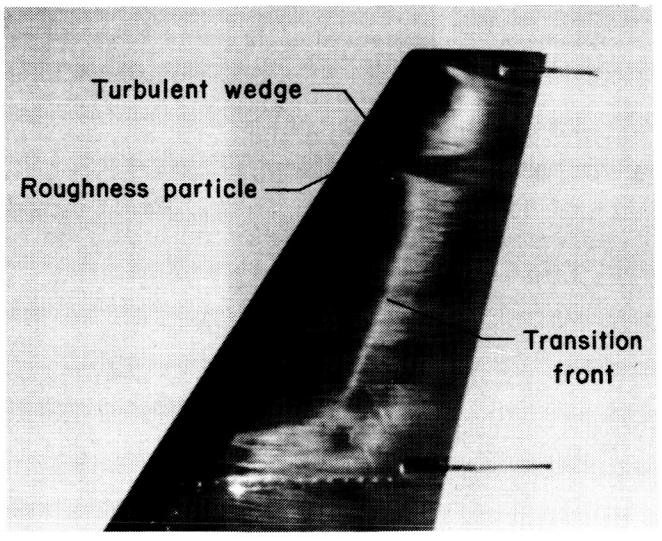

L-86-1401

Boundary-layer transition visualization using liquid crystals on Lear 28/29 airplane winglet.

Storm Hazards Program - 1986 Results

The NASA Storm Hazards Program concluded operations in 1986 with the F-106B airplane receiving 24 additional direct lightning strikes. This brought the total number of lightning strikes to 714 hits in 7 years of flying through thunderstorms. The on-board instrumentation included 12 channels of electromagnetic data with 5- and 10-ns time resolution and several video and film camera systems. In 1986, the on-board camera systems included a pair of video cameras mounted on the left wing tip to allow time series photography of swept-stroke lightning paths from the nose boom to the tail.

Results obtained in 1986 confirmed the earlier experiences of higher strike rates at colder temperatures aloft. From 1980 to 1986, only 98 direct strikes were experienced at altitudes below 20,000 ft, where most strikes to commercial and military aircraft in routine operations have been reported. Ground-based data indicated that several strikes may have been cloud-to-ground strikes, and that most lightning strikes obtained at high altitudes were triggered by the presence of the aircraft. The lightning electromagnetic measurements have established a statistical basis for peak rate of current change and peak rate of electric flux density change during tests between a 15,000- and 40,000-ft altitude; the peak rate of current change was found to be several times larger than previous design criteria. The photograph from a left wing tip video camera shows a lightning channel attached to the nose boom with the channel beginning to sweep down the right side of the fuselage. The on-board camera systems have shown that the entire exterior surface of the F-106B airplane may be susceptible to direct lightning attachment, necessitating a rethinking of lightning attachment zone concepts used in aircraft design.

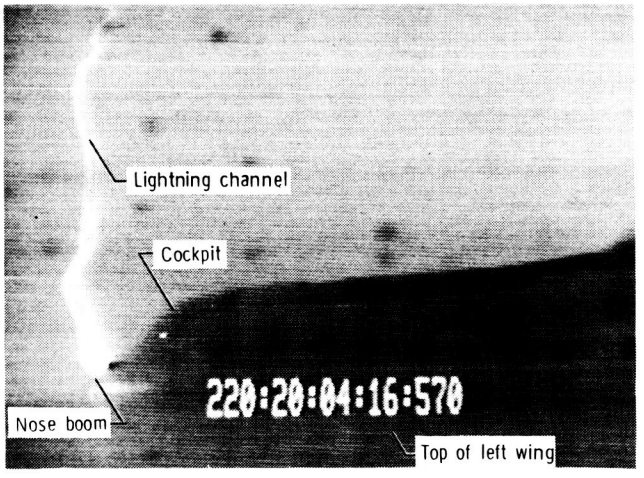

Lightning channel attached to nose boom of F-106B airplane. View is from left wing tip.

Finally, mathematical models that include thunderstorm electrification parameters are being developed to generalize the results from the all-metal F-106B airplane to composite aircraft with low-voltage digital systems.
(Bruce Fisher, 3274)

F-106 Supersonic Transition Flight Experiment

A flight test program has been conducted at the Langley Research Center to measure boundary-layer transition location on the wing and vertical tail of the F-106 at supersonic speeds. A leading-edge section of the wing (about mid-span) and vertical tail (on the inboard portion) was smoothed by attaching a fiberglass glove. Each glove was instrumented with flush surface static pressure orifices to measure the streamwise pressure distributions and hot-film gauges to determine the transition location. Eight flights were conducted at Mach numbers to 1.8 and altitudes to 51,000 ft.

In all cases, transition was found to occur near the leading edge on both the wing and vertical tail. Boundary-layer stability calculations were performed for several flight conditions, and these calculations indicate that the most likely cause of transition is a very strong cross-flow instability due to the high leading-edge sweep angles of both the wing and vertical tail.
(Dennis W. Bartlett and Fayette S. Collier, Jr., 2045)

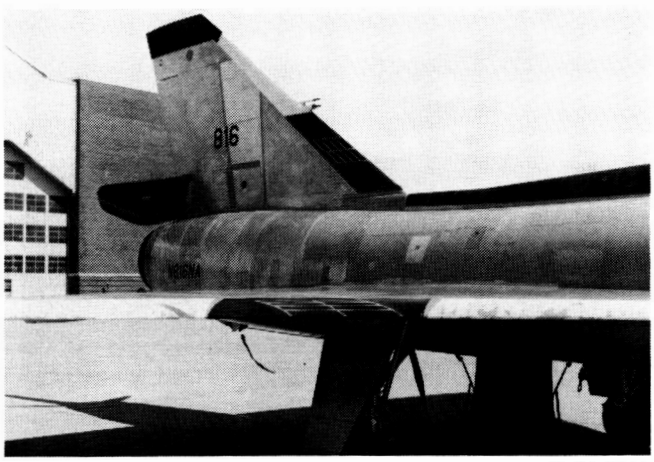

L-86-3839

F-106 smooth leading-edge glove installation.

Natural Laminar-Flow Engine Nacelle Flight Experiments

An experiment has been conducted with natural laminar-flow (NLF) nacelles as part of a Langley Research Center program concerning viscous drag reduction. One objective of these experiments is to explore the extent to which NLF may be achieved on engine nacelles in flight. Another objective is to examine the effect of the external acoustic environment on the stability of the boundary layer on nacelles with different forebody contours.

An experimental Grumman OV-1 is the test aircraft. The present test configuration is shown in the figure. A full-scale flow-through NFL nacelle is attached to a pylon under the right wing of the OV-1. The nacelle is highly instrumented with static and fluctuating pressure transducers. Outboard of the nacelle is a streamlined pod containing a noise source and a small video camera. Sublimating chemicals are used on the nacelle surface to establish the location of the transition front. The flow patterns are observed from the video camera and by an observer in a chase aircraft. The right-hand turboprop is feathered for zero rotation, and pressure data are measured with the sound source off and with it radiating toward the nacelle.

The most recent flight tests showed that for a Reynolds number of about 12×10^6, the transition location was aft of the 50 percent station on the NLF nacelle (i.e., at least half of the nacelle was in a laminar boundary layer). In these tests it was not possible to observe any change in transition due to the acoustic environment. In order to obtain that

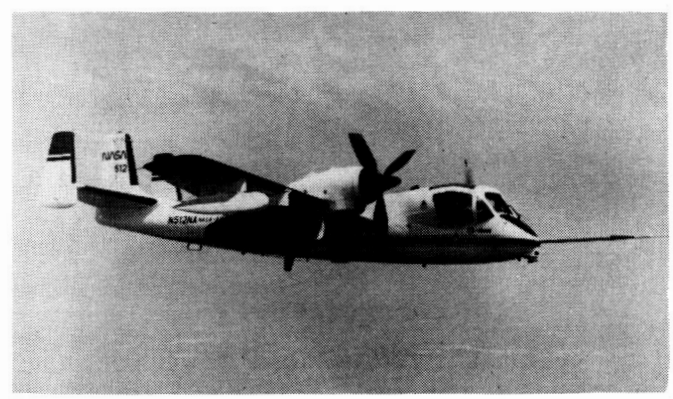

L-86-4986

Test aircraft configuration.

C-2

data, it is necessary to replace the present nacelle forebody with one that has a fuller contour near the lip. With this "less stable" laminar boundary layer, the acoustic environment may cause the boundary layer to trip. Flight testing with the new forebody is expected to resume in February 1987.
(Earl C. Hastings, Jr., 4870)

Stall/Spin Resistance and Separated-Flow Control Research Development of Spin Resistance Criteria for Light Airplanes

Wind tunnel and flight experiments conducted over the past decade have identified promising means to improve the spin resistance of light airplanes. In order to manufacture and certify such airplanes, a standard is needed to describe the desirable traits of a spin-resistant airplane and to provide a measure by which the airplane can be evaluated. Using results from the NASA Stall/Spin Research Program, researchers at the Langley Research Center assisted the General Aviation Manufacturers Association (GAMA) in the development of criteria for spin-resistant airplanes. In May 1985, GAMA proposed these criteria to the Federal Aviation Administration as an alternative to existing standards for light airplane certification.

Near and beyond the stall, a spin-resistant airplane should respond to control inputs in the normal manner and should resist development of the rapid rolling and yawing motions necessary for spin entry. The proposed criteria address these characteristics through assessment of lateral controllability during stalls, stall characteristics during uncoordinated flight, and overall controllability following sustained control abuse (attempted spin entries).

To provide additional data for evaluation of the criteria during the rule-making process, Langley Research Center tested a representative four-place single-engine light airplane against the criteria. The airplane was tested with its basic wing configuration and with a discontinuous wing leading-edge configuration that had been shown to enhance spin resistance in previous NASA tests. The baseline configuration failed 22 percent of the criteria stall tests and 67 percent of the spin entry scenarios. The modified leading-edge configuration passed all of the tests. The criteria, therefore, were shown to be achievable and to require a significant increase in spin resistance beyond that of current airplanes.
(H. Paul Stough, III, 3274)

L-83-6174

C-23X research airplane with wing leading-edge modification tested.

Stall/Departure Resistance Characteristics of Personal-Owner Trainer-Type Aircraft Configuration

A cooperative research program with the DeVore Aviation Corporation was conducted to investigate the stall/departure resistance characteristics of a model of a personal-owner trainer-type aircraft equipped with an outboard wing leading-edge droop. Wind tunnel tests were conducted in the 12-Foot Low Speed Tunnel, and radio-controlled model tests were conducted using a powered 1/4-scale model as shown in the figure. The model was instrumented, and flight data were transmitted to a ground control unit that records the information for further data reduction and analysis. The flight tests were conducted primarily to study high-angle-of-attack maneuvers and stall behavior; however, level flights were also conducted to assess stability and control behavior at these conditions.

Results from the wind tunnel tests indicate that wing leading-edge droops applied to the outboard

portion of the wing were effective in delaying flow separation and, hence, the onset of wing stall and autorotation tendencies. Results of radio-controlled model fight tests showed that the configuration with the outboard wing leading-edge droops installed exhibited good stall departure resistance through an angle of attack of 30°. Without the leading-edge droop installed, the model experienced an abrupt uncontrollable stall departure at an angle of attack of approximately 15°. These flight test results correlate well with predictions based on wind tunnel tests.

(Long P. Yip, 2184)

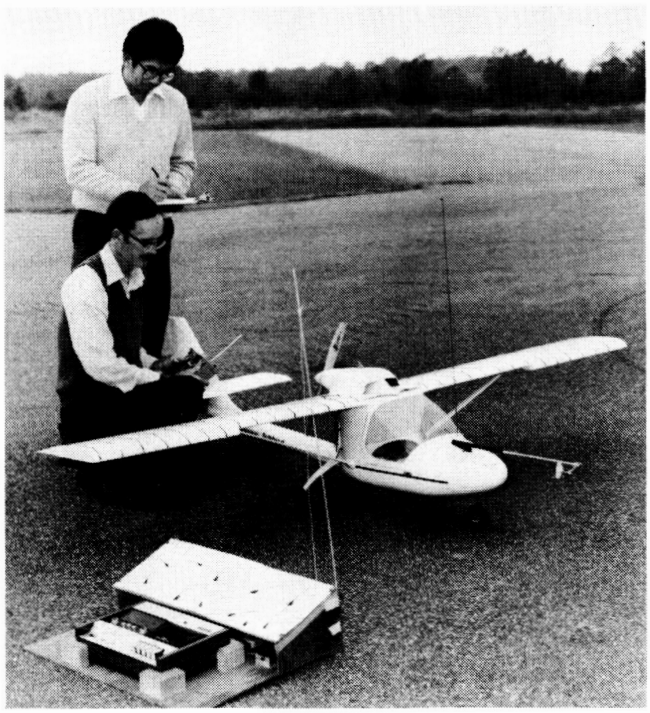

L-86-10,890

Radio-controlled model of personal-owner trainer-type airplane configuration.

X-29 High-Angle-of-Attack Flight Dynamics

As part of a program to study the high-angle-of-attack α flight dynamics of the X-29 configuration, drop model tests were conducted on a 22-percent dynamically scaled model. The objectives of the study were: (1) to investigate and document the flight behavior of the configuration throughout the stall/poststall envelope; (2) to develop and validate control law concepts to provide desired high-α characteristics; and (3) to obtain flight data to develop high-fidelity simulation models of the airplane.

The first series of tests explored the flight dynamics of the configuration throughout its angle-of-attack envelope. Two major problem areas were identified: (1) a region of unstable roll damping near stall which caused large-amplitude roll oscillations, or wing rock, and (2) strong yawing moments (caused by asymmetric shedding of vortices from the slender forebody) which can drive the airplane into a dangerous spin. These characteristics agreed well with predictions from earlier wind tunnel tests. Control law concepts were developed and implemented on the drop model system to address these problems. Subsequent flights showed that these systems were very effective in suppressing the wing rock and preventing the asymmetry-induced spins. With the modified control system, the model was flown to angles of attack as high as 70° without encountering significant loss of control situations.

The flight time histories have been analyzed using several parameter estimation techniques, and the resulting data are being used to update simulation mathematical models of the airplane. A high angle-of-attack flight test program of the full-scale X-29 is planned. The results from the current drop model program will significantly contribute to the development and validation of high-α control laws which will be crucial to this program.

(Luat T. Nguyen, 2184)

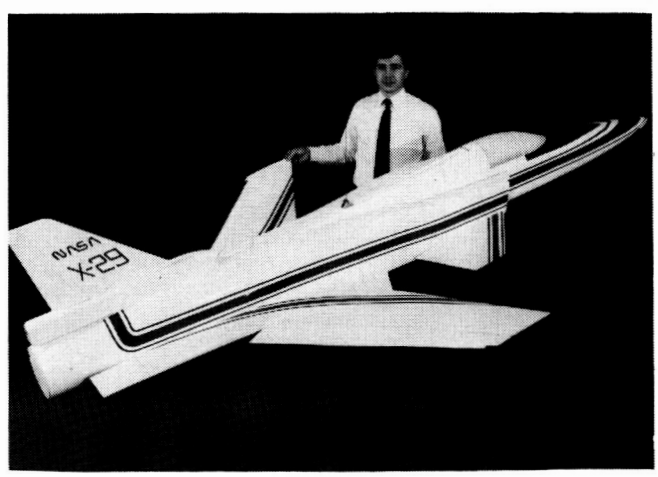

L-86-02

X-29 drop model.

NASA
National Aeronautics and Space Administration

Report Documentation Page

1. Report No.	2. Government Accession No.	3. Recipient's Catalog No.
NASA TM-89144		

4. Title and Subtitle	5. Report Date
Langley Aerospace Test Highlights—1986	May 1987
	6. Performing Organization Code
7. Author(s)	8. Performing Organization Report No.
9. Performing Organization Name and Address NASA Langley Research Center Hampton, VA 23665-5225	10. Work Unit No. 11. Contract or Grant No.
12. Sponsoring Agency Name and Address National Aeronautics and Space Administration Washington, DC 20546-0001	13. Type of Report and Period Covered Technical Memorandum 14. Sponsoring Agency Code

15. Supplementary Notes

16. Abstract

The role of the Langley Research Center is to perform basic and applied research necessary for the advancement of aeronautics and space flight, to generate new and advanced concepts for the accomplishment of related national goals, and to provide research advice, technological support, and assistance to other NASA installations, other government agencies, and industry. This report highlights some of the significant tests which were performed during calendar year 1986 in Langley test facilities, a number of which are unique in the world. The report illustrates both the broad range of the research and technology activities at the Langley Research Center and the contributions of this work toward maintaining United States leadership in aeronautics and space research. Other highlights of Langley research and technology for 1986 are described in *Research and Technology 1986 Annual Report of the Langley Research Center*. Further information about both reports is available from the Office of the Chief Scientist, Mail Stop 103, Langley Research Center, Hampton, Virginia 23665-5225(804-865-3316).

17. Key Words (Suggested by Authors(s))	18. Distribution Statement
Research and technology Tests Facilities Wind tunnels Models	Unclassified – Unlimited Subject Category 99

19. Security Classif.(of this report)	20. Security Classif.(of this page)	21. No. of Pages	22. Price
Unclassified	Unclassified	99	A05

For sale by the National Technical Information Service, Springfield, Virginia 22161-2171